INSTRUMENTATION AND TAR MEASUREMENT SYSTEMS FOR A DOWNDRAFT BIOMASS GASIFIER

by

MING HU

B.S., China Agricultural University, 2007

A THESIS

submitted in partial fulfillment of the requirements for the degree

MASTER OF SCIENCE

Department of Biological and Agricultural Engineering
College of Engineering

KANSAS STATE UNIVERSITY
Manhattan, Kansas

2009

Approved by:

Major Professor
Wenqiao Yuan

Copyright

Abstract

Biomass gasification is a promising route utilizing biomass materials to produce fuels and chemicals. Gas product from the gasification process is so called synthesis gas (or syngas) which can be further treated or converted to liquid fuels or certain chemicals. Since gasification is a complex thermochemical conversion process, it is difficult to distinguish the physical conditions during the gasification stages. And, gasification with different materials can result in different product yields. The main purpose of this research was to develop a downdraft gasifier system with a fully-equipped instrumentation system and a well-functioned tar measurement system, to evaluate temperature, pressure drop, and gas flow rate, and to investigate gasification performance using different biomass feedstock.

Chromel-Alumel type K thermocouples with a signal-conditioning device were chosen and installed to monitor the temperature profile inside the gasifier. Protel 99SE was applied to design the signal conditioning device comprised of several integrated chips, which included AD 595, TS 921, and LM 7812. A National Instruments (NI) USB-6008 data acquisition board was used as the data-collecting device. As for the pressure, a differential pressure transducer was applied to complete the measurement. An ISA1932 flow nozzle was installed to measure the gas flow rate.

Apart from the gaseous products yield in the gasification process, a certain amount of impurities are also produced, of which tar is one of the main components. Since tar is a critical issue to be resolved for syngas downstream applications, it is important to determine tar concentration in syngas. A modified International Energy Agency (IEA) tar measurement protocol was applied to collect and analyze the tars produced in the downdraft gasifier. Solvent for tar condensation was acetone, and Soxhlet apparatus was used for tar extraction.

The gasifier along with the instrumentation system and tar measurement method were tested. Woodchips, Corncobs, and Distiller's Dried Grains with Solubles (DDGS) were employed for the experimental study. The gasifier system was capable of utilizing these three biomass feedstock to produce high percentages of combustible gases. Tar concentrations were found to be located within a typical range for that of a general downdraft gasifer. Finally, an energy efficiency analysis of this downdraft gasifer was carried out.

Table of Contents

List of Figures vii
List of Tables ix
Acknowledgements x
CHAPTER 1 - Introduction 1
1.1 Gasification Process 2
1.2 Classification of Gasifiers 5
1.2.1 Updraft 5
1.2.2 Downdraft 6
1.2.3 Fluidized Bed 7
1.2.4 Entrained Flow 8
1.2.5 Choren Process 9
1.3 Objectives 10
CHAPTER 2 - Literature Review 11
2.1 Biomass Tar Formation 11
2.1.1 Tar Components 11
2.1.2 Tar Yield as a Function of Gasifier Type 14
2.1.3 Tar Formation under Different Biomass Gasification Conditions 15
2.2 Tar Measurement Methods 17
2.2.1 Cold Trapping Method 17
2.2.2 Solid-Phase Adsorption (SPA) Method 20
2.2.3 Molecular Beam Mass Spectrometer (MBMS) Method 20
2.2.4 Solvent-free Method 22
2.2.5 Quasi Continuous Tar Quantification Method 23
2.2.6 Laser Spectroscopy Method 23
2.3 Summary 24
CHAPTER 3 - Instrumentation and Tar Measurement Systems 26
3.1 Instrumentation system 26
3.1.1 Introduction to the Gasifier Unit 26

3.1.2 DC Power for the Blower (AC to DC Converter) 28
3.1.3 Temperature Measurement 30
3.1.4 Pressure Drop and Flow Rate Measurement 34
3.2 Tar measurement system 37
3.2.1 Tar Measurement - Sampling 37
3.2.2 Tar Measurement - Analysis 40
3.3 Summary 41
CHAPTER 4 - Experimental Study 43
4.1 Materials and Methods 43
4.1.1 Biomass Feedstock 43
4.1.2 Gasifier System Operation 44
4.1.3 Intake Air Temperature Control 44
4.1.4 Tar and Syngas Analysis 45
4.2 Results and Discussion 47
4.2.1 Gasifier Chamber Temperature Profile 47
4.2.2 Pressure Drop and Air Flow Rate 51
4.2.2.1 Biomass Loading Affecting Pressure Drop 52
4.2.2.2 Voltage Affecting Pressure Drop 54
4.2.2.3 Pressure Drop Variations at Different Locations 56
4.2.2.4 Pressure Drop at Outlet II 59
4.2.2.5 Pressure Drop of the Flow Nozzle and Syngas Flow Rate 61
4.2.3 Syngas Composition 61
4.2.4 Tar Concentration 61
4.2.5 Gasification Energy Efficiency 62
4.3 Summary 64
CHAPTER 5 - Summary 65
CHAPTER 6 - Future Research Recommendations 66
Appendix A - Operating Manual for Downdraft Biomass Gasifier 73
Appendix B - Temperature Calibration Chart for AD595 75
Appendix C - Data of Temperature Profiles and Pressure Drop 76
Appendix D - Data Table for Experiment Documentation 80

Appendix E - DDGS Properties Analysis 81
Appendix F - Biomass Properties (Gaur and Reed, 1998) 82
Appendix G - Relative Heating Value of Wood as a Function of Moisture Content 83
Appendix H - Calibration of SRI8610 Gas Chromatograph (GC) 84
Appendix I - Calculation of flow rate, syngas density, and energy efficiency 85
Appendix J - Thermodynamic data used by different companies (unit: MJ/Nm^3) (IEA, 2001) ... 88

List of Figures

Figure 1.1 Reaction zones in a downdraft gasifier 3
Figure 1.2 Syngas yields from gasification process (Turare, 2002) 5
Figure 1.3 Updraft fixed-bed gasifier (Knoef, 2005)..... 6
Figure 1.4 Downdraft fixed-bed gasifier (Knoef, 2005)..... 7
Figure 1.5 Fluidized bed gasifiers: bubbling (left) and circulating (right) (Knoef, 2005)..... 8
Figure 1.6 Texaco entrained flow gasifier (NETL online resource, www.netl.doe.gov) 9
Figure 1.7 Choren process (Choren, 2007)..... 10
Figure 2.1 Biomass tar formation (Evans and Milne, 1987)..... 12
Figure 2.2 Tar maturation scheme (Elliott, 1988)..... 12
Figure 2.3 Tar yield as a function of the maximum temperature exposure 13
Figure 2.4 Typical particulate and tar loadings in biomass gasifiers (Baker et al. 1986)..... 15
Figure 2.5 Tar sampling system setup (Kinoshita et al., 1994) 16
Figure 2.6 The normalized EPA method for collecting particulates from combustion stack gases (EPA 1983) 18
Figure 2.7 Detectable components typical presented in producer gas with Xenon PID lamp (BTG, 2008)..... 19
Figure 3.1 The downdraft gasifier system and its DC motor..... 27
Figure 3.2 Schematic of the downdraft fixed-bed gasifier 28
Figure 3.3 Circuit of the rectifier box 29
Figure 3.4 The rectifier box 29
Figure 3.5 AD 595 for Type-K Thermocouple conditioning (single power supply)..... 30
Figure 3.6 Printed Circuit Board (PCB) for Thermocouple signal conditioning..... 31
Figure 3.7 Thermocouple signal conditioning and data processing 32
Figure 3.8 Actual thermocouple arrangement inside the gasifier. 32
Figure 3.9 Maximum flow air heater (Omega Engineering) 33
Figure 3.10 Pressure transducer connection and data processing..... 34
Figure 3.11 Theoretical flow nozzle installation 35

Figure 3.12 Actual flow nozzle installation 35
Figure 3.13 Schematic of tar sampling system 38
Figure 3.14 The NALGENE in-line filter holder installation 39
Figure 3.15 The tar sampling device 39
Figure 3.16 Tar analysis 40
Figure 4.1 Biomass feedstock samples (left to right: woodchips, corncobs, and DDGS) 43
Figure 4.2 Tar samples (left, solutions; right, dried) 45
Figure 4.3 Syngas composition analysis using a SRI 8610s GC 46
Figure 4.4 PeakSimple for GC data analysis 46
Figure 4.5 Temperature profile inside the gasifier for woodchips gasification 48
Figure 4.6 Temperature profile of woodchips gasification after the starting run 49
Figure 4.7 Temperature profile of corncobs gasification after the starting run 50
Figure 4.8 Temperature profile of DDGS gasification after the starting run 51
Figure 4.9 Pressure drop measurement through the gasifier system 52
Figure 4.10 Pressure drop comparison at different locations through the gasifier system (power input = 120 V) 53
Figure 4.11 Pressure drop comparison at different power inputs (voltages) 55
Figure 4.12 Pressure drop at different locations across the gasifier system 58
Figure 4.13 Pressure drop at outlet II for woodchips gasification 59
Figure 4.14 Pressure drop at outlet II for corncobs gasification 60
Figure 4.15 Pressure drop at outlet II for DDGS gasification 60
Figure 4.16 Energy efficiency for woodchips gasification 63

List of Tables

Table 1.1 Biomass feedstock availability in Kansas 2
Table 2.1 Chemical components in biomass tars (Milne and Evans, 1998) 12
Table 2.2 Tar classification (Sousa, 2001; Podgórska, 2006) 14
Table 3.1 Gasifier system specification 27
Table 3.2 Thermocouples setup inside the gasifier 33
Table 4.1 Total carbon contents of three biomass samples 43
Table 4.2 DDGS properties (average values) 44
Table 4.3 Intake air temperature (ambient air temperature = 4 °C) 45
Table 4.4 Pressure drop across the flow nozzle and syngas flow rate 61
Table 4.5 Syngas composition 61
Table 4.6 Tar concentration 62
Table 4.7 Calorific values (MJ/Nm^3) for syngas components (IEA, 2001) 63
Table 6.1 Output voltage vs. thermocouple temperature at ambient +25 °C (adapted from AD595 specification, Analog Devices) 75
Table 6.2 DDGS gasification 76
Table 6.3 Corncobs gasification 77
Table 6.4 Woodchips gasification 78
Table 6.5 Pressure drop comparison (unit: inch of water) 79
Table 6.6 Test and analysis log for gasification experiment 80
Table 6.7 DDGS properties (data provided by Land O'Lakes Purina Feed) 81
Table 6.8 The relative heating value of wood as a function of moisture content 83
Table 6.9 Calculation of flow rate 85
Table 6.10 Calculation of syngas density 86
Table 6.11 Calculation of energy efficiency 87
Table 6.12 Gasification energy efficiency for woodchips 87

Acknowledgements

First of all, I would like to express my greatest appreciation to my major professor, Dr. Wenqiao Yuan, for his academic guidance and support through my two-year graduate study, and for his sharing wisdom with me both in research and life. Two years of communication makes me better understand the importance of time management, the meaning of commitment to research, and the way how I need to carry them out.

I also want to thank all the professors who served as my committee members, Drs. Kirby Chapman, Keith Hohn, and Donghai Wang. Thanks for taking time reviewing my thesis and the valuable comments. Especially, I own my many thanks to Dr. Hohn for his allowing me to use the gas chromatograph equipment in his lab, and Dr. Wang for his sharing his laboratory facilities. All these made my project go on more smoothly and convenient.

Mr. John Hany from Land O'Lakes Purina Feed shall receive my sincere thanks. I felt grateful for his providing the distillers' dried grains with solubles (DDGS) sample and sharing property data of that.

Gratefulness goes to Mr. Darrell Oard for his always ready for help. He has always been my role model as a great engineer. Also, I need to mention Ms. Barb Moore and Ms. Edna Razote. Barb is always there since the first date I was admitted to this department. Thanks to Edna's advice on gas sampling which made that part of my project easier.

Thank all the department mates, especially my group members in Yuan's Lab. It's been good memories for the days we shared.

Last but not least, my family – my parents, my grandmother, and my sister. They deserve my heartfelt thanks. Without them, nothing can be made possible.

CHAPTER 1 - Introduction

The history of gasification dates back to the seventeenth century. Since the conception of the idea, gasification has passed through several phases of development. During the 1840s, the first commercially used gasifier, which was an updraft style, was built and installed in France. Gasifiers were then developed for different fuels and industrial power and heat applications (Quaak et al., 1999). The 1970s brought a renewed interest in the technology for power generation at small scales due to oil crisis (Stassen and Knoef, 1993). Since then, fuels other than wood and charcoal have been applied as feedstock materials.

As a century old technology, gasification flourished quite well before and during World War II. Gasifiers were largely used to power vehicles during that period. Many of the gasoline and diesel driven vehicles during that period were converted to producer gas driven. The technology was discontinued soon after World War II, when liquid fuel became easily available. Today, because of increased fuel prices and environmental concerns, there is a renewed interest in this century old technology. The use of downdraft gasifiers fueled with wood or charcoal to power cars, lorries, buses, trains, boats and ships have already proved their worth (Turare, 2002). Gasification has become a more modern and quite sophisticated technology.

Biomass is a complex mixture of organic compounds and polymers (Graboski and Bain, 1979). The major types of compounds are lignin and carbohydrates (cellulose and hemicellulose) whose ratios and resulting properties are species dependent. Lignin, the cementing agent for cellulose, is a complex polymer of phenylpropane units. Cellulose is a polymer formed from glucose; the hemicellulose polymer is based on hexose and pentose sugars. Basically, biomass includes wood, crop residues, solid waste, animal wastes, sewage, and waste from food processing, etc. Agricultural wastes such as cotton stalks, saw dust, nutshells, coconut husks, rice husks and forestry residues - bark, branches and trunk can be used as feedstock. Theoretically, almost all kinds of biomass materials with moisture content less than 30% can be gasified, however, in reality not every biomass fuel can lead to successful gasification (Turare, 2002). Most of the development work is carried out with common fuels such as coal, charcoal and wood. The key to a successful design of gasifier is to understand the properties and thermal behavior of the fuel fed into the gasifier system. It was recognized that fuel properties such as

surface area, size, shape as well as moisture content, volatile matter and carbon content affect gasification performance (McKendry, 2002).

The state of Kansas has abundant biomass resources (Walsh, 1999). Biomass feedstock availability in the state is shown in Table 1.1. When delivered price is less than $40 per dry ton, agricultural residues account for the largest percentage of the cumulative biomass quantities in the state. Urban wood wastes and dedicated energy residues are also in rich availability. Other biomass materials, such as forest residues, and primary mill residues, are in relatively small amount. Generally, the cumulative quantities promise an adequate storage for biomass utilization in Kansas.

Table 1.1 Biomass feedstock availability in Kansas

Estimated Annual/Cumulative Biomass Quantities (dry ton/yr), by Delivered Price, KS				
	< $20/dry ton	< $30/dry ton	< $40/dry ton	< $50/dry ton
Forest Residues	-	47,000	68,000	88,100
Primary Mill Residues	1,000	9,000	20,000	-
Agricultural Residues	-	0	8,570,003	8,570,003
Dedicated Energy Residues	-	0	2,859,261	11,438,271
Urban Wood Wastes	736,289	1,227,148	1,227,148	1,227,148
Cumulative Biomass Quantities	737,289	1,283,148	12,733,412	21,343,522

Note:

1. Estimates of biomass quantities potentially available in five general categories: forest residues, mill residues, agricultural residues, urban wood wastes, and dedicated energy crops.

2. Availabilities are sorted by anticipated delivered price (harvesting, transportation).

3. Quantities are cumulative quantities at each price (i.e., quantities at $50/dt include all quantities available at $40/dt plus quantities available between $40 and $50/dt).

1.1 Gasification Process

The essence of a gasification process is the conversion of solid carbon fuels into carbon monoxide and hydrogen by a complex thermochemical process, as shown in the general formula below.

$$\textit{Biomass} + O_2 \textit{ (or } H_2O) \rightarrow CO,\ CO_2,\ H_2O,\ H_2,\ CH_4 + \textit{other hydrocarbons}$$
$$\rightarrow \textit{tar} + \textit{char} + \textit{ash}$$
$$\rightarrow HCN + NH_3 + HCl + H_2S + \textit{other sulfur gases}$$

Splitting of a gasifier into strictly separate zones is not realistic, but it is conceptually essential. Generally, there are four zones in a gasifier, the drying, pyrolysis, combustion and reduction zones, as illustrated in Figure 1.1 (illustrated in a downdraft model).

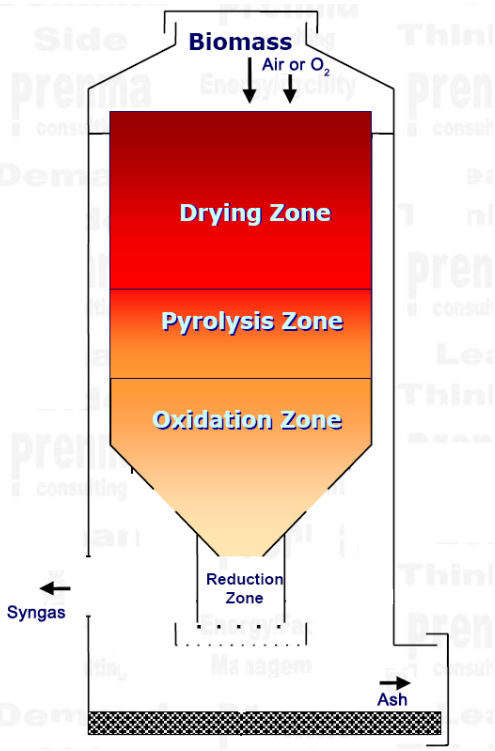

Figure 1.1 Reaction zones in a downdraft gasifier

Drying

At temperatures above 100 °C, water (moisture content within the biomass) is removed and converted into steam. In the drying zone, fuels do not experience any kind of decomposition.

Pyrolysis

Biomass is pyrolyzed under conditions being free from air, namely destructive distillation or thermal decomposition of biomass. The products of biomass pyrolysis have three states: solid charcoal, liquid wood tar and pyroligneous liquor, and combustible gas. Pyrolyzing at different temperatures may produce products with different contents. The higher the temperature is, the greater the amount of combustible gas and liquids, and the less the amount of solid charcoal. The reaction is influenced by the chemical composition of biomass fuels and the operating conditions. Charcoal obtained from pyrolysis zone is further reacted in the reduction zone to yield syngas. Tar and pyroligneous liquor produced in pyrolysis is a liquid containing more than 200 components, like acetic acid, methanol, acetic aldehyde, acetone, ethyl acetate, etc. These pyrolysis products can be further reacted in the subsequent reaction zones as well. It is noted that no matter how a gasifier is built, there will always be a low temperature zone where pyrolysis takes place, generating condensable hydrocarbons (Turare, 2002).

Oxidation/combustion

Introduced air in the oxidation zone contains, besides oxygen and water vapors, inert gases such as nitrogen and argon. These inert gases are considered to be non-reactive with fuel constituents. The oxidation takes place at the temperature of 700-2000 ◦C. Heterogeneous reaction takes place between oxygen in the air and solid carbonized fuel, producing carbon monoxide. (Note: Plus (+) and minus (-) signs indicate the release and supply of heat energy during the process, respectively.)

$C + O_2 \rightarrow CO_2 + 406$ [MJ/kmol]

Hydrogen in the fuel reacts with oxygen in the air blast, producing steam.

$2H + ½O_2 \rightarrow H_2O + 242$ [MJ/kmol]

Reduction

In the reduction zone, several high temperature chemical reactions take place in the absence of oxygen. The principal reactions that take place in the reduction zone are described below.

Boudouard reaction:

$CO_2 + C \rightarrow 2CO - 172.6$ [MJ/kmol]

Water-gas reaction:

$C + H_2O \rightarrow CO + H_2 - 131.4$ [MJ/kmol]

Water shift reaction:

$CO_2 + H_2 \rightarrow CO + H_2O + 41.2$ [MJ/kmol]

Methane production reaction:

$C + 2H_2 \rightarrow CH_4 + 75$ [MJ/kmol]

The main reactions show that heat is required during the reduction process. Hence, the temperature of gas goes down during this stage. If a complete gasification takes place, all the carbon is burned or reduced to carbon monoxide and some other mineral matter are vaporized. The remaining are ash and some char (unburned carbon).

The synthesis gas (syngas) or producer gas is the mixture of combustible and non-combustible gases. The quantity of gas constituents depends upon the types of fuels and operating conditions. Typical producer gas constituents are shown in Figure 1.2. The heating value of producer gas usually varies from 4.5 to 6 MJ/m^3 (standard conditions) depending upon the quantity of its constituents (Natarajan et. al, 1998). Carbon monoxide is produced from the

reduction of carbon dioxide and its quantity varies from 15 to 30% by volume basis. Hydrogen is also a useful product of the reduction process in the gasifier, which is 10 to 20%. Methane, carbon monoxide, and hydrogen are responsible for higher heating value of the producer gas. The amount of methane present in the producer gas is very small. Carbon dioxide and nitrogen are non-combustible gases in the producer gas. Compared to other gas constituents, nitrogen presents the highest amount (45 to 60%) in the producer gas. Water vapors in the producer gas occur due to moisture content of air introduced during oxidation process, injection of steam or moisture content of biomass fuels.

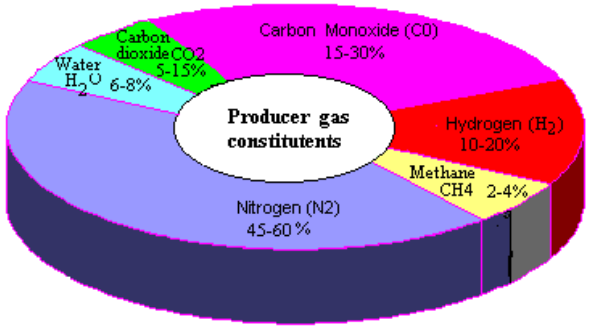

Figure 1.2 Syngas yields from gasification process (Turare, 2002)

1.2 Classification of Gasifiers

A gasifier consists of usually cylindrical chamber with spaces for fuel, air inlet, gas exit, and grate. It can be made of firebricks, steel, concrete and oil barrels, etc. A complete gasification system consists of a gasification chamber, purification unit and energy converter – a burner or internal combustion engine. Based on the design of gasifiers and types of fuels used, there exists different kinds of gasifiers. Portable gasifiers are mostly used for running vehicles. Stationary gasifiers combined with engines are widely used in rural areas of developing countries for many purposes including cooking, heating, generation of electricity and running irrigation pumps, and so on. The most commonly built gasifiers are classified as:

1.2.1 Updraft

The schematic of an updraft gasifier is shown in Figure 1.3. An updraft gasifier has clearly defined zones for partial combustion, reduction, and pyrolysis. Air is introduced at the

bottom and acts as countercurrent to fuel flow. The gas is drawn at a higher location (close to the top). Updraft gasifiers achieve the highest efficiency as the hot gas passes through the fuel bed and leaves the gasifier at low temperatures. The sensible heat given by the gas is used to preheat and dry the fuel. Updraft gasifiers can be easily designed and installed. They are thermally efficient because the ascending gases pyrolyze and dry the incoming biomass, transferring heat so that the exiting gases leave very cool. Disadvantages of updraft gas producer are excessive amount of tar in raw gas (which is due to insufficient heat for cracking the tars) and poor loading capability since the syngas is also exiting close to the site where biomass is loaded.

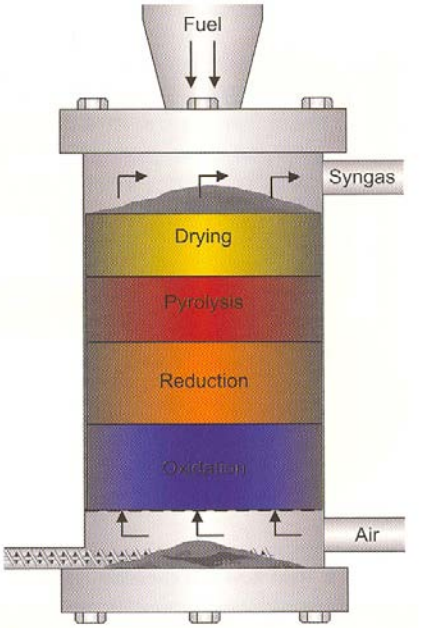

Figure 1.3 Updraft fixed-bed gasifier (Knoef, 2005)

1.2.2 Downdraft

The schematic of a downdraft gasifier is shown in Figure 1.4. In the updraft gasifier, gas leaves the gasifier with high tar concentration that may seriously affect the operation of downstream applications such as internal combustion engines. This problem is minimized in downdraft gasifier, of which air is introduced into downward flowing packed bed or solid fuels and gas is drawn off at the bottom. Tars in the raw gas can be cracked or broken down in the heat reaction zones (i.e., oxidation and reduction) to shorter non-condensable hydrocarbons and partially converted to syngas. A lower overall efficiency is a common problem in small downdraft gasifiers because of the heat 'wasted' for cracking tars and other heat loss in the gasification process. Since this type of gasifier has strict requirements on biomass properties

(i.e., particles sized between 1 and 30 cm, low ash content, and moisture less than 30%), it has difficulties in handling higher moisture and ash content fuels. The time needed to ignite and bring plant to working temperature with good gas quality is shorter than updraft gas producer.

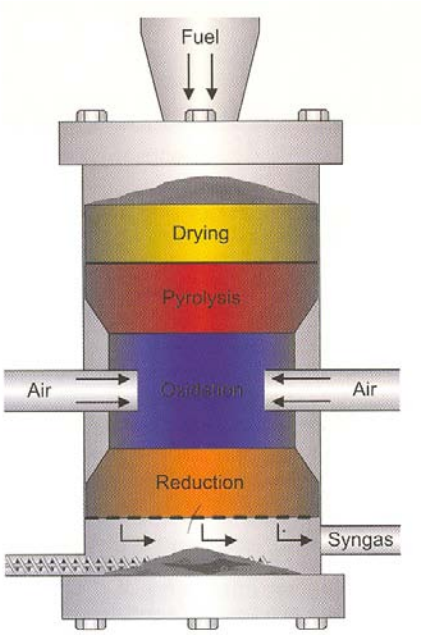

Figure 1.4 Downdraft fixed-bed gasifier (Knoef, 2005)

1.2.3 Fluidized Bed

The schematics of fluidized bed gasifiers are shown in Figure 1.5. The operation of the fixed bed gasifier demands a high fuel quality, particularly a homogenous piece size. Fluidized bed type gasifiers are more flexible in terms of operation, fuel, scale and the use of gasification agents. Inert bed material is used (e.g. silica sand) to achieve homogenous conditions and rapid heat transfer in the fluidized bed. Fluidized bed technique enables long operation periods and continuous ash removal and bed material renewal. The operation temperature is limited by the ash (and bed material) sintering temperature below 900 °C. Because tar content depends on operation temperature, a medium tar and particle laden gas is produced.

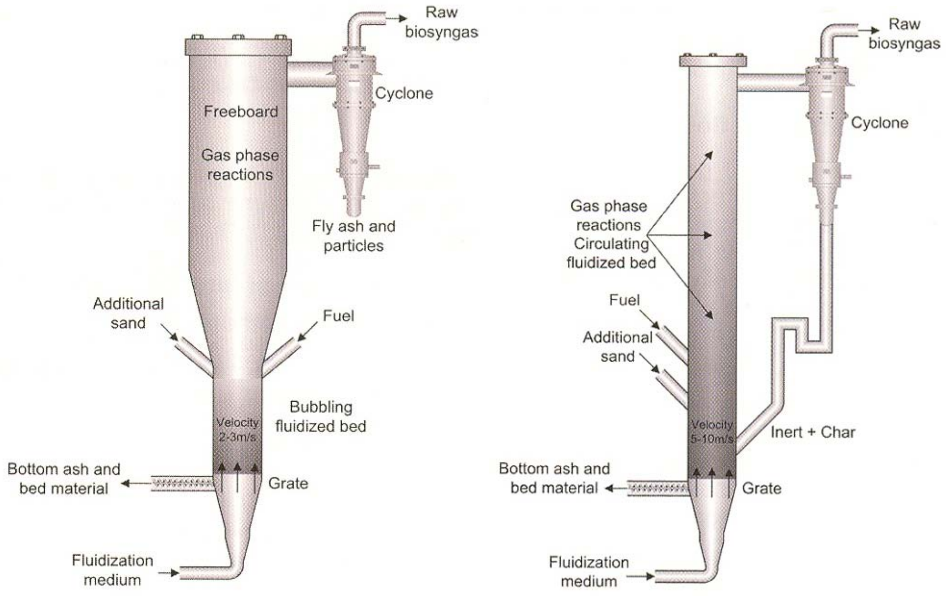

Figure 1.5 Fluidized bed gasifiers: bubbling (left) and circulating (right) (Knoef, 2005)

1.2.4 Entrained Flow

The schematic of an entrained flow gasifier is shown in Figure 1.6. Entrained flow gasifier needs pulverized fuel and is operated above the ash melting point (>1000 °C). Ash is removed as liquid phase and due to the high temperature tar content is very low. Two types of entrained flow gasifiers can be distinguished: slagging and non-slagging. In a slagging gasifier, the ash forming components melt in the gasifier, flow down the walls of the reactor and finally leave the reactor as a liquid slag. Generally, the slag mass flow should be at least 6% of the fuel flow to ensure proper operation. In a non-slagging gasifier, the walls are kept free of slag. This type of gasifier is suitable for fuels with only little ash.

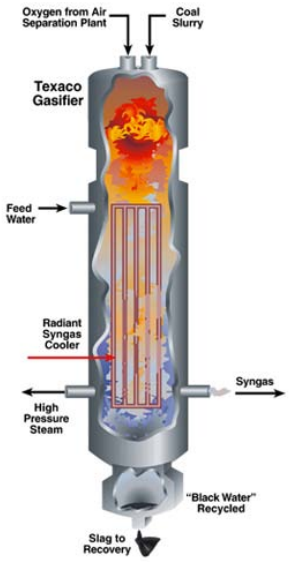

Figure 1.6 Texaco entrained flow gasifier (NETL online resource, www.netl.doe.gov)

1.2.5 Choren Process

The Choren Company was founded in 1990 by staff of the former East German Deutsche Brennstoffinstitut with the objective of developing a commercial biomass gasification process as a basis for manufacturing transport fuels. Choren addresses the tar issue of biomass gasification by using a three-stage process (Figure 1.7) (Blades et al., 2005). In the first stage, the biomass is continually carbonized through partial oxidation (low temperature pyrolysis) with air or oxygen at temperatures between 400 and 500 °C. The pyrolysis gas and char are extracted separately. The pyrolsis gas is then subjected to high-temperature gasification in the second stage. During the second stage of the process, the gas containing tar is post-oxidized hypostoichiometrically using air and/or oxygen in a combustion chamber operating above the melting point of the fuel's ash to turn it into a hot gasification medium. During the third stage of the process, the char is ground down into pulverized fuel and is blown into the hot gasification medium. The pulverized fuel and the gasification medium react endothermically in the gasification reactor and are converted into a raw synthesis gas. The Choren process is said to be capable of gasifying a wide range of feed materials to produce high-quality gas with low tar content and low emission levels. The capital cost for system construction and operation tend to be higher than other gasifiers.

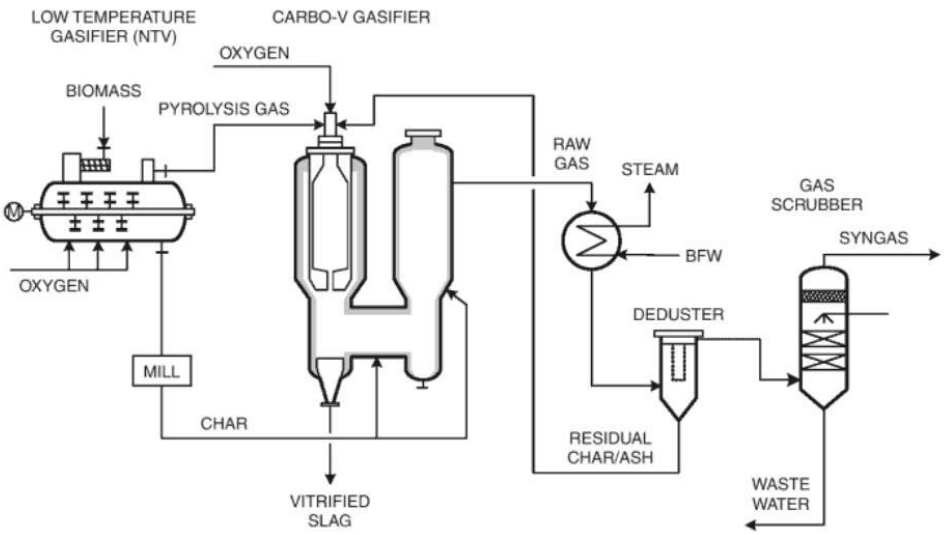

Figure 1.7 Choren process (Choren, 2007)

1.3 Objectives

To utilize the abundant biomass resources in Kansas, we developed a unique downdraft gasifier system for low bulk density biomass materials. The core part of the system is a gasifier reaction chamber. There is a purification system followed the gasifier. It is consist of a water-cooling system and a filter chamber with charcoal. As a part for testing of the syngas, a burner is connected to the purification system.

The overall purpose of this research was to design and construct two systems for the downdraft gasifier: an instrumentation system and a tar measurement system. The specific objectives of the research project were to:

- Fabricate an instrumentation system to study the temperature profile inside the gasifier, the pressure drop, and the gas flow rate, so as to observe the physical gasification conditions.
- Construct a tar measurement system to determine the tar concentration in the syngas.
- Evaluate the performance of the systems, in terms of syngas composition, tar concentration, and energy efficiency, by gasifying three different kinds of biomass materials - wood chips, corncobs, and Distiller‘s Dried Grains with Solubles (DDGS).

CHAPTER 2 - Literature Review

2.1 Biomass Tar Formation

2.1.1 Tar Components

At an IEA gasification task meeting, it was stated that all organics boiling at temperatures above that of benzene should be considered as tar (Brussels, 1988). Generally, biomass tar is referred to condensable organics in the syngas produced in the gasification process of biomass, and it is assumed to be largely aromatics (Milne and Evans, 1998). Using molecular beam mass spectrometry (MBMS) suggests a systematic approach to classifying pyrolysis products as primary, secondary, and tertiary (Evans and Milne, 1987) (Figure 2.1). The primary and tertiary products are mutually exclusive, that is, the primary products are destroyed before the tertiary products appear. A commonly used tar maturation scheme, proposed by Elliott (1988), who reviewed the composition of biomass pyrolysis products and gasifier tar from various conversion processes, is shown in Figure 2.2. The scheme shows the tar maturation process as a function of temperature. It indicates the transition as a function of process temperature from primary products to phenolic compounds to aromatic hydrocarbons. Table 2.1 indicates the classes of chemical compounds based on GC/MS analysis of collected “tars” (Milne and Evans, 1998). From this table, tar components varying as temperatures increase is distinguished in each major regime.

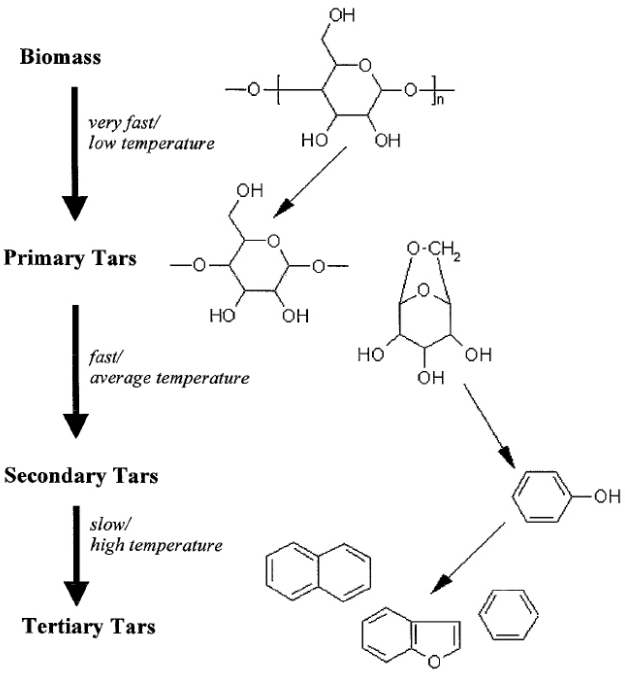

Figure 2.1 Biomass tar formation (Evans and Milne, 1987)

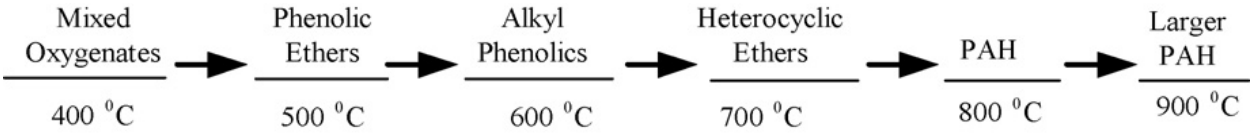

Figure 2.2 Tar maturation scheme (Elliott, 1988)

Table 2.1 Chemical components in biomass tars (Milne and Evans, 1998)

Conventional Flash Pyrolysis (450–500 °C)	High-Temperature Flash Pyrolysis (600–650 °C)	Conventional Steam Gasification (700–800 °C)	High-Temperature Steam Gasification (900–1000 °C)
Acids	Benzenes	Naphthalenes	Naphthalene*
Aldehydes	Phenols	Acenaphthylenes	Acenaphthylene
Ketones	Catechols	Fluorenes	Phenanthrene
Furans	Naphthalenes	Phenanthrenes	Fluoranthene
Alcohols	Biphenyls	Benzaldehydes	Pyrene
Complex Oxygenates	Phenanthrenes	Phenols	Acephenanthrylene
Phenols	Benzofurans	Naphthofurans	Benzanthracenes
Guaiacols	Benzaldehydes	Benzanthracenes	Benzopyrenes
Syringols			226 MW PAHs
Complex Phenols			276 MW PAHs

From previous research results, it is indicated that temperature is an important factor affecting tar composition (Baker et al., 1988; Kinoshita et al., 1994; Li et al., 2004; Qin et al., 2007) showed a conceptual relationship between the yield of tars and the reaction temperature, shown in Figure 2.3. They cited levels of tar for various reactors with updraft gasifiers having 12 wt% of wood and downdraft less than 1%. For oxygen-blown fluid beds, the levels of tar were

4.3% at 750 °C and 1.5% at 810 °C. An ideal assumption is that tars are thermally cracked to CO, H_2, and other light gases with temperature. This is true with primary product cracking, and yields of 50% by weight of CO are possible by thermal cracking. However, it is not true for the condensed tertiary products, which grow in molecular weight with reaction severity. As a result, many researchers have conducted various experiments to remove tars from biomass gasification process with increasing operating temperature. The decision to run a gasification system at high severity to crack tars, however, should be balanced by a consideration of the remaining tars composition. The dilemma is that, high temperatures favor greater efficiency and rates but also lead to a more refractory nature of the tar (Milne and Evans, 1998).

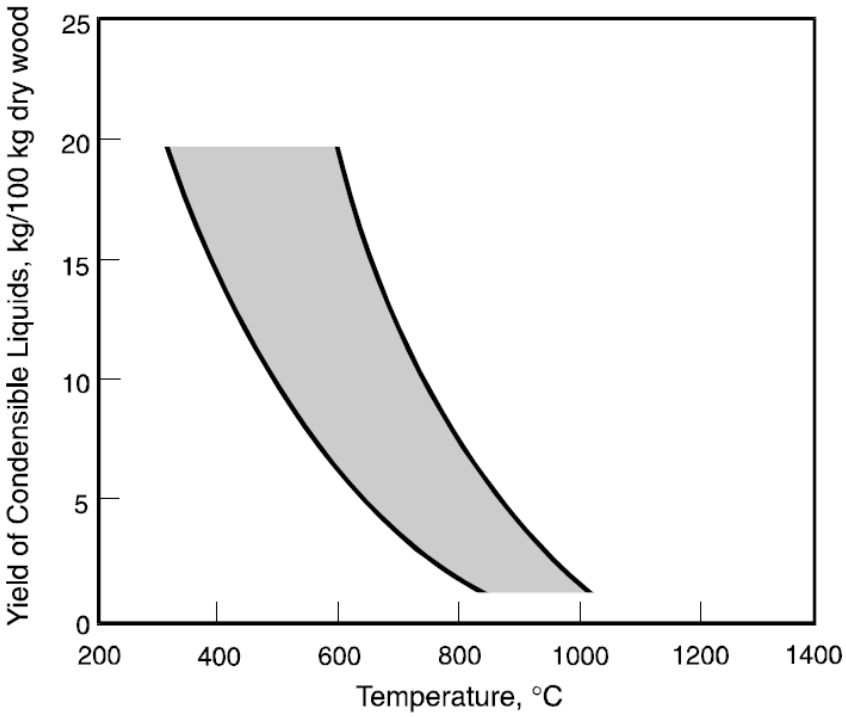

Figure 2.3 Tar yield as a function of the maximum temperature exposure

Base on the molecular weight of tar compounds, a popular classification of tar is shown in Table 2.2 (Sousa, 2001; Podgórska, 2006). They divided tar components into five groups, and each group has its specific property and representative compounds.

Table 2.2 Tar classification (Sousa, 2001; Podgórska, 2006)

Tar class	Class name	Property	Representative compounds
1	GC-undetectable	Very heavy tars, cannot be detected by GC	Determined by subtracting the GC-detectable tar fraction from the total gravimetric tar
2	Heterocyclic aromatics	Tars containing hetero atoms; highly water soluble compounds	Pyridine, phenol, cresols, quinoline, isoquinoline, dibenzophenol
3	Light aromatic (1 ring)	Usually light hydrocarbons with single ring; do not pose a problem regarding condensability and solubility	Toluene, ethylbenzene, xylenes, styrene
4	Light PAH compounds (2–3 rings)	2 and 3 rings compounds; condense at low temperature even at very low concentration	Indene, naphthalene, methylnaphthalene, biphenyl, acenaphthalene, fluorene, phenanthrene, anthracene
5	Heavy PAH compounds (4–7 rings)	Larger than 3-ring, these components condense at high-temperatures at low concentrations	Fluoranthene, pyrene, chrysene, perylene, coronene

Note: GC - gas chromatograph, PAH - polyraromatic hydrocarbon

2.1.2 Tar Yield as a Function of Gasifier Type

The amount of tar is a function of the temperature/time history of the particles and gas, the feed particle size distribution, the gaseous atmosphere, and the method of tar extraction and analysis. Each type of gasifier has its unique operation and reaction conditions, which results in different tar composition and yield. Figure 2.4 presents typical tar (note: tar refers to compounds boiling higher than at 150 °C) and particulate loadings generated in biomass gasifier as reported by Brown et al. (1986). As a general conclusion, it has been proven and explained scientifically and technically that updraft gasifiers produce more tars than fluidized beds and fluidized beds more than downdrafts (Milne and Evans, 1998). In updraft gasifiers, the tar nature is buffered somewhat by the endothermic pyrolysis in the fresh feed from which the tars primarily arise. In downdraft gasifiers the severity of final tar cracking is high, due to the conditions used to achieve a significant degree of char gasification. Tar loading in raw syngas from updraft gasifiers has an average value of about 100 g/Nm^3, fluidized bed and CFBs have an average tar loading of about 10 g/Nm^3, downdraft gasifiers produce the cleanest syngas with tar loading typically less than 1 g/Nm^3. Baker et al. (1986) also concluded very similar research results, which stated a very general tar level in respect to different gasifier types. It is also established that well-functioning updraft gasifiers produce a largely primary tar, with some degree of secondary character; downdraft gasfiers mostly produce tertiary tar, and fluidized beds produce a mixture of secondary and tertiary tars. Entrained flow gasifiers produce very low level of tar due to the high temperatures, possible mainly tertiary tar if exists.

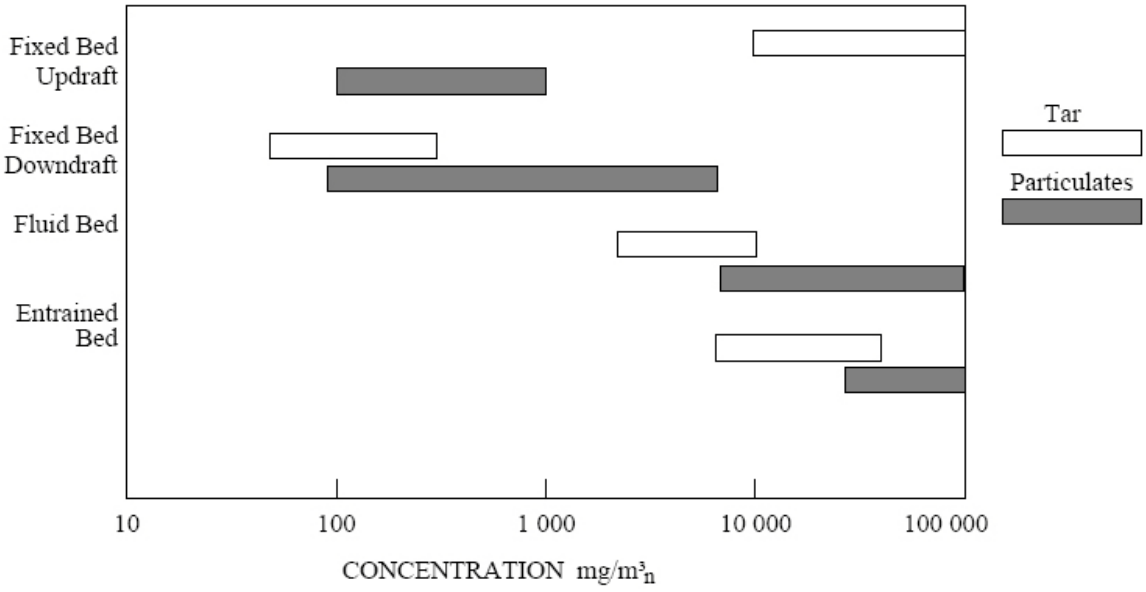

Figure 2.4 Typical particulate and tar loadings in biomass gasifiers (Baker et al. 1986)

Many publications reported the quantities of tar produced by various types of gasifiers, under various geometries and operating conditions (Abatzoglou et al. 1997a; Bangala 1997; CRE Group, Ltd. 1997; Graham and Bain 1993; Hasler et al. 1997; Mukunda et al. 1994a, b; Nieminen et al. 1996). Tars reported in raw gases for various types of gasifiers is a bewildering array of values, in each case (updraft, downdraft, and fluidized-bed) spanning two orders of magnitude. Three of many reasons for this have no relation to the gasifier performance, but are a result of the different definitions of tar being used, the circumstances of the sampling, and the treatment of the condensed organics before analysis.

2.1.3 Tar Formation under Different Biomass Gasification Conditions

Baker et al. (1988) showed a conceptual relationship between the yield of tars and the reaction temperature. Li et al. (2004) ran biomass gasification in a circulating fluidized bed, of which tar yield was measured by in-line tar sampling using a sampling train simplified from the tar protocol (Knoef, 2000). The experimental data indicated that the tar concentration primarily depended on the operating temperature. Researchers from the Hawaii Natural Energy Institute studied how gasification conditions affecting tar formation using a bench-scale indirectly-heated fluidized bed gasfier (Kinoshita et al., 1994). Three parameters were tested, including temperature, equivalence ratio, and residence time. Tar samples were collected by a GC with a flame ionization detector, using a capillary column. Under all conditions tested, tar yield in the

product gas ranged from 15 to 65 g/kg biomass, tar concentration ranged from 15 to 86 g/Nm^3, and benzene and naphthalene were the dominant species under most conditions, ranging from 22 to 58% and 4 to 16% of total tars, respectively. Temperature and equivalence ratio have significant effects on tar yield and tar composition. Lower temperatures favor the formation of more aromatic tar species with diversified substituent groups, while higher temperatures favor the formation of fewer aromatic tar species without substituent groups. Their tar sampling system setup is shown as follows (Figure 2.5). A sintered metal filter removed particulates, and the filter housing was maintained at 450 ^{o}C to prevent condensation of tars in the filter. A slip-stream of product gas went to the cooling section to condense tars. A water jacket was beyond the sintered metal filter to condense water vapor in the hot gas. The light fraction of the tars escaping the dry-ice condenser-trap was removed downstream by two solvent scrubbers connected in series. Methanol was the solvent used in these two scrubbers.

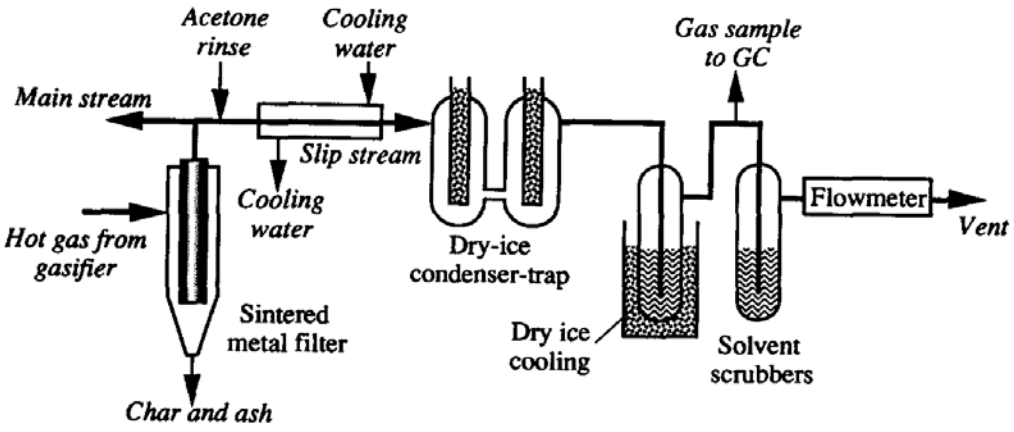

Figure 2.5 Tar sampling system setup (Kinoshita et al., 1994)

Qin et al. (2007) studied characterization of tar from sawdust gasified in the pressurized fluidized bed under different operating temperatures and pressures. For pressures of 0.5 to 2.0 MPa, the similar distributions indicated that the pressure had little effect on the molecular weight distribution of the sawdust air gasified tar under different experimental conditions. The structure of heavy compounds showed an increase of the aromatic character with the increase in pressure. The high pressure decreased the devolatilization rate and consequently enhanced the cracking reactions; the liable bonds could either be dissociated or spontaneously condensed into stable bonds.

2.2 Tar Measurement Methods

The sampling and analytical methods for tar characterization have varied from simple "color of the cotton wool" type of methods (Walawender et al. 1985) to sophisticated and complicated systems, by which different components from light oils to high-molecular-weight polycyclic aromatic hydrocarbon (PAH) components can be collected and analyzed (Brage et al., 1996). Both isokinetic and non-isokinetic sampling trains were employed in tar sampling. The commonly referred method is cold-trapping tar sampling. Apart from the popular cold trapping path, there are also several alternative tar measurement methods to date, like Solid Phase Absorption (SPA) method that was developed at KTH, Sweden (Brage et al., 1996), a solvent-free method proposed by researchers from Iowa State University (Xu et al., 2005), a molecular-beam mass spectrometer method (Daniel et al., 2007) and an optical measurement system based on laser spectroscopy developed by German scientists (Karellas et al., 2007). On top of that, researchers at the University of Stuttgart developed a quasi continuous tar quantification method (Moersch et al., 1998). Sricharoenchaikul et al. (2002) studied formation of tars during black liquor gasification conducted in a laboratory-scale laminar entrained-flow reactor (LEFR), of which condensable organic and tar compounds were collected with a three-stage scrubber (Sricharoenchaikul et al., 2002). The lack of a standard method of tar sampling has led to a variety of tar collection methods, and this has created problems in comparing results from different studies. Acetone, methylene chloride, dichloromethane, methanol, toluene, and water have all been widely used as solvents to condense and collect tar. Non-solvent methods, such as condensing tar on cotton or fiberglass filters, have also been employed (Donnot et al., 1985; Stobbe et al., 1996). A large variety of sampling and analysis methods have been developed to determine the tar concentration in biomass-derived producer gas (Haser et al., 1998; Moersch et al., 1997), which makes the comparison of operating data among researchers and manufacturers very difficult. In this review, we will briefly discuss these different sampling technologies, including measurement setup and apparatus used.

2.2.1 Cold Trapping Method

Most tests are based on condensation in a liquid or adsorption on a solid material. Subsequently, the collected samples are analyzed gravimetrically or by means of a GC. EPA Method 5 (EPA, 1983) for sampling particulate emissions from flue gas is the basis for most

gasifer sampling trains, as shown in Figure 2.6. This method was originally designed for sampling particulate emissions from combustion flue gases. It was also used to collect gas and organic liquid samples from stack gases. Modifications have been necessary because of the higher tar and particulate loadings of gasifier streams. Collected liquids (or, solution) can be analyzed by high-performance liquid chromatography with UV fluorescence spectroscopy (Desilets et al., 1984; Corella et al., 1991), size-exclusion chromatography-UV (Adegoroye et al., 1991), gas chromatography-flame ionization detection (GC-FID) (Brage et al., 1991; Kinoshita et al., 1994; Blanco et al., 1992), and gas chromatography-mass spectroscopy (GC-MS) (Bodalo et al., 1994; Padkel and Roy, 1991; Blanco et al., 1991).

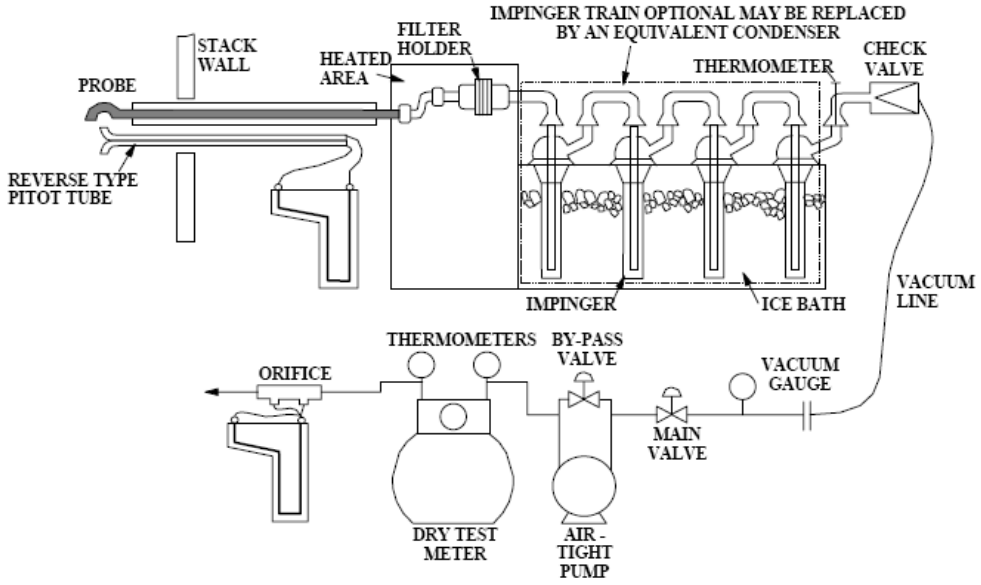

Figure 2.6 The normalized EPA method for collecting particulates from combustion stack gases (EPA 1983)

For isokinetic sampling systems, common elements for measuring the amount of tar and particulate are a heated filter (glass fiber, cellulose, quartz-fiber, ceramic) for trapping the dust particles and a condenser for trapping the tar. A general problem of this type of sampling is that some of the particles collected by the sample filter may have been in gaseous form in the product gas (BTG, 1995). In addition, some heaviest tar compounds condense on the sample filter and some create soot particles in the sampling probe. Moreover, some of the heaviest tar compounds are insoluble in certain solvents or seem to polymerize on the filter paper to form insoluble soot particles. No clear solution to overcome this problem. Soot forming reactions are probably

enhanced by the high temperature, so sampling at lower temperature is recommended. The work of ETSU/DTI included sampling from different gasifiers (CRE Group, 1997). Authors of that work undertook as comprehensive as possible identification of tars from various gasifiers. Fresh sample analysis is recommended to ensure representability of the tar present during the gasification process. There are a large number of notes on sampling and analysis from the literature, which presents the diversity of sampling and analysis methods that have been used. A later project regarding tar sampling and analysis methods has been conducted in BTG ever since early 2008. They compared offline and online (Online tar analysis based on Photo-ionisation, shown in Figure 2.7) measurement methods. The selectivity of tar compounds was illustrated in this figure assuming Xenon was used as gas corresponding to an energy equivalent of 8.4 eV. All components having an Ionization Potential (IP) below 8.4 eV would be detected; components having a higher IP would not be detected. The components in the orange area were most likely detected.

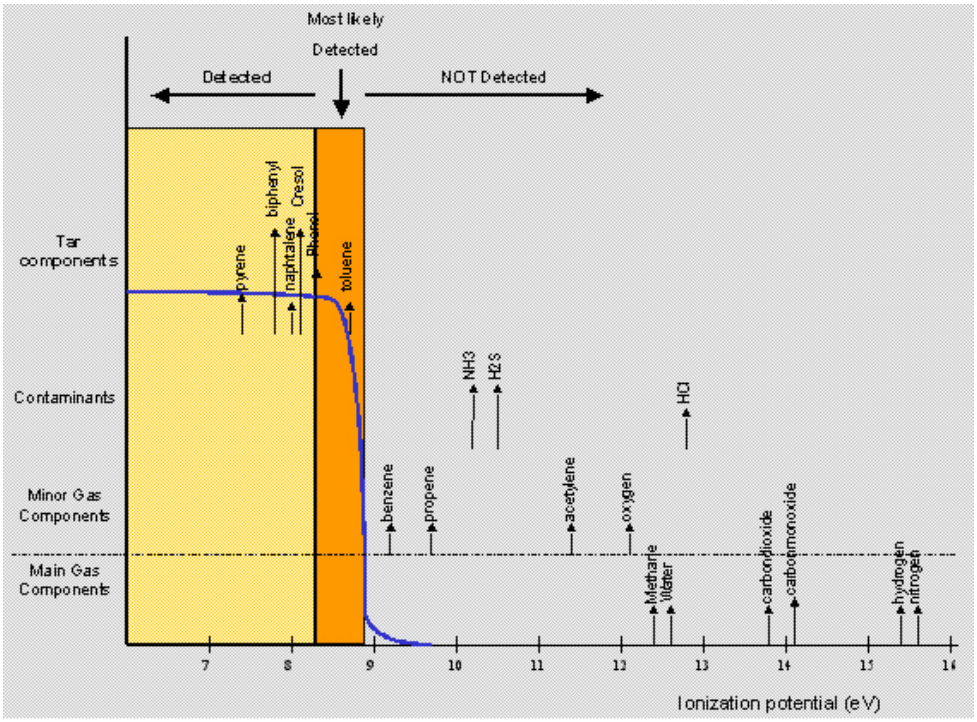

Figure 2.7 Detectable components typical presented in producer gas with Xenon PID lamp (BTG, 2008)

2.2.2 Solid-Phase Adsorption (SPA) Method

The solid-phase adsorption (SPA) method is chosen to analyze individual tar compounds ranging from benzene to coronene, which was originally developed by Royal Institute of Technology at Sweden (KTH). A gas sample is sucked through an amino-phase sorbent collecting all tar compounds, then, by using different solvents the aromatic and phenolic compounds are collected separately and analyzed using a GC. Specifically, in this method 100mL of gas is withdrawn from a sampling line using a syringe or pump for each sample, of which the sampling line operating temperature is maintained stable at 250-300 °C to minimize tar condensation. The aromatic fraction is extracted using dichloromethane, and the solution is analyzed by GC-MS. Afterwards, a second phenolic fraction is eluted using 1:1 (volume ratio) dichloromethane/acetonitrile. Within this method, a nonpolar capillary column is applied, focusing on the analysis of mostly non-polar fluidized-bed tars. Given its limits, this method is applied to measurement of class 2-5 tars (see Table 2.2), which could be fast, simple and reliable (Osipovs, 2008). The limit of this method lies in, with a high benzene concentration in biomass tar, some of the benzene are not collected. An improved system added one more adsorbent cartridge loaded with another sorbent, activated coconut charcoal, which is widely used for adsorption of volatile organic compounds (including benzene), to the older system. Dufour et al. (2007) compared the SPA method with the traditional cold trapping method, both methods are based on GC-MS analysis, when they measured the wood pyrolysis tar, of which they employed multibed solid-phase adsorbent tubes followed by thermal desorption (SPA/TD) (Dufour et al., 2007). This new application and comparison proved that SPA/TD is more accurate than impingers especially for light PAHs.

2.2.3 Molecular Beam Mass Spectrometer (MBMS) Method

Evans and Milne (1987) applied molecular-beam, mass spectrometric (MBMS) sampling method to the elucidation of the molecular pathways in the fast pyrolysis of wood and its principal isolated constituents. In a follow-up research paper, they also presented the analysis of effluents from gasification and combustion systems, and found out a full range of products from the major classes of primary, secondary, and tertiary reactions (Evans and Milne, 1987). Dayton et al. (1995) from NREL demonstrated the application of MBMS technology to the study of alkali metal speciation and release during switchgrass combustion. Most recently, researchers

from the same lab, NREL, used the same technology to measure gasifier tar concentrations in a model compound study and during actual biomass gasification, and results were compared to the traditional method of impinger sampling (Carpenter et al., 2007). A brief description of the design and operation of MBMS is introduced as follows.

A molecular beam forms as the sampled gases/vapors are drawn through a 300 μm diameter orifice into the first stage of a three-stage, differentially pumped vacuum system. This free-jet expansion results in an abrupt transition to collisionless flow that quenches chemical reactions and inhibits condensation by rapidly decreasing the internal energy of the sampled gases. The result is that the analyte is preserved in its original state, allowing light gases to be sampled simultaneously with heavier, condensable, and reactive species. The central core of this expansion is extracted with a conical skimmer, located at the entrance of the second stage, and the molecular beam continues into the third stage of the vacuum system. There, components of the molecular beam are ionized using low-energy electron ionization before passing through the mass analyzer. From NREL research experience, 22.5 eV allows for sufficient ionization efficiency while minimizing fragmentation of larger molecules (Carpenter et al., 2007). The ions are detected with an off-axis electron multiplier, and spectra are generated from the measured signal intensity as a function of the ion molecular weight. The mass range of interest (up to m/z (mass-to-charge ratio) 750 with this system) is repeatedly scanned so that the time-resolved behavior of the system under study can be observed. Because the sample is introduced continuously by this technique, quantitative measurement of organic and inorganic constituents in the gasifier process stream can potentially be done once per second. The MBMS system is equipped with several integrated controls that facilitate sampling of a variety of chemical process streams. On-board temperature, pressure, and flow control is achieved with I/O control system interfaced with a PC. Mass flow controllers allow inert gases to be introduced for sample dilution and internal standards. Liquid standards are injected using two high-pressure liquid chromatography (HPLC) pumps. Data from each of these auxiliary channels are collected for subsequent quantitative analysis. The MBMS enables real-time, continuous monitoring over a large dynamic range [10^{-6}–10^{2}% (v/v)]. It can be used to sample directly from harsh environments, including high-temperature, wet, and particulate-laden gas streams. One limitation of the MBMS is that there is no pre-separation of the observed peaks. Although fragmentation is minimized by using low-energy ionizing electrons (22.5 eV), isomers cannot be distinguished,

making it difficult to interpret the mass spectra. Complementary analysis, such as impinger sampling, can be important for initial peak identification.

2.2.4 Solvent-free Method

Researchers from Iowa State University designed a so-called dry condenser method (Xu et al., 2005). It condenses heavy tars (organic compounds with boiling points greater than about 105 °C. Benzene is not treated as a constituent of heavy tar in this context, since its boiling point is only 80 °C) in a disposable tube and a fiberglass mat. By operating above the boiling point of water, the heavy tar is not contaminated with moisture. A simple gravimetric analysis of the tube and fiberglass mat allows the mass of heavy tars to be determined.

The measurement system consists of a heated thimble particulate filter, a dry condenser constructed from a household pressure cooker, a chilled bottle to condense water and possibly some light hydrocarbons, a vacuum pump, and a dry gas meter. The dry condenser consists of a 6-m coil of Santoprene tubing and a fiberglass-filled stainless steel canister installed inside the pressure cooker. The removable lid of the pressure cooker is pierced by compression fittings to admit gas flow to and from the pressure cooker. Gas entering the pressure cooker flows serially through the Santoprene tubing and the stainless steel canister before exiting the pressure cooker. Before sealing the pressure cooker, it is filled with sufficient distilled or deionized water to submerge the Santoprene tubing and most of the canister. The pressure cooker is placed on an electric hot plate adjusted to sufficient power to boil water within the pressure cooker. The pressure cock on the cooker is adjusted to boil water at 105 °C, which prevents water vapor in the sampled producer gas from condensing inside the Santoprene tubing and on the fiberglass. Gas exiting the pressure cooker flows through an impinger bottle submerged in an ice bath for the purpose of removing water (and possibly some light hydrocarbons) from the gas before it flows through the vacuum pump. A dry gas meter is used to measure total gas flow through the dry condenser. The pressure and temperature just ahead of the gas meter is recorded periodically throughout the testing run. Determination of tar is accomplished by measuring the weight change of the Santoprene tubing and the fiberglass-packed canister before and after a test. When gas sampling is completed, the Santoprene tubing and fiberglass-filled canister are immediately removed from the pressure cooker and the outer surfaces wiped dry. The ends of the Santoprene tubing are sealed, and the tubing is placed in an oven at 105 °C for 1 h, after which its weight

change is determined while the canister was immediately weighed. Tar concentration in the producer gas is calculated by dividing the total weight gain in the tubing and canister by the total dry gas volume that passed through the dry condenser.

2.2.5 Quasi Continuous Tar Quantification Method

Researchers from University of Stuttgart developed a tar quantification method that allows quasi continuous on-line measurement of the content of condensable hydrocarbons in the gas from biomass gasification, which makes continuous on-line monitoring possible (Moersch et al., 2000). The method is based on the comparison of the total hydrocarbon content of the hot gas and that of the gas with all tars removed. Hydrocarbons are measured with a flame ionization detector (FID, with high sensitivity and linearity). Tar contents between 200 and 20000 mg/m^3 have been measured reliably.

The basic idea of this tar measurement method lies in the comparison of two measurements. In the first measurement, the total content of hydrocarbons in the gas is determined. Subsequently all tars are removed by condensation on a filter and a second measurement is performed to determine the amount of the non-condensable hydrocarbons. The difference of these two measurements yields the amount of condensable hydrocarbons or tars. Due to some drawbacks of the measurement system, like influence of the fluctuations of syngas composition and very small difference of the two measurements when tar contents are too low, an improved setup was also proposed. Two sample loops are set in the new system, which guarantees the reference volume for both flows is identical. Both loops are loaded with samples contemporaneously to remove the fluctuations of the gas concentration. The gas from loop one is flushed to the FID to determine the total hydrocarbons, while gas from loop two is led to a filter adsorbing all condensable substances and then passes to the FID yielding the content of non-condensable hydrocarbons. Analysis time is two minutes with this method (Moersch et al., 2000).

2.2.6 Laser Spectroscopy Method

Researchers from Technische Universität Miinchen in Germany developed a technology for allothermal gasifier producing hydrogen-rich, high-calorific syngas (Karellas and Karl, 2007). An optical measurement system based on laser spectroscopy was applied to measure the basic composition of the product gas and the content of tars in the syngas.

Raman spectroscopy has also been used for the analysis of gases. It has been used in various applications for the investigation of combustion technique (Bombach, 2002). The quantum theoretical explanation of the Raman effect is: when the incident light quantum hν1 collides with a molecule, it can be scattered either elastically, in which case its energy, and therefore its frequency, remains unscattered (Rayleigh scattering), or it can be scattered in an inelastic way (Raman scattering), in which case it either gives up part of its energy to the scattering system (anti-Stokes scattering) or takes energy from it (Stokes scattering) (Bombach, 2002). The Raman scattering is termed rotational or vibrational depending on the nature of the energy exchange that occurs between the incident light quanta and the molecules (Herzberg, 1967; Long, 1977). In TUM's project, an industrial neodium-doped yttrium garnet (Nd:YAG) laser (Lightwave Electronics) has been used as light source. They used pure gases, and mixed gases with defined composition for laser system calibration. After measuring the already mixed gases, they compared the measuring values with already known ones to prove the success of the calibration process. For the laser spectroscopy method, tars are higher hydrocarbons that emit a strong fluorescence signal in a wide wavelength range (Bombach, 2002). This signal is detected as background signal in the profiles when measuring the hot product gas by means of Raman spectroscopy. With the use of numerical method the background of the signal is approximated and the area underneath the background profile gives information about the tar content. Different sampling lines were setup in the measurement system, of which one tar sampling line was conducted based on IEA method (described as "standardized tar protocol" in the project). The standardized tar protocol was applied parallel to the laser measurement in order to find the correlation between the intensity of the optical background signal and tar content. This optical method could be used to investigate the tar content of the product gas.

2.3 Summary

From MBMS study, pyrolysis tar is classified as primary, secondary, and tertiary products. It is also indicated that tar concentration primarily depends on the operating temperature. The amount of tar is a function of the temperature/time history of the particles and gas, the feed particle size distribution, the gaseous atmosphere, and the method of tar extraction and analysis. Each type of gasifier has its unique operation and reaction conditions, which results in different tar composition and yield. A general agreement about the relative order of magnitude

of tar production is updraft gasifiers being the dirtiest, downdraft the cleanest, and fluidized beds intermediate.

The sampling and analytical methods for tar characterization have varied from simple to very complicated systems. To date, there are two main sampling methods applied in this field. One method is commonly referred to as cold-trapping tar sampling, and the other Solid Phase Absorption (SPA) method. In addition, researchers all over the world have developed various approaches, like the solvent-free method proposed by researchers from Iowa State University, the molecular-beam mass spectrometer method and the optical measurement system based on laser spectroscopy developed by German scientists.

The lack of a standard method of tar sampling has led to a variety of tar collection methods, and this has created problems in comparing results from different studies. In this review, we discussed these different sampling and analysis technologies. There is no one single method fitting every aspects of measuring requirement, so none is perfect.

CHAPTER 3 - Instrumentation and Tar Measurement Systems

3.1 Instrumentation system

Temperature profile inside the gasifier and pressure drop through the system are proven to be critical parameters in gasification study. High temperatures are indicators of better carbon conversion rate, therefore better gasification performance. Pressure drop is closely related to the fluid flow rate through the gasifier system. Therefore, design and construction of instrumentation systems is important for a well-monitored gasification process. Accurate measurement of these data would also provide better control of the system so as to optimize the gasification performance. Temperature and pressure data are also useful for validation of computational modeling of gasifiers. For the downdraft gasifier system studied in this project, we designed and built an AC to DC power transmitter for the blower, a temperature measurement system, a pressure drop measurement device, and a gas flow rate measurement device.

3.1.1 Introduction to the Gasifier Unit

The gasifier, which is shown in Figure 3.1, has an overall syngas production rate of 2.8-5.6 cfm when coupled with the burner provided. The gasifier system power output is 7-9 HP. A blower is used to introduce air into the reaction chamber, and syngas output is pumped under the power of the blower. The pressure of the blower is 1.2 kPa. Power supply for this blower is 80W, 120 VDC (specification shown in Table 3.1). A schematic drawing of the gasifier system is shown in Figure 3.2. The complete system includes a gasifier chamber, a purification system, and a burner. Both biomass and gasification medium are introduced through the top, while syngas exits at the bottom. Through the purification system, the syngas is partially cleaned, and is burned out after that (except for the part that is collected as samples for analysis).

Figure 3.1 The downdraft gasifier system and its DC motor

Table 3.1 Gasifier system specification

Syngas output	2.9-5.8 cfm
Power output	7-9 HP
Pressure	1200 Pa
Power	80 W
Electric power supply	120 VDC

Applications –

From experimental test, this unit can be applied to gasify woodchips easily. Low bulk density biomass materials, like DDGS and corn stover may be used as feedstock. The producer gas can be directly burned to supply heat for family or farm use. After careful gas conditioning and treatment, producer gas from this gasifier can be supplied to the internal combustible engine for testing, or it may be used as a source for other downstream applications.

Pros and Cons –

After setting the unit on a skid, it became portable and convenient for use. Its capability of utilizing various biomass materials indicated the potential uses in local farms or families where they have a large amount of agricultural residues.

Tar formation is problematic and may result in operating troubles for the gasifier system. The accumulated tar within the gasifier can block the pipes or other channels in the gasifier, which will cause inconvenient syngas production and even some mechanical issues. Regular cleanup of tars is recommended for this gasifier system. Syngas conditioning is critical if further

application of syngas is in consideration, which is technically requiring time and skills. Waste water is also treated as another environmental problem generated from this unit.

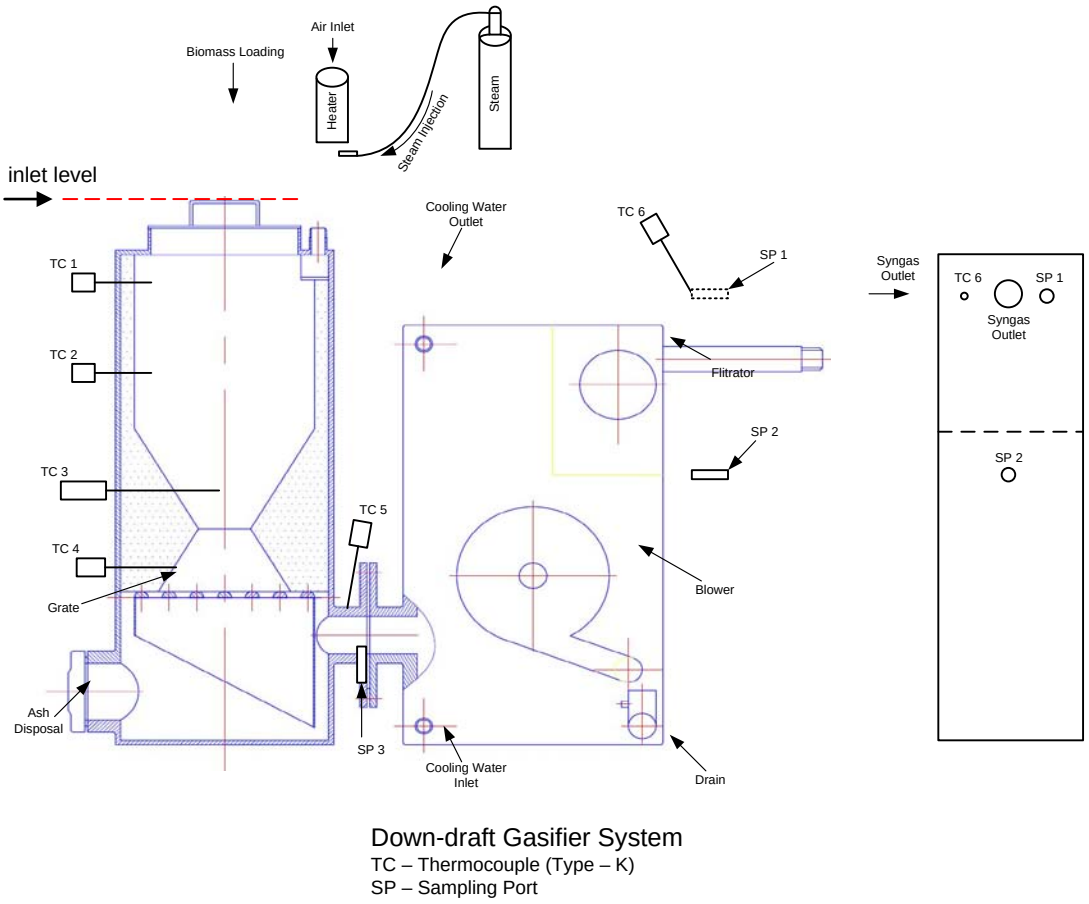

Figure 3.2 Schematic of the downdraft fixed-bed gasifier

3.1.2 DC Power for the Blower (AC to DC Converter)

The intake air is sucked in by a blower. Since the blower is driven by a DC motor, the wall power (120 VAC) needs to be converted to 120 VDC power. Based on the principle of full-wave rectifier circuit, a rectifier box was constructed to convert AC to DC in order to power the blower (Figures 3.3 and 3.4). The rectifier selected permitted a maximum current of 5 amp. A 5 amp fuse was used to protect the circuit.

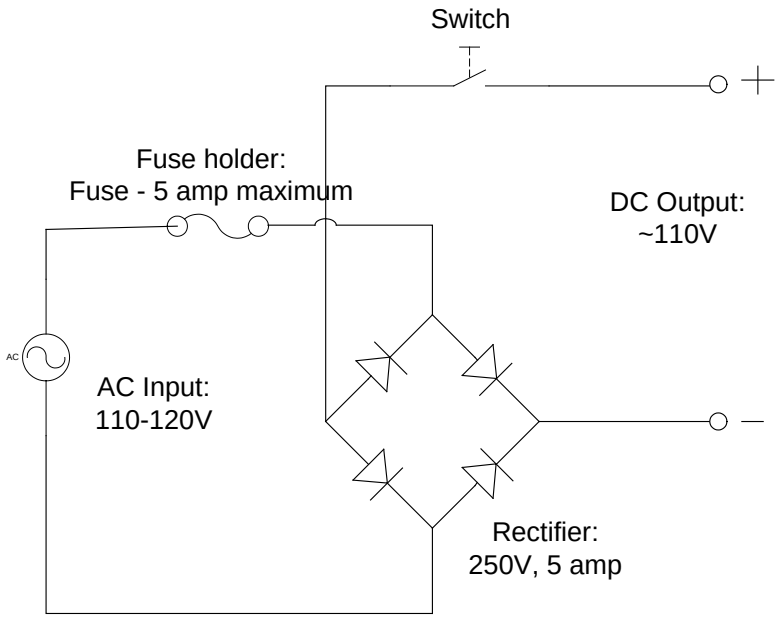

Figure 3.3 Circuit of the rectifier box

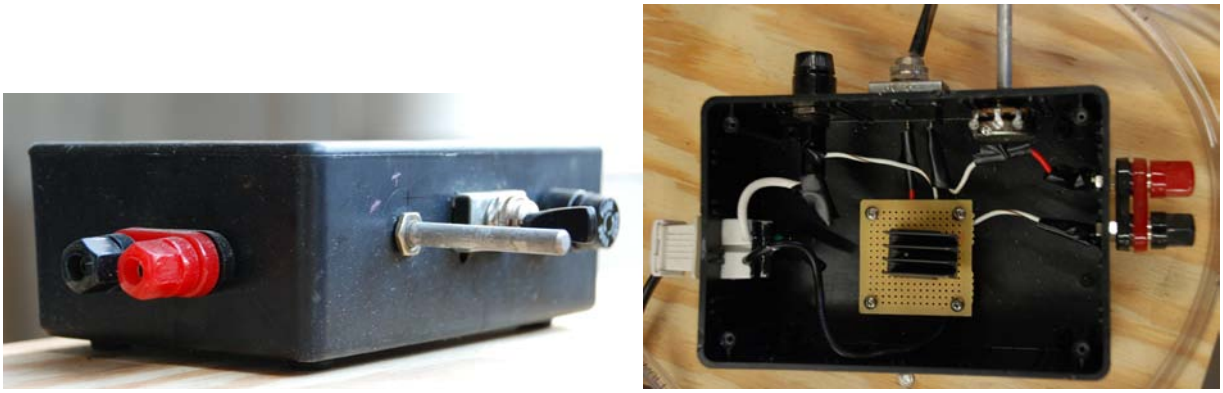

Figure 3.4 The rectifier box

Materials used to construct the rectifier box included a fuse holder (5 amp maximum), switch, rectifier (250 V, 5 amp), heat sink, project enclosure, and flexible banana plugs. As shown in Figure 3.4, the side with banana plugs is DC power output, and the opposite side accepts the AC power. With the help of a 5 amp variable voltage transformer (All Electronics Inc), the power input could be adjusted, which affected the DC motor to drive the blower. Therefore, air blown could be adjusted accordingly in the gasifier system.

3.1.3 Temperature Measurement

Given the high temperature inside the gasifier, we utilized Chromel-Alumel type K thermocouples (standard limits of error: ±2.2 °C or 0.75%, whichever is greater; specific limits of error: ±1.1 °C or 0.4%, whichever is greater) (Omega Engineering) to accomplish the measurement. It is low cost and, owing to its popularity, it is available in a wide variety of probes (grounded junctions were chosen in this project). Type K thermocouples are available in the -200 °C to +1200 °C range. Sensitivity is approximately 41 uV/°C. A thermocouple signal-conditioning device was also designed and tested. Two main integrated chips (ICs), AD 595 (Analog Devices) and TS 921 (STMicroelectronics), were employed to fabricate the device. The temperature calibration chart was provided with AD595 specification (Appendix B).

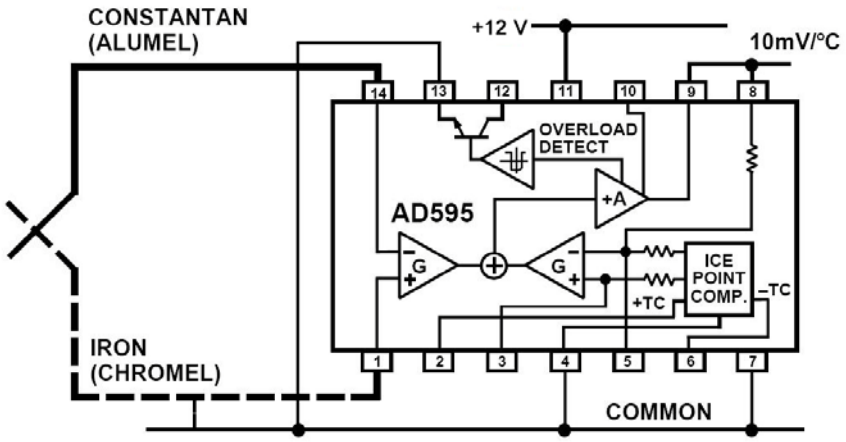

Figure 3.5 AD 595 for Type-K Thermocouple conditioning (single power supply)

The AD595 is a completely self-contained thermocouple conditioner. It is a complete instrumentation amplifier and thermocouple cold junction compensator on a monolithic chip. It combines an ice point reference with a pre-calibrated amplifier to produce a high level (10 mV/°C) output directly from a thermocouple signal. Pin-strapping options allow it to be used as a linear amplifier-compensator or as a switched output setpoint controller using either fixed or remote setpoint control. It can be used to amplify its compensation voltage directly, thereby converting it to a stand-alone Celsius transducer with a low impedance voltage output. The AD 595 is laser trimmed for type K (chromel-alumel) inputs. The temperature transducer voltages and gain control resistors are available at the package pins so that the circuit can be recalibrated

for the thermocouple types by the addition of two or three resistors. These terminals also allow more precise calibration for both thermocouple and thermometer applications.

Using a single +12 V supply, the interconnections shown in Figure 3.5 provided a direct output from a type K thermocouple (AD 595) measuring from 0 °C to +1200 °C. Any convenient supply voltage from +5 V to +30 V may be used, with self-heating errors being minimized at lower supply levels. In the single supply configuration, the +12 V supply connects to Pin 11 with the V– connection at Pin 7 strapped to power and signal common at Pin 4. The thermocouple wire inputs were connected to Pins 1 and 14 either directly from the measuring point or through intervening connections of similar thermocouple wire type. The alarm output at Pin 13 was not used but connected to common or –V. The pre-calibrated feedback network at Pin 8 was tied to the output at Pin 9 to provide a 10 mV/°C nominal temperature transfer characteristic.

The TS921 is a RAIL TO RAIL single BiCMOS operational amplifier with low noise and low distortion. Since the output voltage from AD 595 could not be detected by the data acquisition system, the TS921 was applied as a signal delivery (buffer) using a negative feedback which would simply follow the input voltage (from AD 595) with a stable gain of 1.

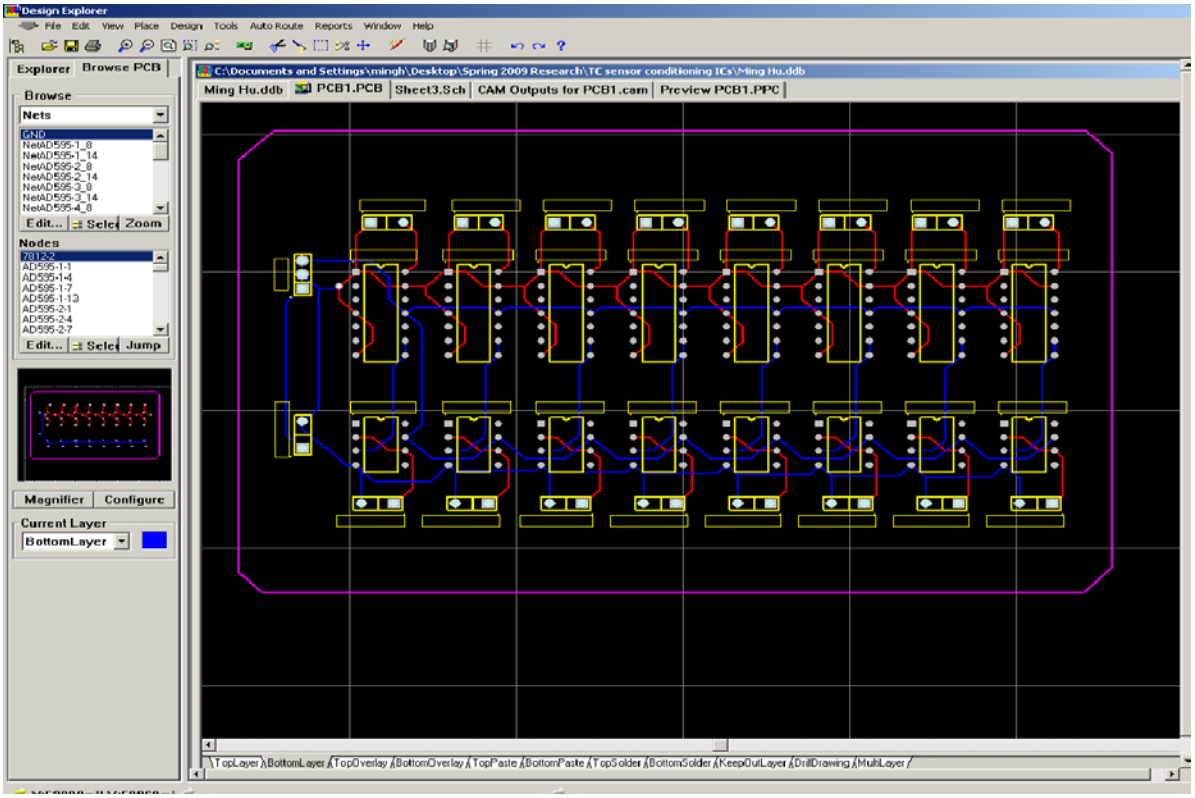

Figure 3.6 Printed Circuit Board (PCB) for Thermocouple signal conditioning

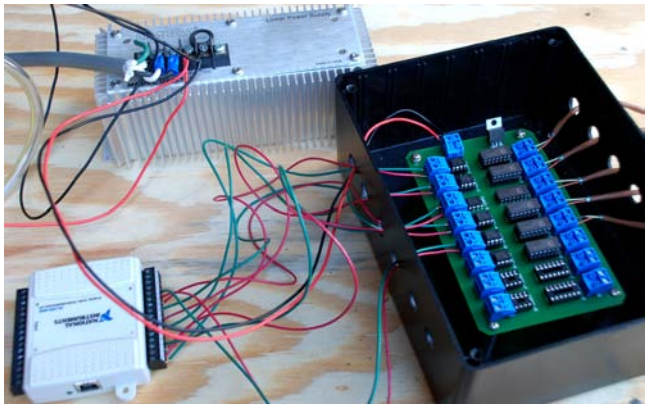

Figure 3.7 Thermocouple signal conditioning and data processing

As shown in Figure 3.6, Protel 99 SE was used to design the PCB board, which included 8 parallel type K thermocouple signal conditioning circuits. In Figure 3.7, it indicated the working condition of the temperature measurement device, which included a 24 VDC power supply (Omega Engineering Inc.), a NI USB-6008 data acquisition board, and the temperature measurement box. It is noted that a DC voltage regulator, LM 7812 (National Semiconductor Corporation), was used to convert the 24 VDC to 12 VDC so as to supply power for the ICs.

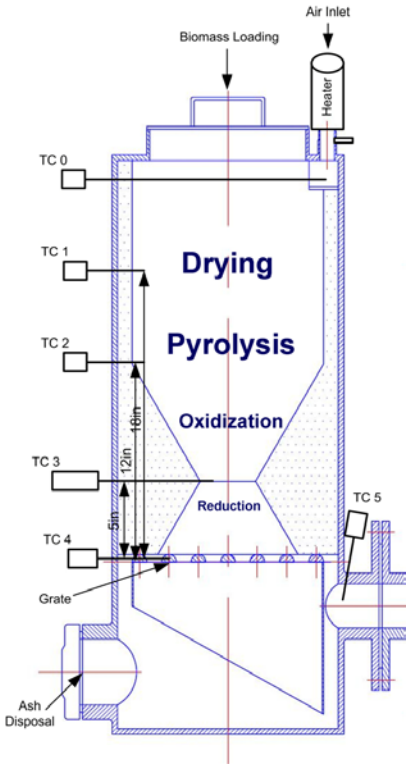

Figure 3.8 Actual thermocouple arrangement inside the gasifier.

In order to monitor the temperature profiles at different reaction zones inside the gasifier, a series of type K thermocouples were set to accomplish this task. Thermocouples were set along the gasifier wall in different locations, as shown in Figure 3.8. The first thermocouple was set to measure the intake air temperature. The intake air temperature was controlled by a high-flow-rate heater (Omega Engineering Inc.) which can be manually adjusted by power supply or air flow rate (Figure 3.9). This air heater was designed with a 60 mm (outsider diameter) aluminum tube and a cross frame heating element for minimum resistance to air flow. A 102 mm round flange with pre-drilled holes at the inlet side were used for mounting the heater. This heater had a practical operating range of up to 200 CFM with temperatures up to 315 °C.

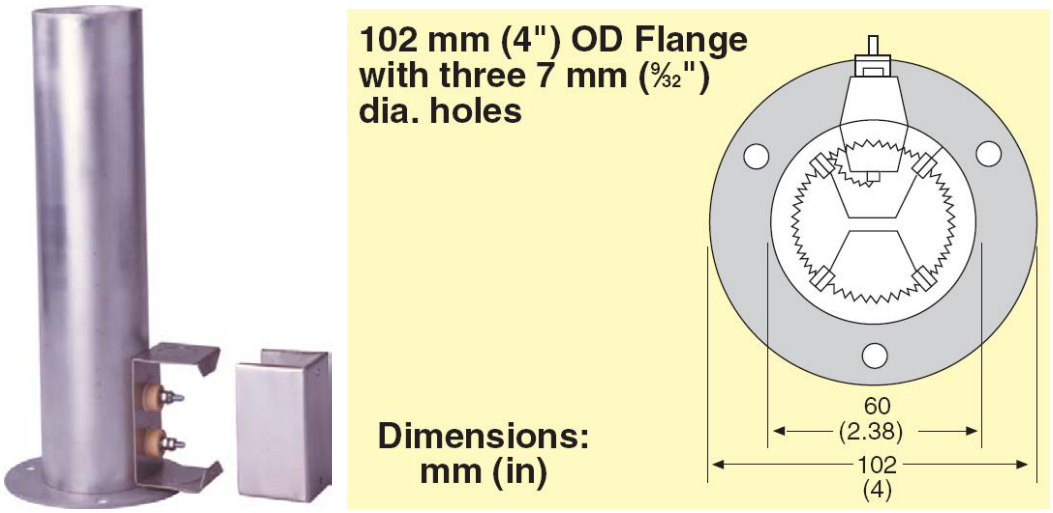

Figure 3.9 Maximum flow air heater (Omega Engineering)

As shown in Table 3.2, the other four thermocouples were set accordingly to a theoretical reaction zone distribution inside a typical downdraft gasifier (Knoef, 2005). They were placed at 18-inch, 12-inch, 5-inch, (all heights related to the grate), and the grate, to estimate temperatures at different reaction zones.

Table 3.2 Thermocouples setup inside the gasifier

Port	TC Code	Approximate reaction zone
Inlet	TC0	N/A
18 inches from the grate	TC1	Drying
12 inches from the grate	TC2	Pyrolysis
5 inches from the grate	TC3	Oxidation
The grate	TC4	Reduction
Exit	TC5	N/A

3.1.4 Pressure Drop and Flow Rate Measurement

In this study, a differential pressure transducer (type: PX274-30DI; accuracy: ±1.0% FS) (Omega Engineering Inc.) was applied to evaluate the pressure change across the gasifier, also that of the flow nozzle. The transducer was pre-calibrated by the manufacture. It was calibrated to deliver 4-20 mA corresponding to a pressure range of 0-30 inches of water, linearly. The USB 6008 board is set up to receive voltage. Therefore, a resistor across the input terminals of the instrumentation was installed to solve this problem. The value of the resistor was determined by Ohms law (V = IR). The connection of the pressure transducer to the data acquisition board was completed using a 470 ohm resistance in series with the transducer (Figure 3.11).

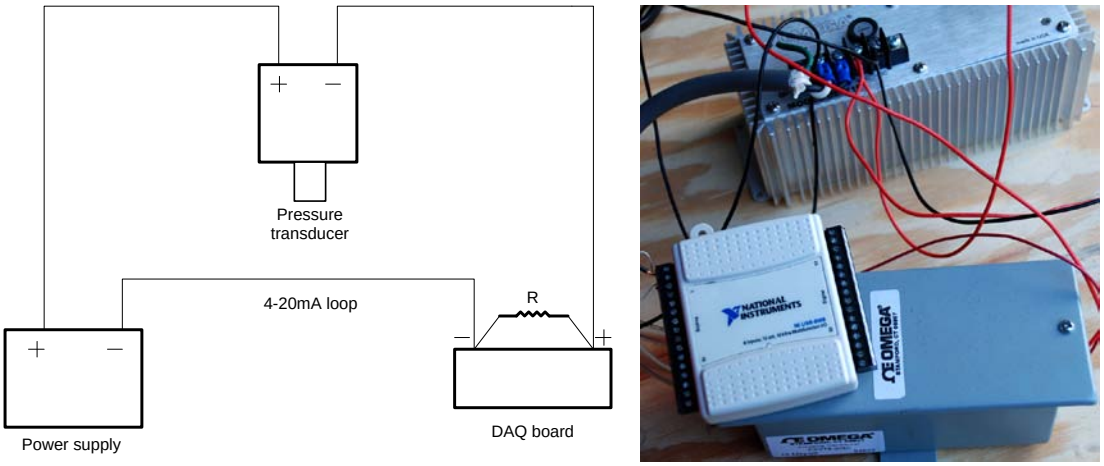

Figure 3.10 Pressure transducer connection and data processing

Measurement of fluid flows in pipes is commonly implemented using orifice, nozzle, and venturi. The air flow rate measurement using nozzle is proven to be precise, but proper installation is critical. Therefore, a flow nozzle (i.e., ISA1932 nozzle) with a throat diameter of 1 inch and straight PVC pipe of 2 in (Diameter Ratio, $\beta=d/D=0.5$) were chosen to accomplish this measurement. The part of the nozzle inside the pipe is circular. The nozzle consists of a convergent section, rounded profile, and a cylindrical throat. Design and manufacture of the flow nozzle are based on the standard and specification. Pressure taps were set 2 inches ahead of the nozzle and 1inch behind it, respectively (distances were based on the upstream face of the nozzle). The minimum upstream and downstream straight lengths were 6 inches and 5 inches, respectively. Construction was completed according to an ASME standard (ASME, 2004). As indicated in following figures, Figure 3.11 is the theoretical installation of flow nozzle, and Figure 3.12 shows the actual construction. For experimental operation, it was connected to the

syngas outlet so as to test the pressure drop between the two pressure taps, during the actual working condition.

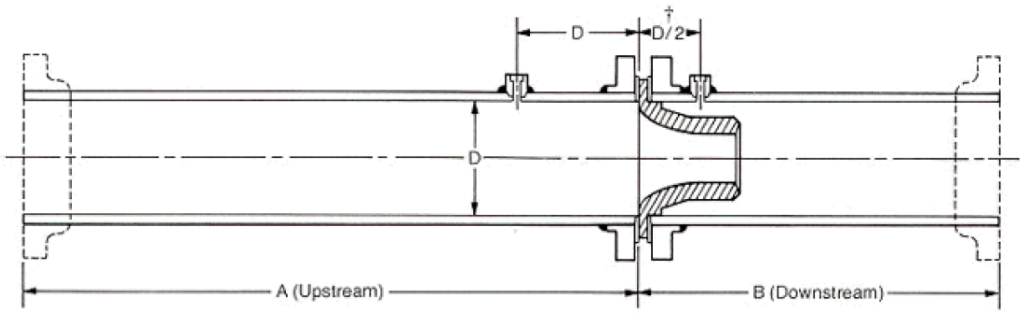

Figure 3.11 Theoretical flow nozzle installation

Figure 3.12 Actual flow nozzle installation

The mass flow rate (q_m) and volume flow rate (q_v) are related to the differential pressure, and both are computed by the following equation (*SI Units*) (ASME, 2004):

$$q_m = \frac{\varepsilon \pi d^2}{4} \frac{C\sqrt{2\Delta p \rho_1}}{\sqrt{1-\beta^4}}$$

$$q_v = \frac{q_m}{\rho}$$

$$C = 0.9900 - 0.2262\beta^{4.1} - (0.00175\beta^2 - 0.0033\beta^{4.15})(\frac{10^6}{R_D})^{1.15}$$

$$\varepsilon = \left\{ \left(\frac{\kappa \tau^{2/\kappa}}{\kappa - 1} \right) \left(\frac{1-\beta^4}{1-\beta^4 \tau^{2/\kappa}} \right) \left[\frac{1-\tau^{(\kappa-1)/\kappa}}{1-\tau} \right] \right\}^{0.5}$$

Where,

C is the discharge coefficient;

ε is the expansibility factor;

Δp is the differential pressure (p_1-p_2), p_1 refers to high pressure at upstream, and p_2 refers to low pressure at downstream (Pa);

ρ_1 is the density of the fluid at the upstream pressure tap (kg/m^3);

ρ is the fluid density at the temperature and pressure for which the volume is stated (kg/m^3);

β is the diameter ratio;

R_D is the Reynolds number referred to D;

τ is the pressure ratio (p_2/p_1);

κ is the isentropic exponent (its value depends on the nature of the gas).

Both values for C and ε can be looked up in the appendix forms at the ASME standard (ASME, 2004). Uncertainties of flow rate measurement includes three parts, that of discharge coefficient C (equals to ±0.8%), that of expansibility factor ε (equals to $\pm 2\Delta p/p_2\%$), and that of pressure loss Δw ($\Delta w = \frac{\sqrt{1-\beta^4(1-C^2)}-C\beta^2}{\sqrt{1-\beta^4(1-C^2)}+C\beta^2}\Delta p$).

Calculation of flow rate was completed in a 2003 Microsoft Excel spreadsheet (Table 6.9, Appendix I). The known parameters for flow rate calculation were d and β. In addition, ΔP and P_1 were measured using the differential pressure transducer under working conditions. The other unknowns needed to be estimated or computed as follows. Firstly, discharge coefficient and expansibility factor, C and ε, could be looked up in the tables of discharge coefficients and expansibility factors (Appendix J). From the pressure measurement, P_2/P_1 was 0.999 (therefore ε=1). A first guess of R_D was made in an iterative computation, and the corresponding C was obtained. Under the first guess, a tentative result of flow rate was obtained. Given this flow rate, the syngas velocity in the pipe was resulted; and given this velocity, the Reynolds number was computed. Compare this number with the guessed number. When they were closest to each other, it was treated as the final guess. The final value for C was 0.9758 (R_D =300,000).

Another parameter needed to be calculated to find flow rate was the syngas density at the temperature and pressure for which the volume was stated. The temperature at outlet II was measured using a thermocouple. It was 49 °C on average. Since pressure drop was very small compared to atmosphere pressure, the pressure at outlet II was treated as 1atm. Syngas density was computed based on the ideal gas law, as indicated in Table 6.10 (Appendix I). Gas density for each component was computed. The density for gas mixture was calculated based on the

percentage and density of each component. The syngas (of woodchips gasification) density at 49 °C, 1atm was 0.8679 kg/m^3.

3.2 Tar measurement system

The main impurities in the syngas of biomass gasification are tar and particulate. Effective and accurate measurement techniques allow determination of the efficiency of the syngas cleaning process and ensure the quality of the cleaned gas to be used in downstream applications, like engines or turbines.

As reviewed in Chapter 2, various sampling and analysis methods have been developed to determine tar concentration in syngas. This makes the comparison of operational data difficult and represents a significant barrier to further development. Compared to other methods, cold trapping method is relatively simple in principle. The system is inexpensive and easy to build. Therefore, this route was chosen as the model for design and construction.

In this study, a modified International Energy Agency (IEA) method was used to measure the tar and particulate concentration. The measurement principle is based on sampling of a gas stream containing tars and particulates driven by a vacuum pump. The test method is carried out in two steps: sampling and analysis.

3.2.1 Tar Measurement - Sampling

As shown in Figure 3.13, the sampling system consists of a filter holder containing fiber glass filter paper, a series of 6 sampling bottles (250 ml) containing acetone (100 ml each), and air flow meter. The sampling bottles were placed in the warm (40 °C ±1 °C, controlled by adding hot water if readings of the thermometer decrease) and cold bath (0 °C controlled by ice) to collect tars which were condensed in the solvent. The two different bathes were set for staged warming and cooling of the sampled gas. Syngas was sampled for a specific period (15 minutes) through the sampling line and filter. The sampling rate was constant, about 9-10 L/min, which was maintained with the aid of a vacuum pump. After sampling, the content of the sampling bottles was decanted into a large bottle for later analysis. All sampling bottles and sampling tubes were rinsed using acetone to collect residue tars and particulates.

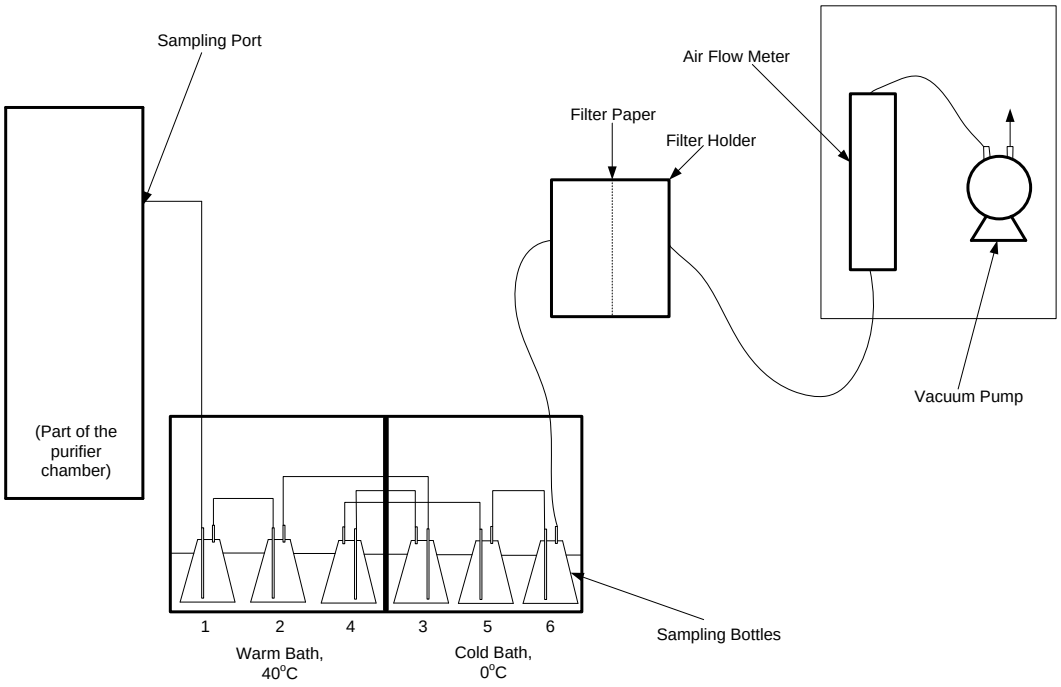

Figure 3.13 Schematic of tar sampling system

It is noted that, both warm bath and cold bath were used in the sampling line, the temperature of sampling bottles 1, 2, and 4 is 40 °C, the temperature of 3, 5, and 6 is 0 °C. The temperature gradient benefited the condensation of tar in acetone. Acetone was the solvent that was used to condense tars. Before using the equipment in connection with a site measurement, all glass equipment was cleaned in three steps. (1) Pre-washing (2) Wash all glassware in hot soapy water using a suitable bottlebrush to clean the internal parts of the glassware. Any glassware that was stained should be soaked for 4 hours, and then rinsed ten times before washing it with soapy water. (3) All glassware should be rinsed three times in tap water, three times in double-distilled water, dried, and stored in a clean place. (Cleaned glassware should be inspected, dried at 150 °C in a drying oven, capped with aluminum foil, and stored in a closed cabinet.)

Materials used to construct the sampling device included the following parts: vacuum pump (Thermo Scientific), glass fibre filter paper (Fisher Science, AP 40) , Thimble filter (25 mm×80 mm) (Whatman), filter holder (NALGENE, as indicated in Figure 3.14), and air flow meter (Dwyer Instruments). The final working condition of the sampling system is indicated in Figure 3.15.

For those filtering materials used in the sampling process, the following procedure was used for pretreatment. (1) Dry the thimble or paper filter in an oven at 110 °C at atmospheric pressure overnight (according to ISO 9096). (2) Remove the filter from the oven and wrap it directly in aluminum foil. (3) Weigh the filter plus aluminum foil using an analytical balance with an accuracy of ±0.1 mg. (4) Weigh the aluminum foil on the same analytical balance and calculate the weight of the filter.

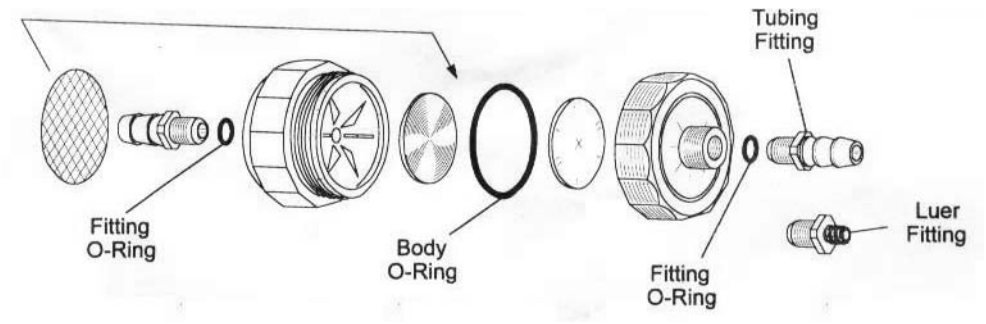

Figure 3.14 The NALGENE in-line filter holder installation

Figure 3.15 The tar sampling device

After the sampling, we collected syngas samples for gas composition analysis with a 3 L Tedlar gas sampling bag (CEL Scientific Corporation). The sampling bag was flushed with N_2 for 3 times, and then dried in the oven overnight at 100 °C. The collected syngas was analyzed using GC within 24 hours as recommended by the sampling bag manufacture.

3.2.2 Tar Measurement - Analysis

Tar sampling started once the gasification approached stable condition which was indicated by the burner flame. This process took 15 minutes to finish. The fiber glass filter paper containing particulate sample was Soxhlet extracted in order to remove adsorbed tar.

Subsequently the amount of particulate was determined gravimetrically. Equipment for gravimetric analysis included Soxhlet apparatus (Figure 3.16), evaporator, analytical balance, and laboratory equipment as volumetric flasks. The tars from the Soxhlet extraction were added to the liquid tar samples. The liquid sample containing tars was evaporated under certain conditions (i.e., heater temperature was set at 80 °C).

To avoid polymerisation of tar this procedure was undertaken immediately after finishing the sampling. First, open the filter housing and transfer the thimble filter to the Soxhlet apparatus. Keep it in the vertical position to avoid loss of particles. Carefully add the appropriate amount (250-500 ml) of acetone to the Soxhlet apparatus. Extract the filter until the acetone was clear. And then, remove the filter from the Soxhlet and keep it in the vertical position. Finally, both the filter paper and filter thimble were dried at 110 °C at atmospheric pressure overnight.

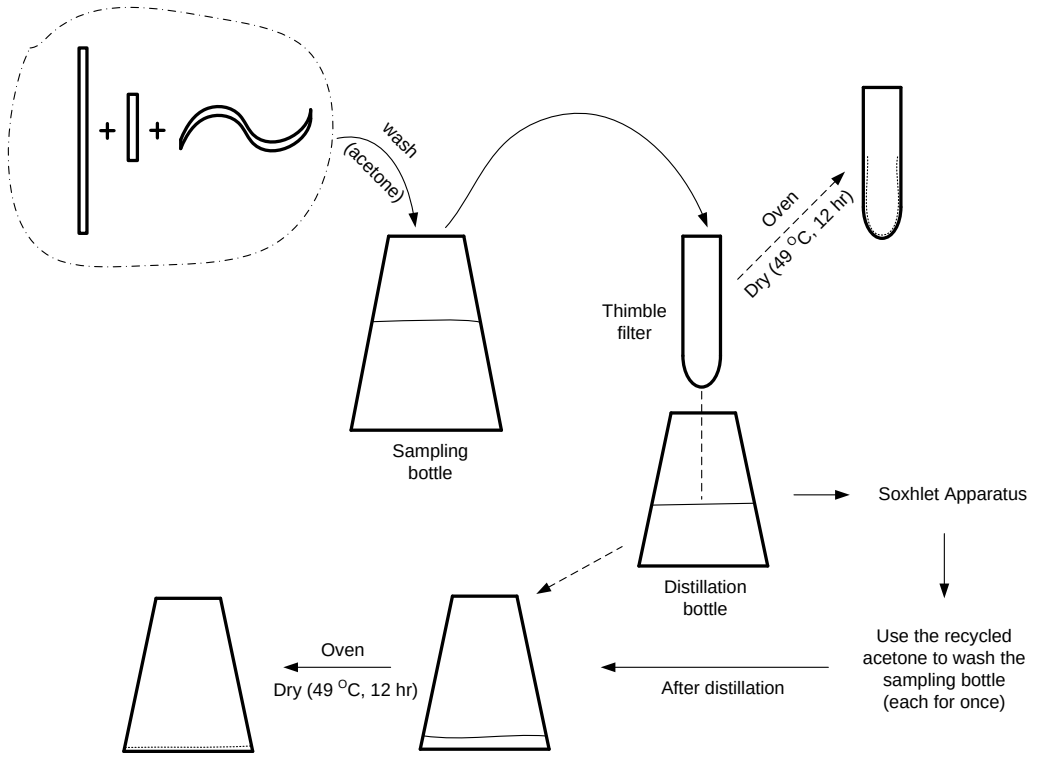

Figure 3.16 Tar analysis

Analysis procedure goes as follows. First, wash the sampling line (stainless pipes and hoses) along the syngas flow direction, collect the acetone mixture in one of the sampling bottles. Use the thimble filter to collect the particulates contained in the acetone mixture, and set up the Soxhlet apparatus in the lab to extract tar. After 5 hours' continuous extraction, remove the thimble from the Soxhlet chamber, dry them (thimble + filter paper) in the oven at 105 °C for 2 hours. Finally, use mass gravimetric method to compute weights of tar and particulate.

Appropriate handling of the leftovers is a must to avoid safety issues. Wash all the flasks and bottles with solvents (acetone and/or ethanol) timely, and dry them in the oven to remove possible residues inside the flasks or bottles.

3.3 Summary

As a thermo-chemical conversion process, biomass gasification experiences significant temperature and pressure variations. For the purpose of successful operation of the gasifier system, it is necessary to accurately measure and monitor the changes of these parameters. In this study, three different instrumentation systems, including temperature measurement, differential pressure estimate, and fluid flow rate calculation, were designed and constructed. On top of that, a full-wave rectifier circuit was applied to convert the AC power to DC power, plus the regulation of AC input via a variable voltage transformer. These devices could be applied to control the intake air temperature by manually varying the input voltage via the variable voltage transformer, monitor the temperature variations inside the gasifier, investigate the pressure drop through the operation system, and calculate the syngas flow rate. The estimation of these parameters benefited the suitable operation of the gasifier system and could be used as useful information to improve the biomass gasification performance. These instrumentation systems were either calibrated or pre-calibrated, and they were tested in the experimental study and proven to be accurate and stable, which will be discussed in details in Chapter 4.

In order to determine tar and particulate concentrations in the syngas of biomass gasification, a tar sampling method based on the IEA tar protocol was developed. As a two-step measurement system, both sampling and analysis procedures were carefully manipulated. Preliminary test of this measurement system indicated that the particulate concentration was too low to be estimated. This may due to the gas conditioning in the purifier system, which reduced the amount of particulate to a very low level. Therefore, in the experimental test, we assumed

that ideally there was zero concentration of particulate and tar measurement system only included tar concentration determination function. As stated and explained in Chapter 4, this study proved the effectiveness of the tar measurement system, and the tar concentration was typical as that of downdraft biomass gasifier indicated in the literature.

CHAPTER 4 - Experimental Study

In order to test the instrumentation and tar measurement systems as well as the gasifier, several experimental tests were conducted with three different biomass materials as feedstock, including woodchips, corncobs, and DDGS. In this part, the experimental results, such as temperature profiles inside the gasifier, pressure drop, syngas flow rate, tar concentration, syngas composition, and energy efficiency, will be discussed.

4.1 Materials and Methods

4.1.1 Biomass Feedstock

Wood chips (City transfer center, Manhattan, KS), Corncobs (Kaytee Products Inc., Chilton, WI), and DDGS (Land O'Lakes Purina Feed, Shoreview, MN) were used as feedstock (Figure 4.1).

Figure 4.1 Biomass feedstock samples (left to right: woodchips, corncobs, and DDGS)

Carbon content for each feedstock was tested in the Soil Testing Laboratory at Kansas State University (Table 4.1). It was indicated from the test, that these three biomass materials generally have similar amount of carbon content, all in the range of 43-44%. For DDGS, the supplier also provided a table of various properties (Table 4.2). It mainly included moisture, protein, fat, total starch, etc.

Table 4.1 Total carbon contents of three biomass samples

Sample ID	Total N %	Total C %
wood chips - 1	0.24	44.26
DDGS - 2	3.78	43.25
corn cobs - 3	0.31	44.66

Table 4.2 DDGS properties (average values)

Midwest Sample	Moisture	Protein	Fat	Pro+Fat	L Value	Total Starch
Averages	11.72	26.91	9.62	36.52	50.25	4.74

Moisture content was determined using an ASAE standard (ASAE, 2008). Two sample containers were loaded with representative samples of at least 25 g. Both samples were weighed and then dried in a drying oven (103 °C for 24 hours).After the samples were removed from the oven, each was weighed immediately. The loss in weight was recorded as moisture. All the moisture contents mentioned in this project are on a wet basis. The Wood chips had a moisture content of 7.5%, and other properties were not analyzed. A general biomass properties analysis is indicated in Appendix F.

4.1.2 Gasifier System Operation

Operation procedure for the system takes several steps. First, set up circulation water, turn off the valve of the stove, and turn on the vent-pipe valve. Add the feedstock materials into the reactor chamber till the throat of the cone area, and use a torch to light them. When the surface layer of feedstock was fully lighted (which was indicated visually), add more feedstock until the inlet level of the chamber (see Figure 3.2). After the biomass materials have been burning for a few minutes, prepare to turn on the burner. Wait until the flame of the burner became stable, start to operate tar-sampling line and collect syngas into sampling bags. After the sampling, it still took a while to finish the run. Wait till all the materials were completely gasified, and then shut off the system and stop the cooling water. Remove the ashes from the disposal port, collect wastewater from the drainage in a 5 gallon plastic bottle (which was recycled by the university Environmental Health and Safety Department).

4.1.3 Intake Air Temperature Control

Depending on the outdoor air temperature, the heating of intake air can be varying from run to run in different conditions. In a test run, when ambient air temperature was 4 °C, the intake air temperatures changed at different input AC powers. Table 4.3 points out the intake air temperature control when air temperature was 4 °C, and air flow rate was set at the point when input voltage (to the blower) was 110 V. Temperature could reach 85 °C when input voltage was 100 V, while it was 80 V air temperature could be heated up to 54 °C. The input voltages were manually adjusted by the 5 amp variable voltage transformer. In the actual experiment runs, air

was introduced without preheating. It was only for the purpose of testing how to manually control the intake air temperature. Therefore, in the energy efficiency estimates, there was no extra heat accounted in the final calculation, but only the higher heating value of the biomass.

Table 4.3 Intake air temperature (ambient air temperature = 4 °C)

Voltage (V)	Temp (^{o}C)
80	54
85	60
90	69
95	75
100	85

4.1.4 Tar and Syngas Analysis

Syngas sample was collected through the sampling port set in the upper wall of purifier chamber using a 3 L Tedlar sampling bag (flushed with N_2 for at least 3 times and dried in the oven at 100 °C for 12 hours). Tar samples were collected using the sampling line. Tar samples are shown in Figure 4.2. In the solution condition, tars were condensed in acetone, which was indicated by the color of the solution, the darker the color was, the more tars were trapped. After the tars were dried in the oven, there was a layer of black residue in the bottom of the flask. It is suggested that both the sample gas and tar should be analyzed immediately after the experiment run.

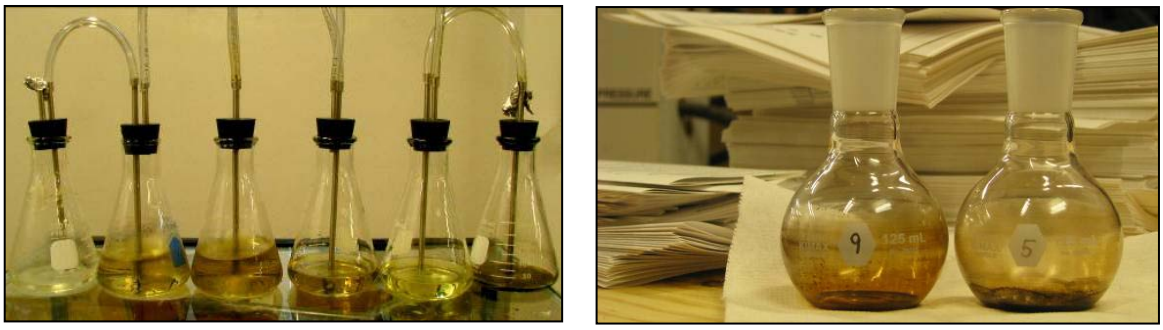

Figure 4.2 Tar samples (left, solutions; right, dried)

Analysis was operated in a chemical engineering lab (Dr. Keith Hohn) where a SRI 8610s gas chromatograph (GC) (SRI Instruments, Torrance, CA) equipped with a thermal conductivity detector (TCD) was set up (Figure 4.3). Helium was used as the carrier gas in the gas chromatograph (it was required TCD switch could not be turned on until the carrier gas was supplied). A syringe was used to pump 1 ml of syngas sample from the sampling bag and inject the sample into the gas chromatograph via the inlet port. For each run, the system needed to

warm up to the setpoint temperature (i.e., 29 °C). In order to obtain complete analysis of each component, it took 20-30 minutes to finish one run. Data analysis of syngas composition was completed using the SimplePeak software (Figure 4.4). Each peak in the curve indicated a molecule component, while its peak area was proportional to its amount. Different molecules exited the GC sampling loop at different times (which was termed as 'retention time', with the unit of second) depending on their molecular weights and some other factors. For the main syngas components, the typical retention time for each of them was, H_2, 1.8s, CO, 7.7-10.6s, CH_4, 5.8-6, CO_2, 6.8s. Calibration chart for the GC analysis is shown in Appendix I.

Figure 4.3 Syngas composition analysis using a SRI 8610s GC

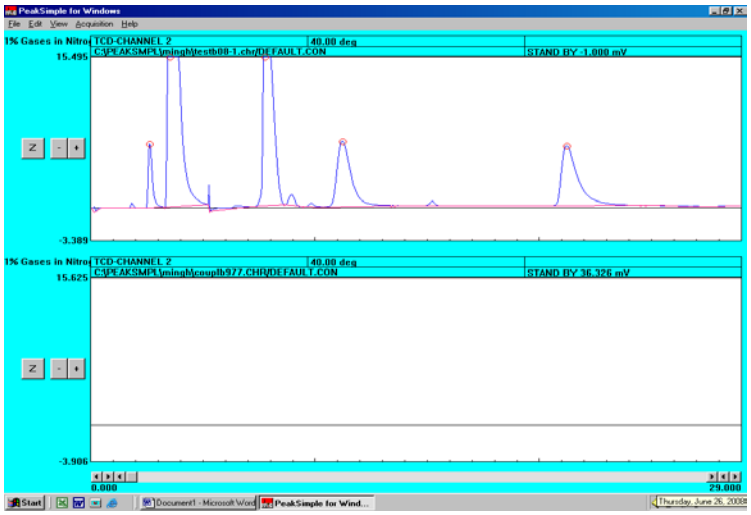

Figure 4.4 PeakSimple for GC data analysis

4.2 Results and Discussion

4.2.1 Gasifier Chamber Temperature Profile

In the test of the temperature profile inside the gasifier, as indicated in Figure 3.8 and Table 3.2 (see Chapter 3), woodchips, corncobs, and DDGS were used to obtain the experimental data. Since the corncobs and DDGS had relatively small sizes which could result in their falling through the grate, woodchips were used to start the system for each run. After woodchip gasification, a burning charcoal bed was formed, in which case the other two biomass materials could be supported and easily gasified. Since the system was a batch model, each type of feedstock was manually introduced to the gasifier chamber. Due to its physical property (especially its size distribution), woodchips were usually gasified quickly (half an hour), while DDGS could support a one-time run up to two hours. Corncobs would make a 40-70 minute run for one-time feed.

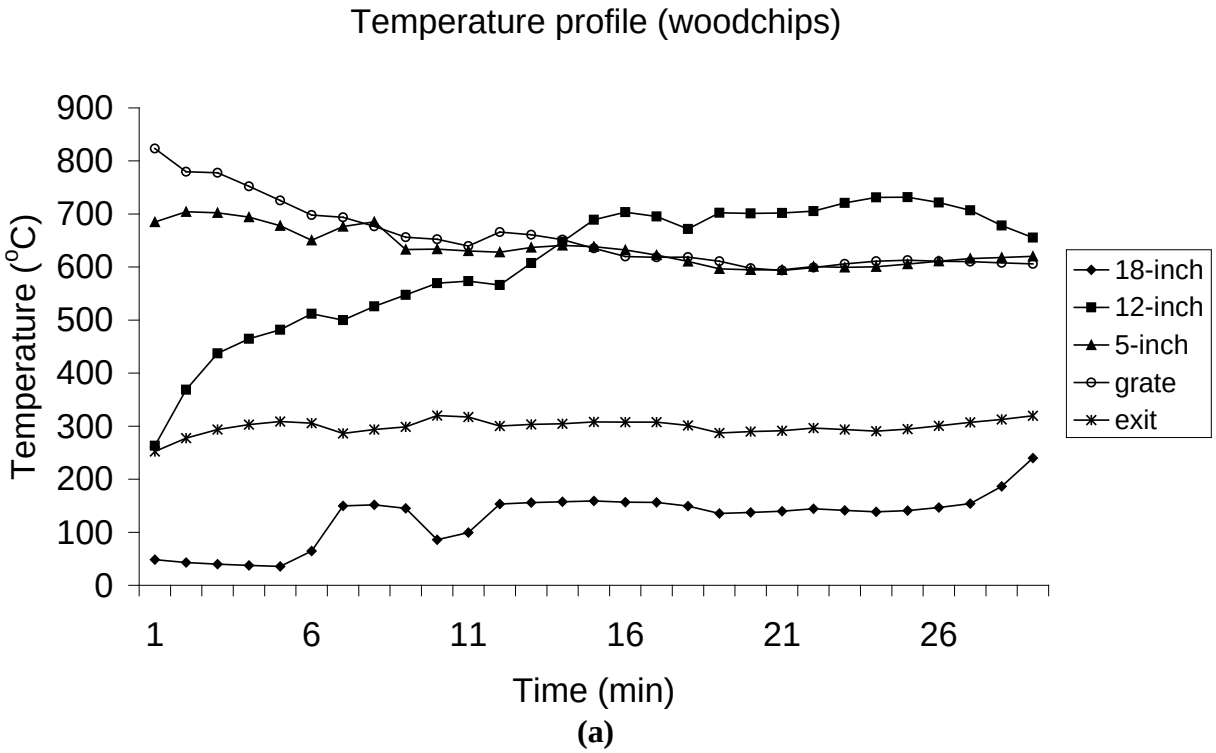

(a)

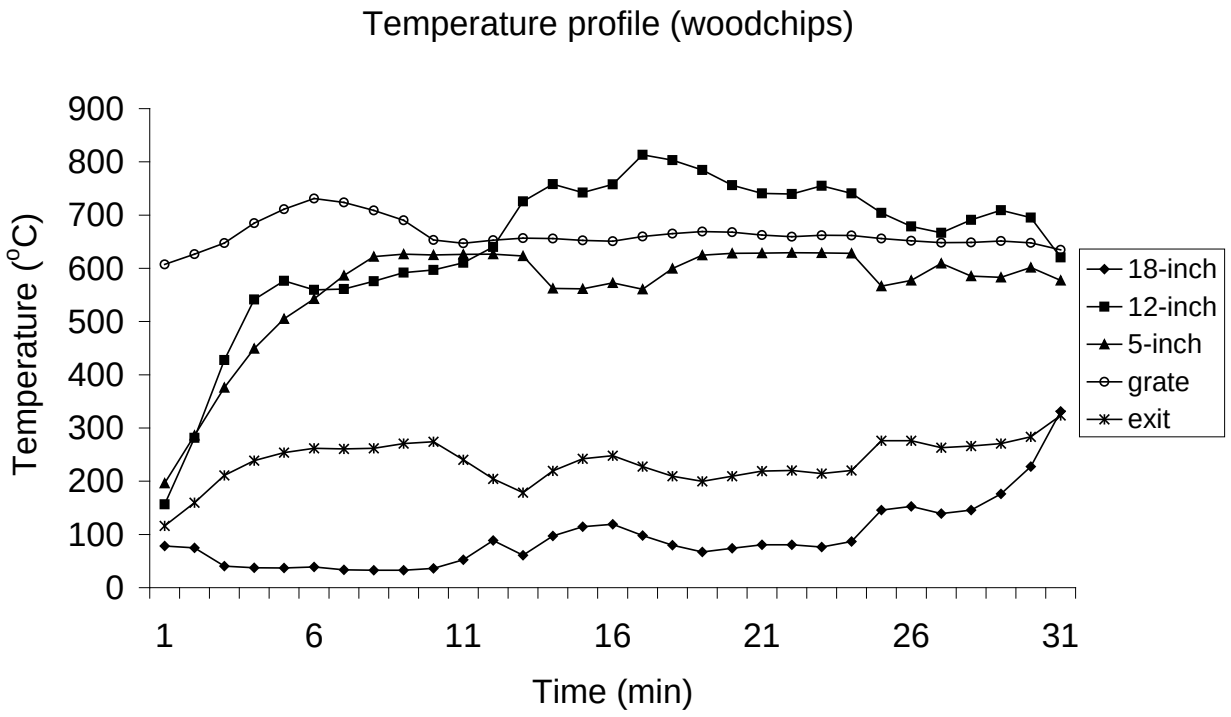

(b)

Figure 4.5 Temperature profile inside the gasifier for woodchips gasification

As indicated in the temperature profile curves shown in Figure 4.5, within different reaction zones, temperatures were typically different from each other (in stable stages). This temperature distribution is very typical for that of a downdraft gasifier. In the starting stage of gasification, since the gasifier chamber was lighted with a small amount of woodchips, temperature at the grate was already very high (i.e., 600-800 °C). An occasion for the first figure (a) was, the temperature at 5-inch was also very high, which was because the woodchips were burned to the throat (where 5-inch was located) and it was heated up to a high temperature. After new biomass was feed into the gasifier, temperature at the grate was decreased, while in other sites temperature increased gradually. In 6-10 minutes, the system approached stable gasification, and temperatures were relatively stable compared to the starting stage. Temperatures were 100-200 °C at 18-inch, 700-800 °C at 12-inch, around 600 °C at 5-inch, and 600-700 °C at the grate. Syngas outlet temperature located within a typical range of 280-300 °C. Both in curves (a) and (b), there was temperature decreasing during the stable stages, like around the 10-11th min in (a) and the 13-14th min in (b), that was because the lid of gasifier chamber was removed and a metal pole was used to stir the biomass feedstock to prevent biomass bridging and allow smooth flow of the biomass. However, in this process, cool air poured in, and temperature

at 18-inch would decrease. In the shut-off stage, biomass was running out, and reactions were approaching to the end. During this period, temperatures at the grate, 12-inch and 5-inch tended to decrease, while temperature at 18-inch and the exit increase (which was because the flame came close to the upper sites, and the heated air was exiting through the system).

After the starting run of the system, another batch of woodchips was fed into the system. Since a supporting bed of burning charcoal was formed, the added feedstock could be gasified very easily and relatively more stable. A typical temperature profile of this process is shown in Figure 4.5(b). As indicated in this curve, temperature at 18-inch was decreased as new biomass was added. Oxidation was retrieved when new biomass was reacted and temperature at 12-inch increased till it approached a steady state. In the stable gasification process, temperature was still within the ranges as in the starting run. A sharp jump of temperature at 18-inch during the ending stage was due to the increase of the burning charcoal bed so the flame could reach the upper sites of the gasifier chamber easily.

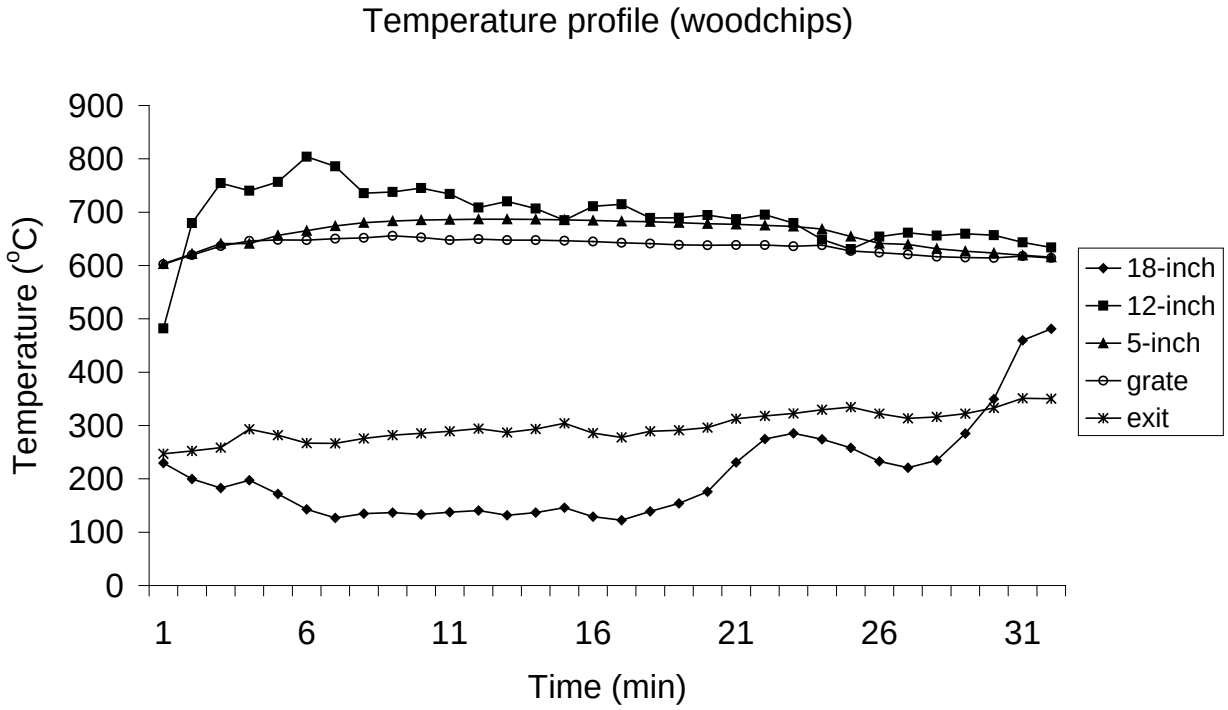

Figure 4.6 Temperature profile of woodchips gasification after the starting run

Corncobs and DDGS were also added into the preheated gasifier system to test their specific temperature profiles, as shown in Figure 4.7 and Figure 4.8. Corncobs gasification was similar to that of woodchips, except that its particle size was smaller than that of woodchips.

Temperature profiles of both (after the starting run) were quite close to each other. After corncobs were added, temperature at 18-inch decreased till stable, while temperatures at 12-inch, 5-inch, and grate increased till stable. Temperature at exit was almost kept unchanged. However, with fine particle sizes, corncobs could support a longer run than the woodchips gasification. When corncobs were burning out, temperature at 18-inch jumped as expected.

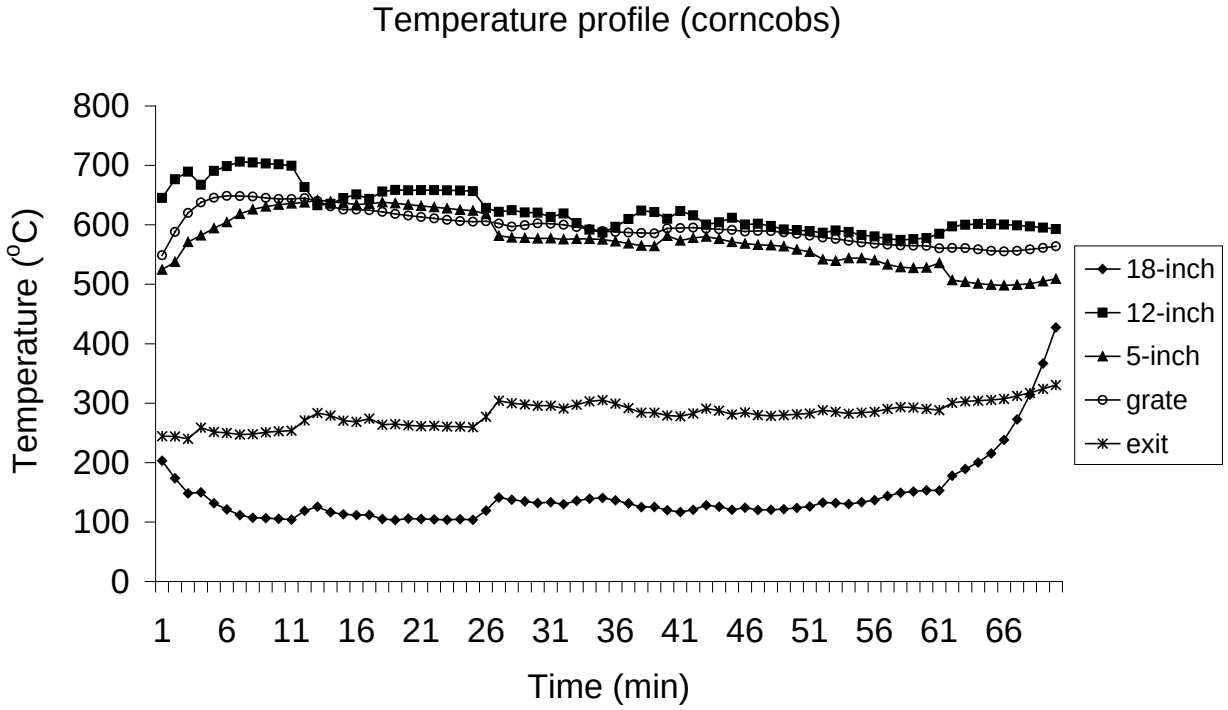

Figure 4.7 Temperature profile of corncobs gasification after the starting run

Comparatively, woodchips and corncobs could be more easily gasified than DDGS. The small particle sizes of DDGS made it difficult to handle inside the gasifier. Since DDGS was too closely packed, air was not easy to go through the DDGS layers to reach in reactions, especially those most important in the oxidation and reduction zones. Therefore, DDGS was randomly stirred with the metal pole to prevent bridging and to make some small holes scattering the DDGS inside the gasifier, enabling air getting in through them. And that was probably why the temperatures in 18-inch, 12-inch, and 5-inch, were greatly shifting during the gasification process. In contrast, temperatures in the grate and exit were much more stable. Even though, since DDGS supported a longer time run, there were several stable stages through the whole process lasting 20-30 minutes. For instance, from the 110th min to the 130th min, there was a relatively stable gasification stage. It was noted that temperatures at 12-inch for DDGS

gasification jumped up to more than 1000 °C, and could maintain at 900-1000 °C. This indicated that DDGS could be a very good biomass feedstock, if it can be properly and easily handled, and its production value can be competitive to its worth as animal feed.

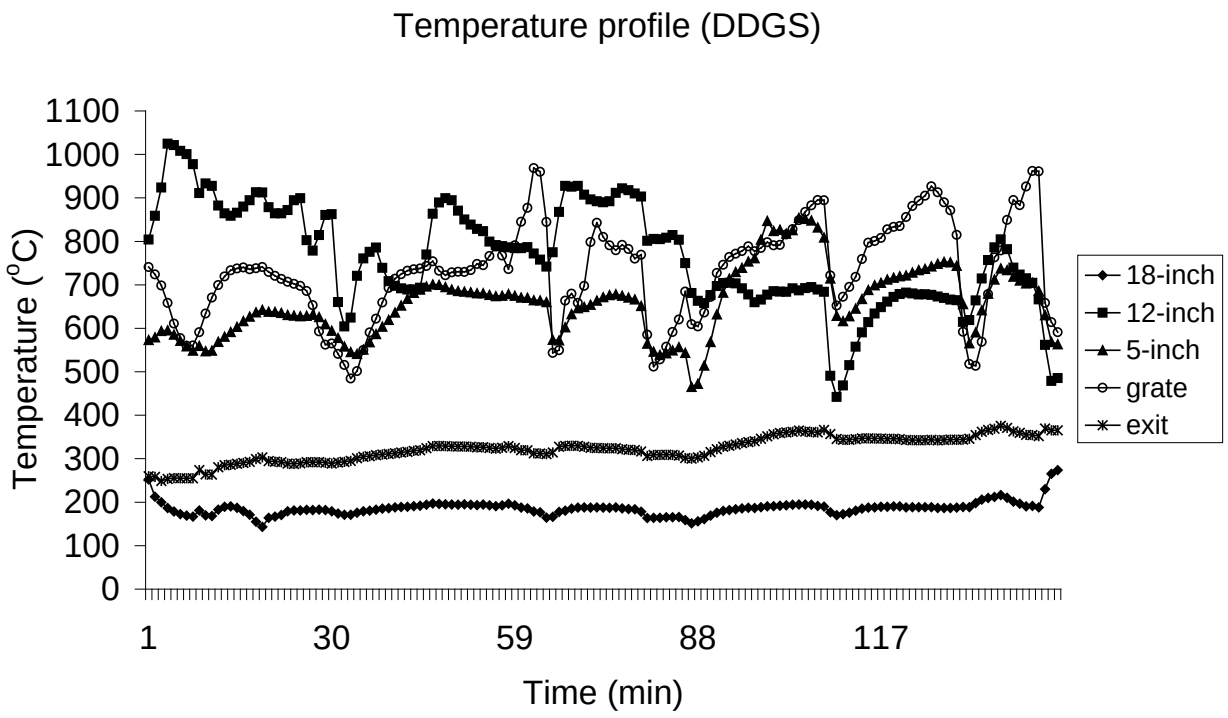

Figure 4.8 Temperature profile of DDGS gasification after the starting run

In summary, temperature measurement inside the gasifier and at the exit port of the gasifier was repeatable. Temperatures for three different biomass gasification processes had their specific distribution, but were quite similar on the whole. In order to obtain more stable temperature profile, it is recommended to pre-treat the biomass (i.e., pelletized) to make it more favorable for the downdraft gasifier.

4.2.2 Pressure Drop and Air Flow Rate

Pressure measurement for the gasifier system was completed in several ways. Firstly, it is necessary to make it clear where pressure drop (note: pressure drop was the relative pressure to the atmosphere, except for that of the flow nozzle) was measured through the gasifier system. It is shown in Figure 4.9. Seven different ports through the gasifier system, inlet, 18-inch, 12-inch (both heights were related to the grate), grate, exit, outlet I, and outlet II, were set to estimate the pressure drop at each place. There were two sets of experiment to finish the tests. For one case,

the biomass was not lighted (therefore, no reactions at all), and the other condition was the real working condition. For the former setting, pressure was measured at each site, while only the outlet II was tested in the working condition due to high temperatures in the gasifier chamber.

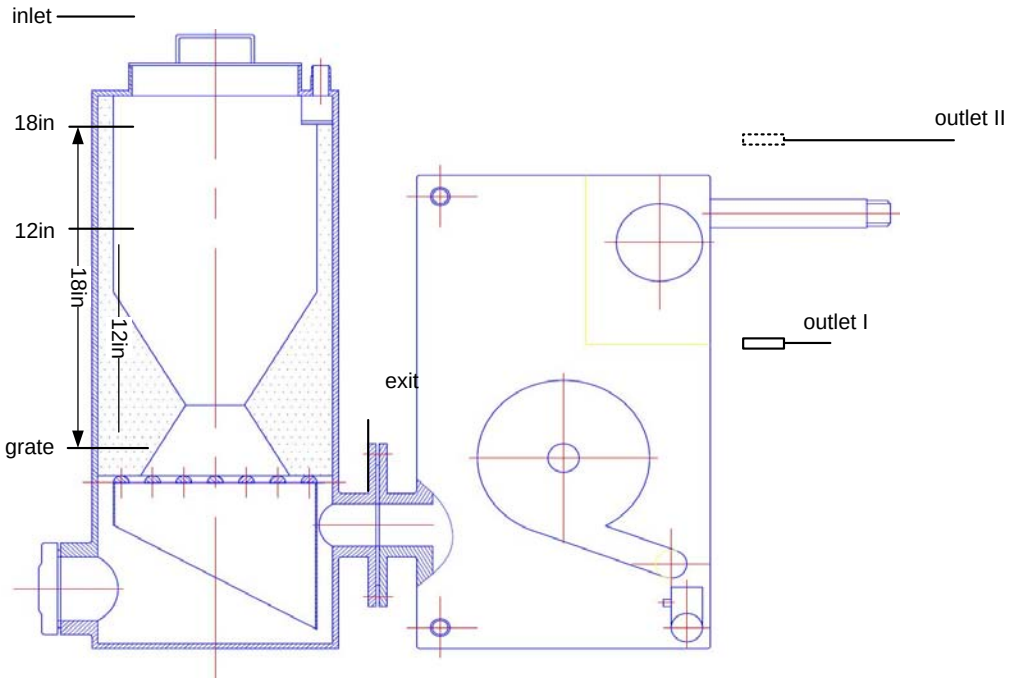

Figure 4.9 Pressure drop measurement through the gasifier system

4.2.2.1 Biomass Loading Affecting Pressure Drop

The 5 amp variable voltage transformer was used to control the voltage input to the blower. Voltages were set to 90 V, 100 V, 110 V, and 120 V. Firstly, without any feed inside the gasifier chamber, run the system under different power, and record the pressure drop at different locations. Three different biomass materials were separately fed into the gasifier, and each resulted in one set of pressure drop data. Each biomass was loaded to the inlet level, so as to maintain the same height inside the gasifier. The difference in pressure drop with different biomass material (including no feed) is shown in Figure 4.10.

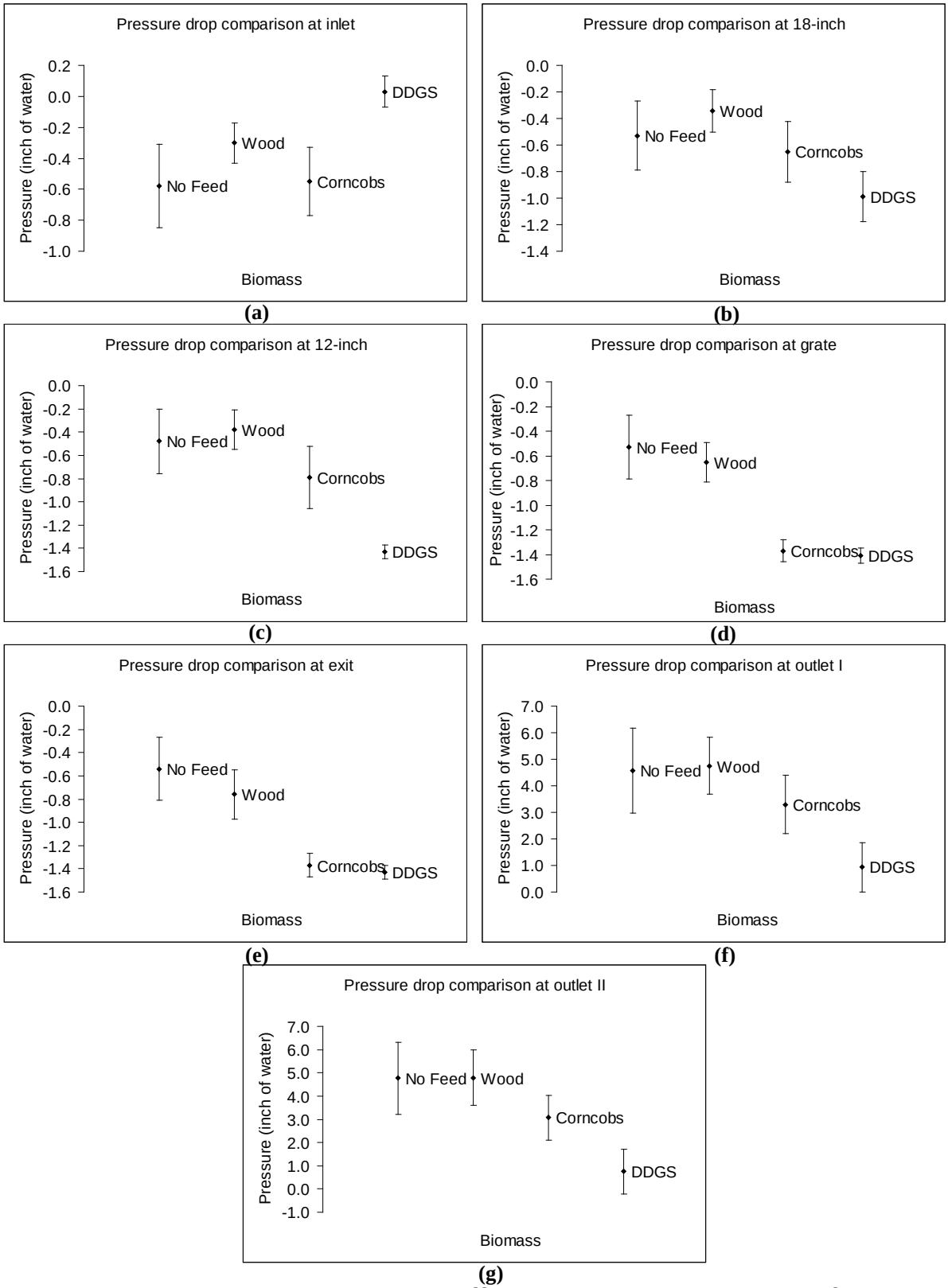

Figure 4.10 Pressure drop comparison at different locations through the gasifier system (power input = 120 V)

As shown in the curve of inlet pressure drop (a), with DDGS fed, the pressure drop was almost 0, which was an indicator that DDGS was so closely packed that even the blower could not bring much pressure change at this location. However, both woodchips and corncobs would allow small pressure drops, and the pressure drop with corncobs fed was close to the empty condition (no feed). In the lower sites of the gasfier, each came closer to the blower. Theoretically, it is easier to form vacuum conditions at the locations close to the blower. That was proved in the figures (b), (c), (d), and (e), by those negative pressure drops. After the blower, the pressure drop became positive. As indicated in the figures (b), (c), (d), and (e), pressure drops were wood<corncobs<DDGS, at the locations ahead of the blower. In contrast, after the blower, in figures (f) and (g), that was DDGS<corncobs<wood. This was due to the particle size distribution of each biomass feedstock. Smaller sizes favored stronger negative pressure drops, and resulted in relatively small positive pressure drop.

4.2.2.2 Voltage Affecting Pressure Drop

For each fixed location, the pressure drop was studied as a function of voltage to the blower. Its effects are shown in Figure 4.11. As a general rule, pressure drop would increase as the input voltage was increased, for each type of biomass feedstock and at each location, as indicated through figures (a) to (g). In curve (a), when DDGS was fed, pressure drop at inlet was very small and kept constant at 0.1 inch of water. In contrast, negative pressure drops were created when woodchips and corncobs were fed into the gasifier, and both increased as input voltages became higher. In figures (d), (e), and (g), pressure drops at the grate, the exit, and outlet II, were slightly changed as DDGS was fed into the gasifier chamber.

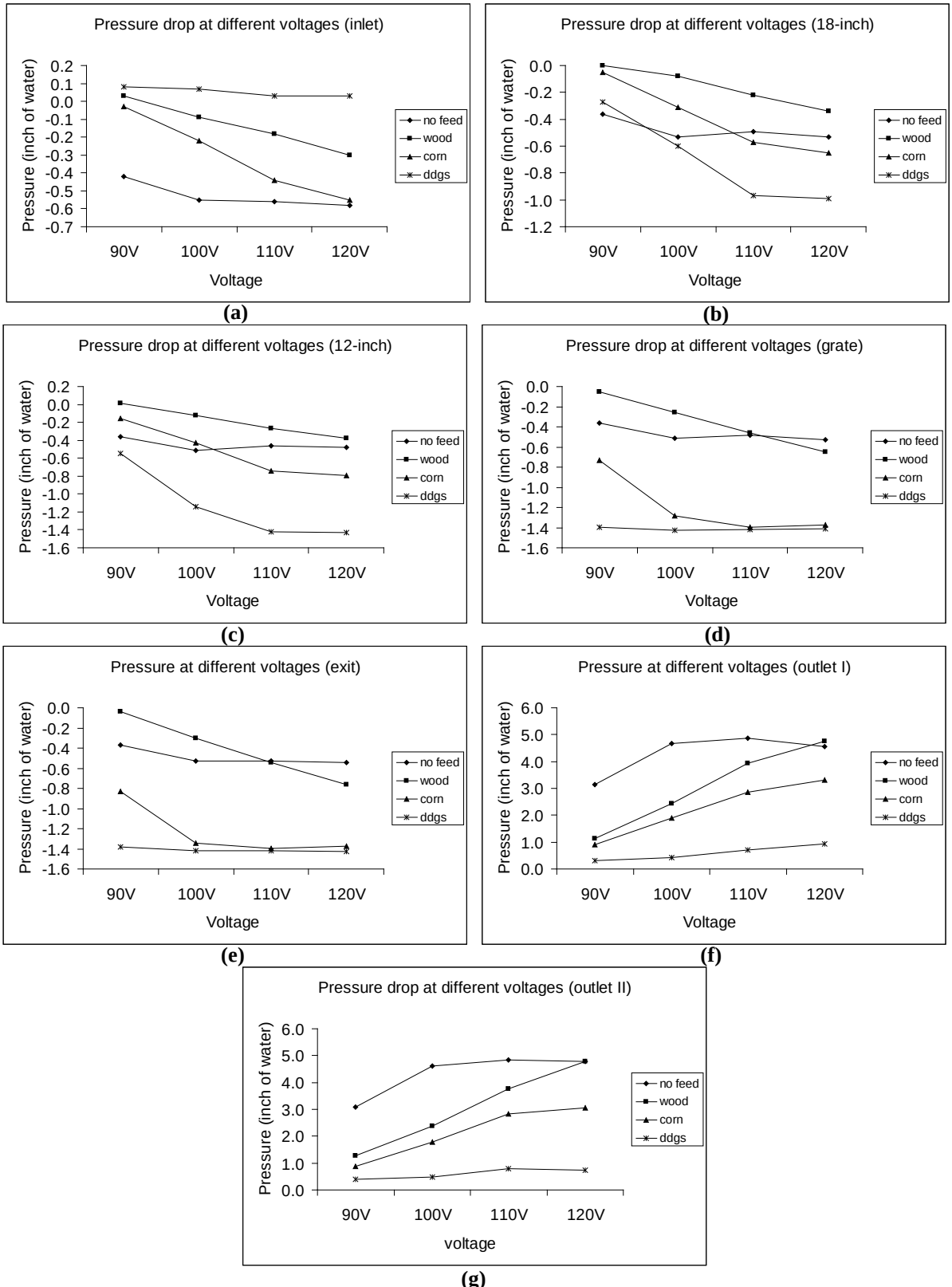

Figure 4.11 Pressure drop comparison at different power inputs (voltages)

Generally, pressure drops at the locations ahead of the blower were smaller than 1.6 inches of water, while pressure drops were within 5 inches of water, after the blower.

4.2.2.3 Pressure Drop Variations at Different Locations

Pressure drop was studied as a function of location, under a specific power input. It is shown in Figure 4.12. All four graphs were in the same shapes that indicated similar variations under different voltages. Compared to no feed, when woodchips were fed, pressure drop became less significant as voltages were increased. For each curve, the pressure drop difference was 2 inches of water at 90 V (a); 2 inches of water at 100 V (b); 1 inch of water at 110 V (c); and almost 0 at 120 V (d). Difference between pressure drop when corncobs were fed and when DDGS was fed became more significant as voltages increased. For each curve, the pressure drop difference was less than 1 inch of water at 90 V (a); more than 1 inch of water at 100 V (b); more than 2 inches of water at 110 V (c); and more than 2 inches of water at 120 V (d).

Also indicated from curves (a) through (d) in Figure 4.12, ahead of the blower, pressure drop approached maximum at exit which was closest to the blower. After the blower, pressure drop decreased after the filtrator, but not that big change in values. Compared to pressure drops after the blower, pressure drops at the locations ahead of the blower were quite close in values.

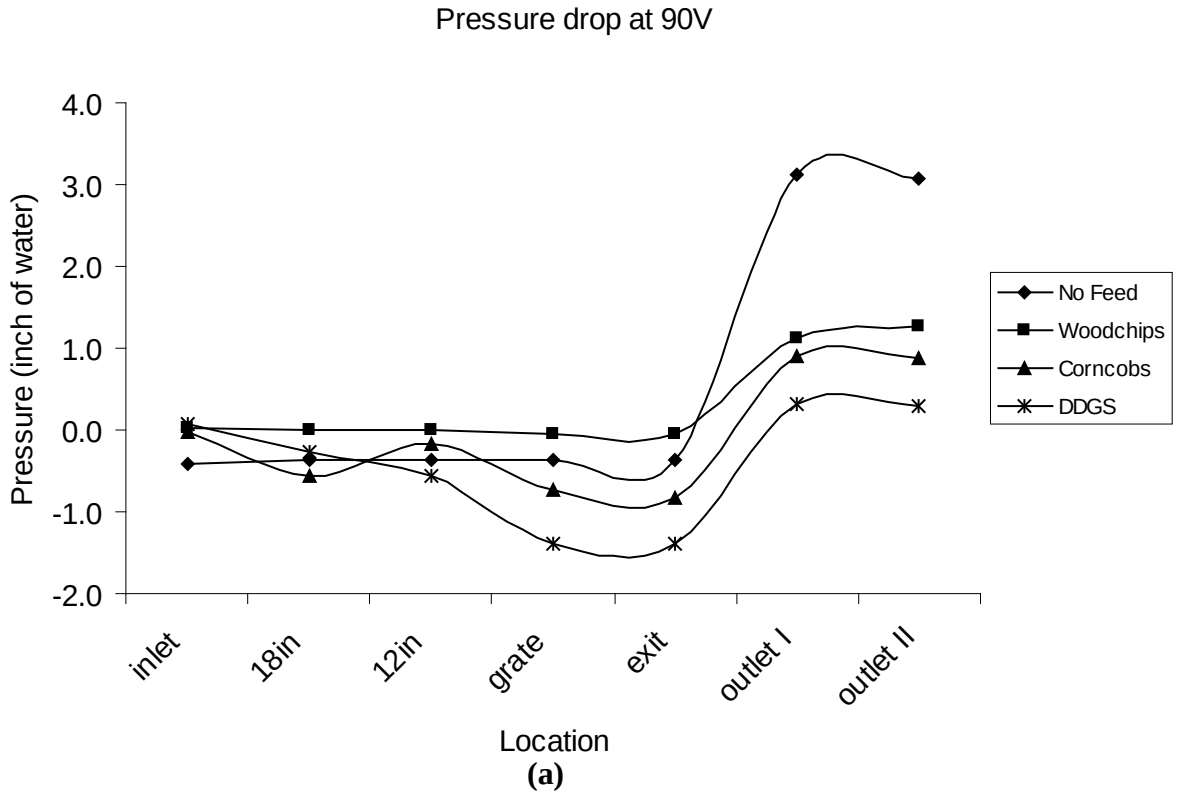
Pressure drop at 90V
Pressure (inch of water)
4.0
3.0
2.0
1.0
0.0
-1.0
-2.0
inlet
18in
12in
grate
exit
outlet I
outlet II
Location
No Feed
Woodchips
Corncobs
DDGS

(a)

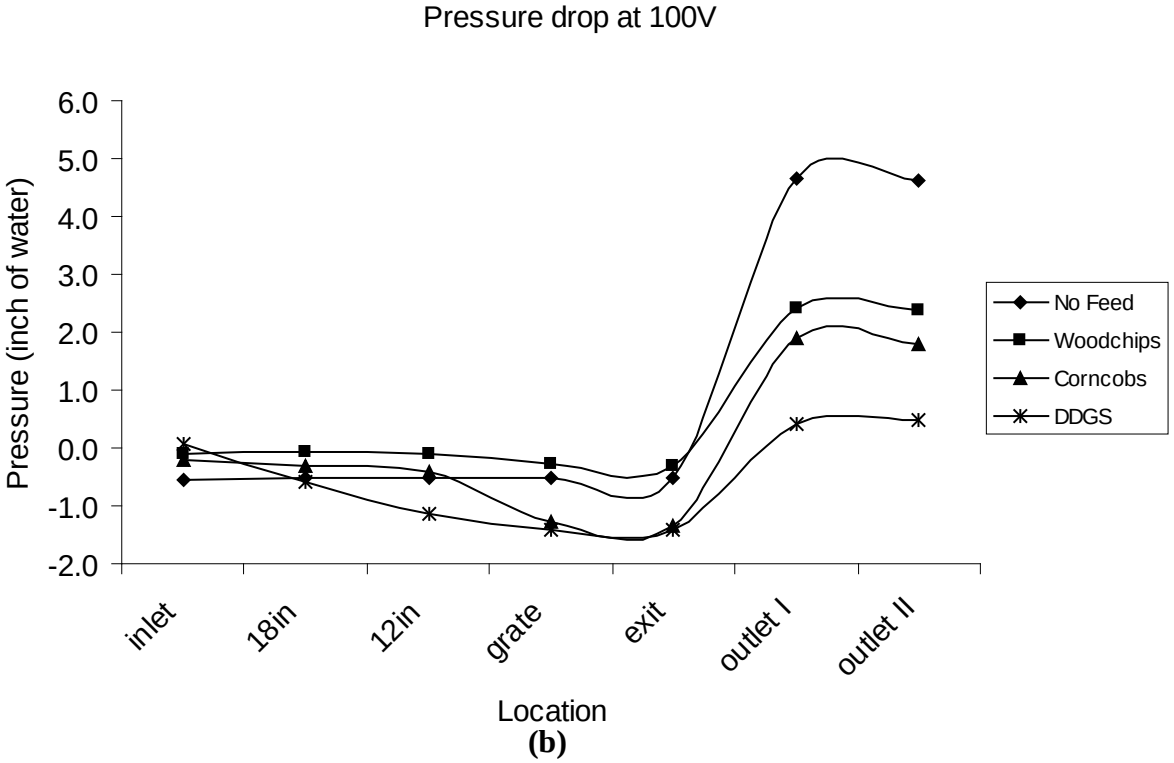
Pressure drop at 100V
Pressure (inch of water)
6.0
5.0
4.0
3.0
2.0
1.0
0.0
-1.0
-2.0
inlet
18in
12in
grate
exit
outlet I
outlet II
Location
No Feed
Woodchips
Corncobs
DDGS

(b)

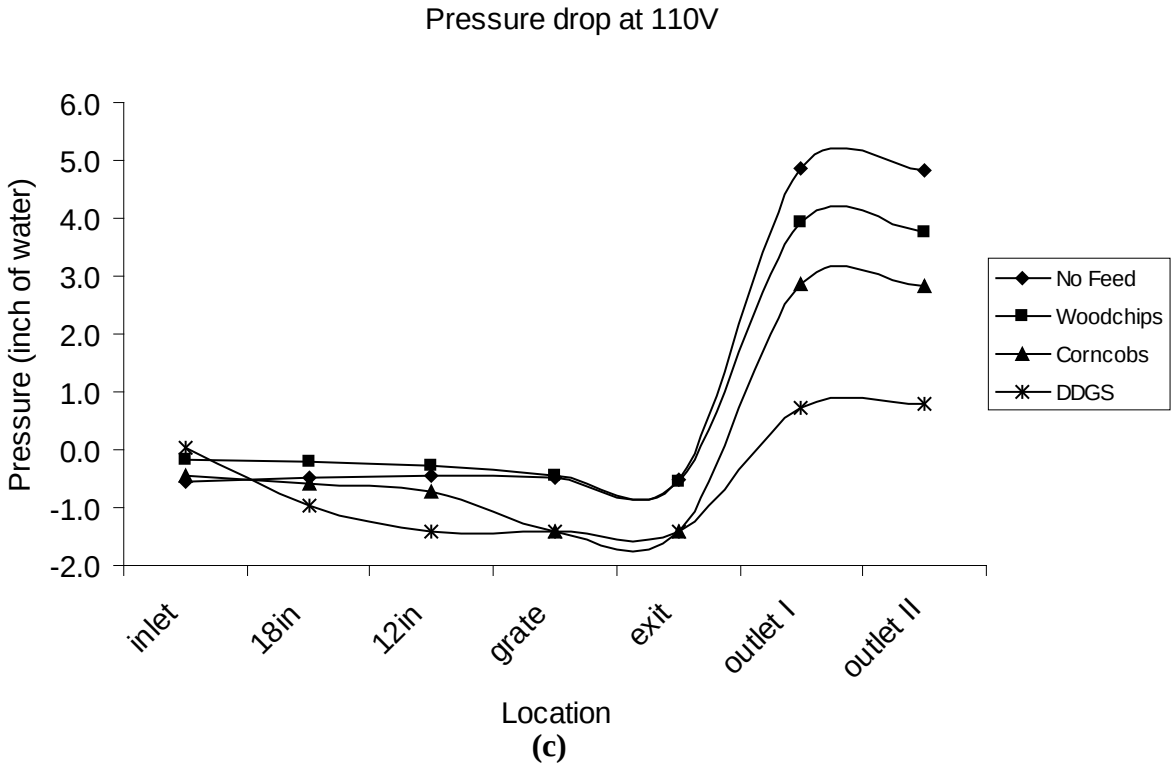

(c)

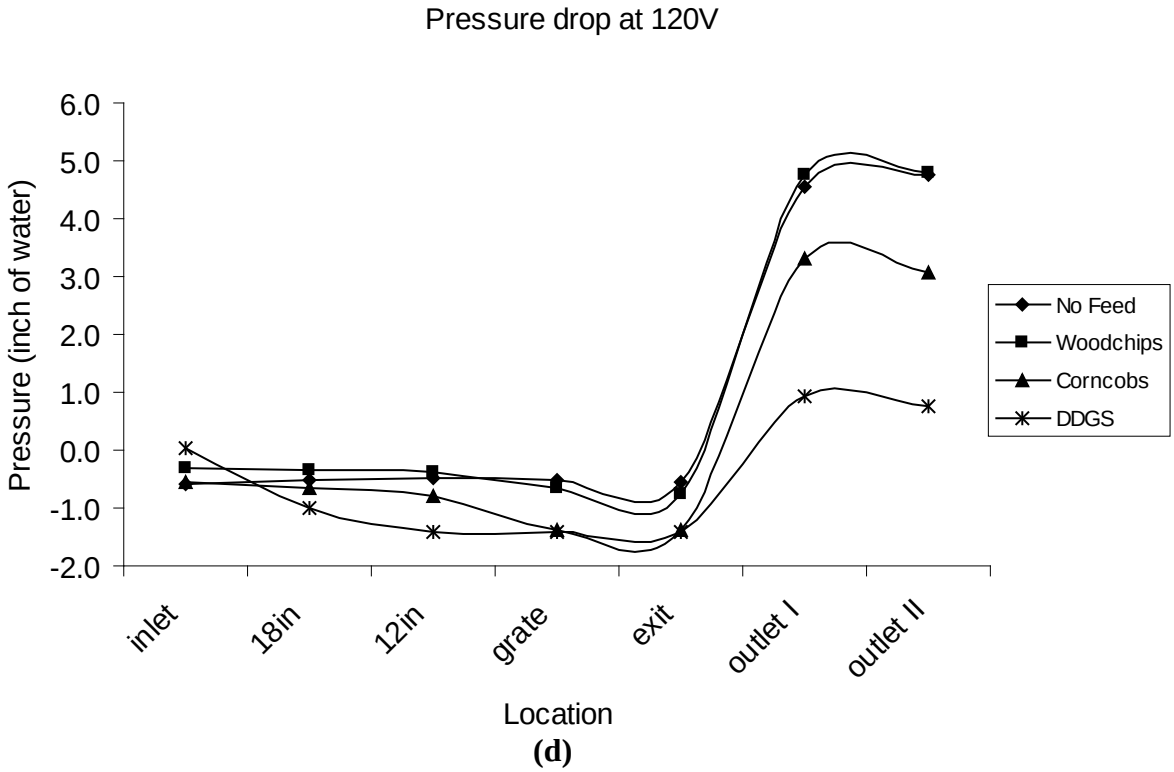

(d)

Figure 4.12 Pressure drop at different locations across the gasifier system

4.2.2.4 Pressure Drop at Outlet II

During each run of the gasification of three different biomass feedstocks, the pressure drop at outlet II was also recorded. This measurement gave information of pressure drop variation during the gasification process at that specific location. Results are shown in Figures 4.13, 4.14, and 4.15 (note: err bars are from the standard deviation which is shown in Appendix C). Through the gasification process, pressure drop at outlet II decreased slightly for each type of biomass feedstock. Pressure drops were in the ranges of 3-5 inches of water for woodchips gasification, 2-4 inches of water for corncobs gasification, and 1-2.5 inches of water for DDGS gasification. The variation of pressure drops was more significant for DDGS gasification than that for corncobs gasification. The variation was not that significant for woodchips gasification, compared to both DDGS and corncobs.

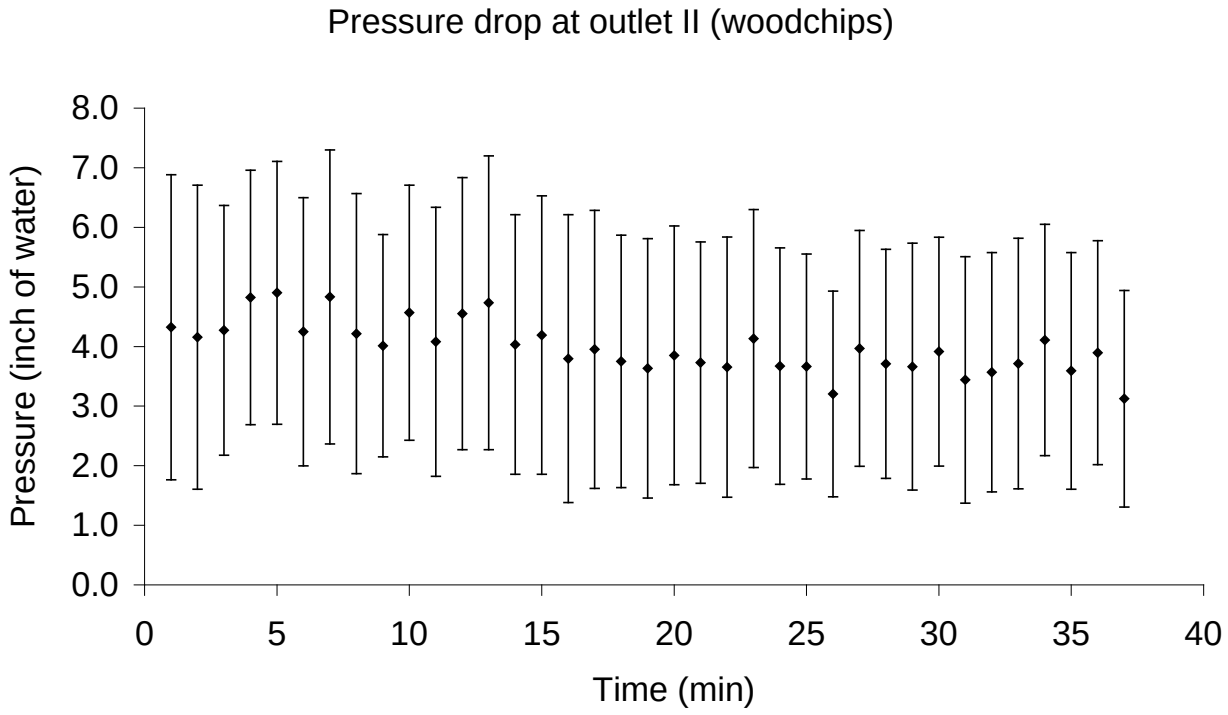

Figure 4.13 Pressure drop at outlet II for woodchips gasification

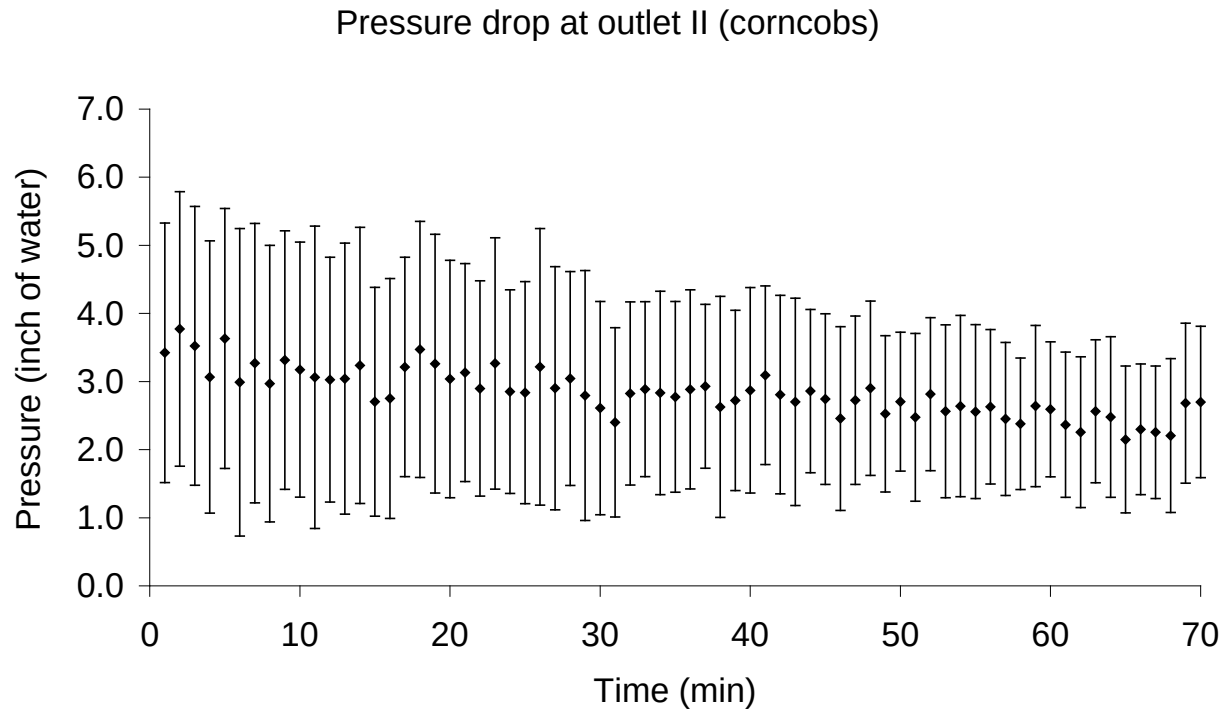

Figure 4.14 Pressure drop at outlet II for corncobs gasification

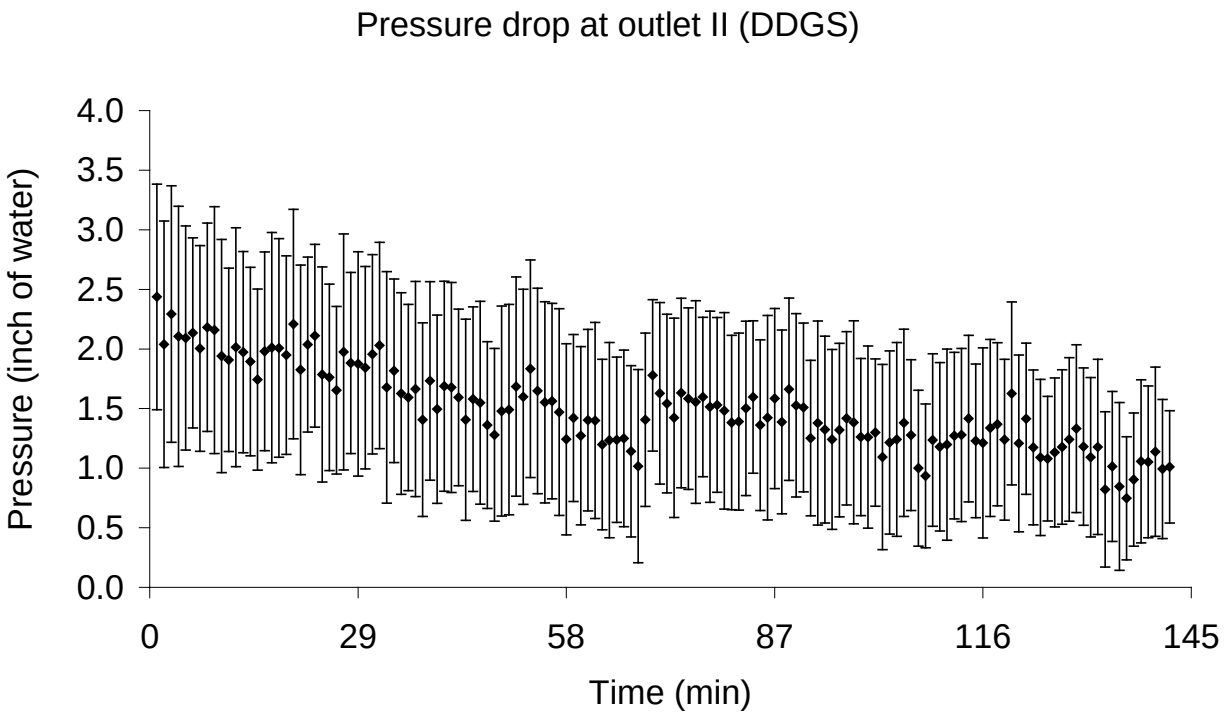

Figure 4.15 Pressure drop at outlet II for DDGS gasification

4.2.2.5 Pressure Drop of the Flow Nozzle and Syngas Flow Rate

Pressure drop across the flow nozzle, which was set in the syngas outlet after the purification system, was estimated to determine the syngas yield rate. It was also an indicator of the stability of the gasifier system. And, when proportionally changed the power input for the DC motor, we could accordingly change the value of intake air flow rate and the syngas yield rate could be varied with a certain pattern. Calculations of the syngas flow rate could be completed under the specific exiting syngas conditions. Table 4.4 indicates the pressure drop across the flow nozzle under different input voltage for the DC motor.

Table 4.4 Pressure drop across the flow nozzle and syngas flow rate

Voltage (V)	ΔP (Pa)	Syngas flow rate (cfm)
90	32.4	9.3
100	69.7	13.7
110	122.0	18.1
120	159.4	20.7

4.2.3 Syngas Composition

Compositions (v%) of the syngas are shown in Table 4.5.

Table 4.5 Syngas composition

Molecule	Wood Chips	DDGS
H_2	20.04%	19.08%
O_2	3.15%	1.18%
N_2	61.64%	50.70%
CO_2	0.04%	7.65%
CO	15.01%	20.02%
CH_4	0.12%	1.34%

For syngas generated from atmospheric, air blown downdraft gasifiers, H_2 usually ranges from 15-21%, and CO 10-22% (Heesch et al., 1999). Our results were consistent with reported values.

4.2.4 Tar Concentration

The gas sampling rates were 9.3 L/min and 9.8 L/min for wood chips and DDGS, respectively. The total sampling volume and tar concentration are listed in Table 4.6. For downdraft gasifiers, the general range of tar concentration is 0.5-5 g/Nm^3 (Milne et al., 1998), depending on gasifier designs and biomass feedstocks. Our results were located in this range.

Table 4.6 Tar concentration

Biomass	Sampling volume	Tar concentration
Wood Chips	140.2 L	1.65 g/Nm^3
DDGS	147.3 L	4.20 g/Nm^3

4.2.5 Gasification Energy Efficiency

Comparison of biomass energy content with syngas energy value resulted in the gasification efficiency.

$$E_{woodchips} = W_{bio} \times (1 - MC) \times \left(HHV_{woodchips}\right)$$

$$E_{syngas} = t \times q_v \times \left(HHV_{syngas}\right)$$

$$\eta = \frac{E_{woodchips}}{E_{syngas}} \times 100\%$$

$$HHV_{woodchips} = 0.4574 \times (C\%) - 2.70$$

$$HHV_{syngas} = 12.769 \times (H_2\%) + 12.622 \times (CO\%) + 39.781 \times (CH_4\%)$$

Where,

$E_{woodchips}$, the energy content of woodchips (MJ)

E_{syngas}, the energy content of syngas (MJ)

$W_{woodchips}$, the mass of woodchips (kg)

MC, the moisture content of woodchips (%)

t, the duration of stable gasification (minute)

q_v, volume flow rate of syngas (cfm)

η, the gasification efficiency (%)

$HHV_{woodchips}$, HHV of woodchips (MJ/kg)

HHV_{syngas}, HHV of syngas (MJ/m^3)

$C\%$, the carbon content in woodchips (dry basis)

$H_2\%$, $CO\%$, and $CH_4\%$, the percentage of syngas components

Calculation of HHV of woodchips was based on the following formula (Brown, 2003).

$$\text{HHV in MJ/dry kg} = 0.4574 \times (\text{C\% on dry biomass}) - 2.70$$

The resulted HHV for woodchips was 17.54 MJ/kg (dry basis).

Based on the thermodynamic data used by National Renewable Energy Laboratory (IEA, 2001) (see Appendix J), the following calorific values were used to compute the HHV (unit: MJ/m^3 at standard conditions) of syngas (Table 4.7).

Table 4.7 Calorific values (MJ/Nm^3) for syngas components (IEA, 2001)

Component	H_2	CO	CH_4	C_2H_6	C_2H_4	C_2H_2
HHV	12.769	12.622	39.781	69.693	63	58.059
LHV	10.788	12.622	35.814	63.748	59.036	56.078

Based on the syngas composition of woodchips gasification and their calorific values, the syngas HHV was calculated, which was 4.50 MJ/m^3. It was assumed that syngas heating value was constant in this calculation, regardless of the wood moisture contents. Therefore in the calculation of energy efficiency, for woodchips gasification, syngas heating value was 4.50 MJ/m^3, higher heating value for wood chips was 17.54 MJ/kg. Calculation was completed in an Excel spreadsheet in Table 6.11 (Appendix I).

Eight runs of woodchips gasification were tested, of which the energy efficiencies were estimated (Figure 4.16). It was noted that energy efficiency at the starting run was relatively lower compared to the runs after the burning charcoal was formed. Energy efficiency for wood chips gasification was 36.0% ± 7.7%.

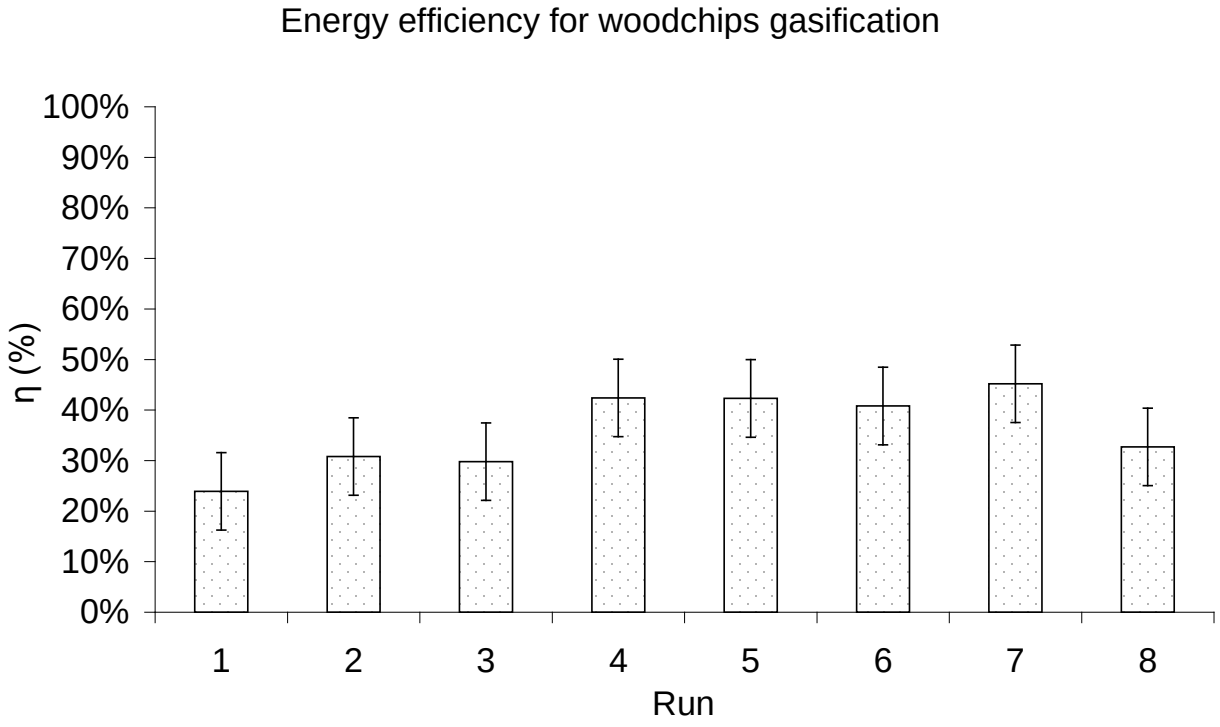

Figure 4.16 Energy efficiency for woodchips gasification

4.3 Summary

Three different types of biomass feedstock, woodchips, corncobs, and DDGS, were used to conduct the experimental study. Woodchips were used to initiate the starting run, and after that a burning charcoal was formed to support new feedstock added into the gasifier chamber. As indicated in the temperature profile curves, temperature values were typically different from each other in different reaction zones.

Intake air temperature was manually controlled by the high-flow-rate heater together with the variable voltage transformer. However, in the experiment runs of the three biomass feedstock, air was not preheated.

Pressure drop and air flow rate were measured and calculated. During the non-working condition, three biomass materials were loaded in the gasifier, data was collected to compare the pressure drops at different locations through the gasifier system, also under the power inputs set at four different levels. Negative pressure drop tended to increase when it came close to the blower, while positive pressure drop after the blower was decreased after the filtrator.

The test showed that the syngas composition, carbon monoxide (15%-20%v) and hydrogen (19%-20%v), and tar concentration, 1.65-4.20 g/Nm^3 were typical for a downdraft gasifier. Energy efficiency for wood chips gasification was 36.0% on average.

CHAPTER 5 - Summary

A downdraft gasifier system was instrumented and tested. Three instrumentation components were designed and built into the gasifier system: real-time temperature monitoring, differential pressure measurement, and gas flow rate measurement. Moreover, a full-wave rectifier circuit was applied to convert the AC power to DC power plus the regulation of AC input via a variable voltage transformer. A high-flow-rate heater was also setup to control intake air temperature. A tar sampling method based on the IEA tar protocol was developed. Experimental studies using three different biomass materials were performed to test the design and construction of these two systems.

Major achievements of this research are:

- Chromel-Alumel type-K thermocouples with a signal-conditioning device were chosen and installed to monitor the temperatures inside the gasifier. A differential pressure transducer and an ISA1932 flow nozzle were installed to measure pressure drop and gas flow rate of the system, respectively. Measured temperature profile inside the gasifier was comparable to that of a typical downdraft gasifier. Measured gas flow rate was close to the gasifier specification.
- A modified IEA tar protocol was used to determine tar concentration in syngas. Acetone was used as the condensation solvent to trap tars in the syngas. Wood chips and DDGS were tested as the feedstocks for biomass gasification experiments. The test showed that the syngas composition, carbon monoxide (15%-20%v) and hydrogen (19%-20%v), and tar concentration, 1.65-4.20 g/Nm^3 were typical for a downdraft gasifier. Energy efficiency for wood chips gasification was 36.0% on average.

CHAPTER 6 - Future Research Recommendations

The purpose of this research was focused on instrumentation and tar measurement of a downdraft gasifier. Based on research work completed, this project can be further developed in all following studies.

- Change the intake air temperature, biomass moisture content, and air flow rate to test how operating parameters would affect gasification performance.
- Test more types of biomass feedstock to study the capability of the downdraft gasifier system and compare the performance for each biomass.
- Verify the tar measurement system by comparing with some other methods.
- Add steam injection and provide better insulation (to reduce heat loss), so as to improve the existing system.

References

Abatzoglou, N.; Fernandez, J.-C.; Laramee, L.; Jollez, P.; Chornet, E. 1997a. "Application of Gasification to the Conversion of Wood, Urban and Industrial Wastes," in Developments in Thermochemical Biomass Conversion, Vol. 2. Edited by A.V. Bridgwater and D.G.B. Boocock. London: Blackie Academic & Professional, pp. 960–972.

Adegoroye, A., N. Paterson, X. Li, T. Morgan, A.A. Herod, D.R. Dugwell, and R. Kandiyoti. 2004. The characterisation of tars produced during the gasification of sewage sludge in a spouted bed reactor. *Fuel* (83): 1949-1960.

ASAE Standards, 2008. S358.2 DEC 1988 (R2008). Moisture measurement – forages. St. Joseph, MI: American Society of Agricultural Engineers.

ASME Standards. 2004. MFC-3M-2004: Measurement of fluid flow in pipes using orifice, nozzle, and venture. New York, N.Y.: ASME.

Baker, E.G., R.H. Moore, L.K. Mudge, and D.C. Elliott. 1986. "Engineering Analysis of Biomass Gasifier Product Gas Cleaning Technology," Richland, WA: Battelle Memorial Institute, Biofuels and Municipal Waste Technology Division, PNL-5534.

Baker, E.G.; M.D. Brown, D.C. Elliott, and L.K. Mudge.1988. "Characterization and Treatment of Tars from Biomass Gasifiers," Denver, CO: AIChE 1988 Summer National Meeting. 1–11.

Bangala, D. 1997. "Reformage Catalytique de Naphtalene et Ai-chlos-benzene," Ph.D. Thesis, Universite de Sherbrooke, Faculte des Sciences Appliques, Department de Genie Chimque.

Biomass Technology Group (BTG). 1995b. "Development of a Standard Procedure for Gas Quality Testing in Biomass Gasifier Plant/Power Generation Systems." Final report. The Netherlands: BTG Biomass Technology Group, JOU2-CT93-0408, NOVEM. EWAB-9608.

Biomass Technology Group (BTG). 2008. Tar & Tar Measurement. Available at: http://www.btgworld.com/index.php?id=21&rid=8&r=rd. Accessed 16 December 2008.

Blades, T., M. Rudloff, and O. Schulze. 2005. Sustainable SunFuel from CHOREN's Carbo-V® Process. CHOREN Industries Freiberg, Presented at ISAF XV, San Diego

Blanco, C.G., J. Blanco, P. Bernad, and M.D. Guillen. 1991. J. Chromatogr.(539): 157

Blanco, C.G., J.S. Canga, A. Dominguez, M.J. Iglesias, and M.D. Guillen. 1992. J. Chromatogr. (607): 295

Bodalo, A., G. Leon, M.L. Asanza, and E. Gomez. 1994. *J.H. Resolut. Chromatogr.* (17): 20

Bombach, R. 2002. Application of Raman spectroscopy: Species concentration and temperature measurements for catalytically stabilized combustion. ERCOFTAC SUMMER SCHOOL, March 2002, Zurich.

Brage, C., and K. Sjostrom. 1991. Separation of phenols and aromatic hydrocarbons from biomass tar using aminopropylsilane normal-phase liquid chromatography. *J. Chromatogr. A* (538): 303-310

Brage, C., Q. Yu. and K. Sjöström. 1996. Characteristics of evolution of tar from wood pyrolysis in a fixed-bed reactor. *Fuel* (75): 213-219.

Brown, M.D., E.G. Baker, and L.K. Mudge. 1986. Evaluation of processes for removal of particulates, tars, and oils from biomass gasifier product gases. In: Proc. Energy from Biomass & Waste X. London-New York: Elsevier Sci. 655-676.

Brown, R. 2003. Biorenewable resources: engineering new products from agriculture. Wiley-Blackwell: NJ

Brussels. 1988. IEA Thermal Gasification of Biomass Task, EC and USDOE Meeting on Tar Measurement Protocol. March 18–19, Brussels, Belgium. Meeting Presentation Information.

Carpenter, D.L., S.P. Deutch, and R.J. French. 2007. Quantitative measurement of biomass gasifier tars using a molecular-beam mass spectrometer: comparison with traditional impinger sampling. *Energy & Fuel* 21(5): 3036-3043.

Corella, J., M.P. Aznar, J. Delagado, and E. Aldea. 1991. Steam gasification of cellulosic wastes in a fluidized bed with downstream vessels. *Ind. Eng. Chem. Res.* (30): 2252-2262.

CRE Group Ltd. 1997. "Identification and Processing of Biomass Gasification Tars," Energy Technology Support Unit (ETSU), Department of Trade and Industry, DTI Contract No. B/T1/00418/00/00.

Dayton, D.C., R.J. French, and T.A. Milne. 1995. Direct Observation of Alkali Vapor Release during Biomass Combustion and Gasification. 1. Application of Molecular Beam/Mass Spectrometry to Switchgrass Combustion. *Energy Fuels*, 9 (5): 855-865.

Desilets, D.J., P.T. Kissinger, F.E. Lytle, M.A. Horne, M.S. Ludwicszak, and R.B. Jacko. 1984. Determination of polycyclic aromatic hydrocarbons in biomass gasifier effluents with liquid chromatography/diode array spectroscopy. *Envron. Sci. Technol.* (18): 386-391.

Donnot, A., J. Reningovolo, P. Magne, and X. Deglise. 1985. Flash pyrolysis of tar from the pyrolysis of pine bark. *J. Anal.Appl.Pyrolysis.* (8): 401

Dufour A, P. Girods, E. Masson, S. Normand, Y. Rogaume, and A. Zoulalian. Comparison of two methods of measuring wood pyrolysis tar. *J Chromatogr A.* (1164):240-247.

Elliott, D.C. 1988. Relation of reaction time and temperature to chemical composition of pyrolysis oils. In: Soltes J,Milne TA, editors. Pyrolysis oils from biomass; producing, analysing and upgrading, ACS Symposium Series 376. Washington, DC: American Chemical Society. 55–78.

EPA. 1983. EPA Federal Register 36, No. 247, 24878. Method 5. Determination of particulate emissions from stationary sources. In: 40 Code of Federal Regulations, Part 60, App. A-Reference methods. Revised 1 July 1983. Washington: EPA. 437-452.

Evans, R.J. and T.A. Milne. 1987. Molecular characterization of the pyrolysis of biomass. *Energy & Fuels.* 1(2):123–137

Evans, R.J., and T.A. Milne. 1987. Molecular characterization of the pyrolysis of biomass. 2. Applications. *Energy Fuels* 1 (4):311-319

FAO. 1986. Document: Wood gas as engine fuel. Forest Industries Division, Food and Agriculture Organization, United Nations, 00100 Rome, Italy.

Gaur, S. and T. Reed. 1998. Thermal data for natural and synthetic fuels, Marcel Dekker, New York.

Graboski, M. and R.L. Bain. 1979. "Properties of Biomass Relevant to Gasification," Chapter 3 of A Survey of Biomass Gasification - Volume 2, Solar Energy Research Institute, SERI/TR-33-239, National Renewable Energy Laboratory, Golden, CO.

Haser, P., and T. Nussbaumer. 1998. Guideline for sampling and analysis of tars and particulates from biomass gasifiers. Swiss Federal Office of Energy, Berne.

Hasler, P.; Bühler, R.; Nussbaumer, T. 1997. “Evaluation of Gas Cleaning Technologies for Small Scale Biomass Gasifiers.” Zurich: Swiss Federal Office of Energy and Swiss Federal Office for Education and Science.

Heesch, E.J.M., A.J. Pemen, M. Keping, S.V.B Yan, S.V.B. Paasen, and K.J. Ptasinski. 1999. Experimental program of the pulsed corona tar cracker. In: Proc. 12th IEEE Int Pulsed Power Conf. IEEE, New York.

Herzberg, G. 1967. Molecular spectra and molecular structure, I. Spectra of diatomic molecules. 2nd ed. Princeton, NJ: Twelfth printing; 1967.

International Energy Agency (IEA). 2001. Heating value of gases from biomass gasification. Report prepared for IEA Bioenergy Agreement, Task 20 – Thermal Gasification of Biomass. Report no. TPS-01/16.

Karellas, S., and J. Karl. 2007. Analysis of product gas from biomass gasification by means of laser spectroscopy. *Optics and Lasers in Engineering* (45): 935-946.

Kinoshita, C.M., Y. Wang, and J. Zhou. 1994. Tar formation under different biomass gasification conditions. *Journal of analystical ans applied pyrolysis* (29):169-181.

Knoef, H.A.M. 2000. The UNDP/World Bank monitoring program on small scale biomass gasifiers (BTG's experience on tar measurement). *Biomass and Bioenergy* (18): 39-54.

Knoef, H.A.M. 2005. *Handbook Biomass Gasification*. Netherlands: BTG Biomass Technology Group.

Li, X.T., J.R. Grace, C.J. Lim, A.P. Watkinson, H.P. Chen, and J.R. Kim. 2004. Biomass gasification in a circulating fluidized bed. *Biomass and Bioenergy* (26): 171-193.

Long, D.A. 1977. Raman spectroscopy. New York, NY: McGraw-Hill.

McKendry, P. 2002. Energy production from biomass (part 3): gasification technologies. *Bioresource Technology*. 83: 55-63

Milne, T.A., R.J. Evans, and N.Abatzoglou. 1998. Biomass gasification "tars": their nature, formation and conversion. NREL, Golden, CO. Report no. NREL/TP-570-25357.

Moersch, O.; Spliethoff, H.; Hein, K.R.G. 1997. "A New System for Tar Sampling and Analysis," in Biomass Gasification and Pyrolysis. Edited by M. Kaltschmitt and A.V. Bridgwater. Newbury, UK: CPL Press, pp. 228–234.

Moersch, O.; H. Spliethoff, and K.R.G. Hein. 1998. "Quasi continuous tar quantification with a new online analyzing method", 10th European Conference and technology exhibition, Biomass for Energy and Industry, Wurzburg, Germany, 8-11 June 1998, Proceedings of the international conference. 1638-1641.

Moersch, O., H. Spliethoff, and K.R.G. Hein. 2000. Tar quantification with a new online analyzing method. *Biomass and Bioenergy* (18): 79-86

Nieminen, M.; Simell, P.; Leppälahti, J.; Ståhlberg, P.; Kurkela, E. 1996. "High-Temperature Cleaning of Biomass Derived Fuel Gas," in Biomass for Energy and Environment: Proceedings of the 9th European Bioenergy Conference, June 1996. Edited by P. Chartier et al. Pergamon, pp. 1080–1085.

Osipovs, S. 2008. Sampling of benzene in tar matrices from biomass gasification using two different solid-phase sorbents. *Anal Bioanal Chem* (391):1409-1417.

Pakdel, H., and C. Roy. 1991. Hydrocarbon content of liquid products and tar from pyrolysis and gasification of wood. Energy & Fuels (5):427–436

Podgórska, A., K. Sylwester, B. Wlodzimierz. 2006. Effect of operating conditions on tar and gas composition in high temperature air/steam gasification (HTAG) of plastic containing waste. Fuel Process Technol (87): 223–33.

Qin, Y., H. Huang, Z. Wu, J. Feng, W. Li, and K. Xie. 2007. Characterization of tar from sawdust gasified in the pressurized fluidized bed. *Biomass and Bioenergy* (31): 243-249.

Quaak, P., H. Knoef, and H.E. Stassen. 1999. Energy from biomass: a review of combustion and gasification. World Bank Technical Paper No. 422

Sousa, L.C.R..2001. Gasification of wood, urban waste wood (Altholz) and other wastes in a fluidised bed reactor. Ph.D. thesis. Swiss Federal Institute of Technology Zurich.

Sricharoenchaikul, V., W.J. Frederick, Jr., and P. Agrawal. 2002. Black Liquor Gasification Characteristics. 2. Measurement of Condensable Organic Matter (Tar) at Rapid Heating Conditions. *Ind. Eng. Chem. Res. (*41): 5650–5658

Stassen, H. E. M. and H. A. M. Knoef. 1993. Small-scale gasification systems. The Netherlands: Biomass Technology Group, University of Twente.

Stobbe, S. J. Oatley, and R.C. Brown. 1996. Indirectly heated biomass gasification using Latent-heat Ballasting of a Fluidized reactor. In proceedings of the 31st Intersociety. Energy conversion engineering conference, 1996. IECEC 96.

Turare, C. 2002. Biomass Gasification – Technology and Utilization. Humanity Development Library: Document text. ARTES Institute, Glucksburg (Germany)

Walawender, W.P., S.M. Chern, and L.T. Fan. 1985. Wood chip gasification in a commercial downdraft gasifier. In: Overend, R.P., Milne, T.A. & Mudge, L.K. (eds.) Fundamentals of thermochemical biomass conversion. London: Elsevier. 911-921.

Walsh, M. E., R. L. Perlack, A. TUrhollow, D. G. de la Torre Ugarte, D. A. Becker, R. L. Graham, S. E. Slinshy, and D. E. Ray. 2000. Biomass feedstock availability in the United States: 1999 state level analysis. Oak Ridge, TN: Oak Ridge National Laboratory, April 1999, updated January 2000

Xu, M., R.C. Brown, G. Norton, and J. Smeenk. 2005. Comparison of a solvent-free tar quantification method to the International Energy Agency's tar measurement protocol. *Energy & Fuels* (19): 2509-2513.

Appendix A - Operating Manual for Downdraft Biomass Gasifier

1. *Gasifier run:*
   (1) Circulation water set up.
   (2) Through the left water inlet, add water in to the chamber underneath the filter case till 12-14 cm (controlled by an overflow outlet).
   (3) Turn off the valve of the stove, turn on the vent-pipe valve.
   (4) Connect the variable transformer to the wall power. Power on.
   (5) Add 50 vol % of the wood chips into the reactor chamber, add a small amount of ethanol to the upper cover of the chips, together with 5-6 pieces of charcoal, use torch to light them so as to start the gasification process (record this initial time).
   (6) When the wood chips are fully lighted, add more wood chips until the chamber is 90% volume full.
   (7) After the chips have been burning for a few minutes (record the time), prepare to turn on the stove.
   (8) Turn on the pulse switch on the stove first, and then let the switch (which controls the gas from the purifier to the stove) on.
   (9) Wait until the flame of the stove becomes stable (treat it as a signal of stable gasification status, record time), using the sampling port after the purifier to collect syngas sample (~80% of the 3 L sampling bag, ~2.4 L).
   (10) Start to operate Tar/Particulate sampling line (record time). Make the sample for about 10~15 minutes (record time). Also read sampling flow rate every 3 minutes.
2. *Syngas sample collection:*
   (1) Connect the filter holder (with 2 pieces of glass fiber filter set up) to the post-purifier sampling port
   (2) Connect the outlet of the filter holder to the inlet of sampling bag
   (3) Collect around 2.4 L syngas sample (80% capacity of the bag)
3. *Tar/Particulate sampling:*
   (1) Airproof/airtight test.
   (2) Connect the tube to the sampling point, set up the filter holder, connect the flow meter to tube extended from the last sampling bottle, turn on the vacuum pump. Put the sampling bottles #1, 2, 4 in the warm water bath; #3, 5, 6 in the ice bath.
   (3) Record the initial time of the sampling. Operate the sampling test for 15~30 minutes. Record the time when we stop sampling.
   (4) Collect the filter paper and other stuffs (stainless pipes and hoses) for analysis.
4. *Tar/Particulate analysis:*
   (1) Wash the sampling line along the syngas flow direction, collect the acetone mixture in one of the sampling bottles.
   (2) Use the thimble filter to collect the PM contained in the acetone mixture.
   (3) Turn on the heater. Set the heater temperature to 80 °C (acetone boiling point =56.53 °C).
   (4) Set up the Soxhlet apparatus in the lab.

(5) Carefully fill the filter paper (with tars and particulates) into the thimble, which is loaded into the main chamber of the Soxhlet extractor.
(6) Place the Soxhlet extractor onto a flask containing the solvent (acetone, 100 ml).
(7) Connect the cooling water in port to the tap, and the cooling water out port to the sink. Equip the extractor to the condenser.
(8) As the temperature gradually increases, the main chamber slowly fills with the warm solvent. The tars contained in the particulate filter paper will be partly solved in acetone. Before the solvent fills the chamber "full" (till the siphon point), remove the acetone to the recycled bottle.
(9) Use recycled acetone to wash each sampling bottle for one time.
(10) Remove the thimble from the Soxhlet chamber, dry them (thimble + filter paper) in the oven (105 °C, 2 hours).
(11) Solvent evaporation.
(12) Weigh dried "thimble + filter paper" (particulates) and "residues" (tars), use mass gravimetric method to evaluate weight of particulates.

Appendix B - Temperature Calibration Chart for AD595

Table 6.1 Output voltage vs. thermocouple temperature at ambient +25 °C (adapted from AD595 specification, Analog Devices)

Thermocouple temperature (°C)	Type K voltage (mV)	AD595 Output (mV)	Thermocouple temperature (°C)	Type K voltage (mV)	AD595 Output (mV)	Thermocouple temperature (°C)	Type K voltage (mV)	AD595 Output (mV)
20	0.798	200	360	14.712	3641	750	31.214	7722
25	1	250	380	15.552	3849	760	31.629	7825
30	1.203	300	400	16.395	4057	780	32.455	8029
40	1.611	401	420	17.241	4266	800	33.277	8232
50	2.022	503	440	18.088	4476	820	34.095	8434
60	2.436	605	460	18.938	4686	840	34.909	8636
80	3.266	810	480	19.788	4896	860	35.718	8836
100	4.095	1015	500	20.64	5107	880	36.524	9035
120	4.919	1219	520	21.493	5318	900	37.325	9233
140	5.733	1420	540	22.346	5529	920	38.122	9430
160	6.539	1620	560	23.198	5740	940	38.915	9626
180	7.338	1817	580	24.05	5950	960	39.703	9821
200	8.137	2015	600	24.902	6161	980	40.488	10015
220	8.938	2213	620	25.751	6371	1000	41.269	10209
240	9.745	2413	640	26.599	6581	1020	42.045	10400
260	10.56	2614	660	27.445	6790	1040	42.817	10591
280	11.381	2817	680	28.288	6998	1060	43.585	10781
300	12.207	3022	700	29.128	7206	1080	44.439	10970
320	13.039	3227	720	29.965	7413	1100	45.108	11158
340	13.874	3434	740	30.799	7619			

Appendix C - Data of Temperature Profiles and Pressure Drop

Table 6.2 DDGS gasification

Temperature (°C)					ΔP (outlet II) (inch of water)	
18-inch	12-inch	5-inch	grate	exit	average	stdev
153	193	418	522	195	2.4	0.9
144	191	440	556	197	2.0	1.0
140	222	459	587	200	2.3	1.1
143	278	471	615	210	2.1	1.1
142	340	491	643	215	2.1	0.9
131	404	522	662	210	2.1	0.8
110	486	574	667	192	2.0	0.9
129	559	554	669	216	2.2	0.9
133	597	562	670	224	2.2	1.0
140	618	564	675	233	1.9	1.0
142	637	567	681	238	1.9	0.8
145	652	567	690	243	2.0	1.0
146	685	574	697	246	2.0	0.8
117	702	640	688	218	1.9	0.8
117	698	659	684	219	1.7	0.8
118	702	669	681	221	2.0	0.8
120	719	673	679	223	2.0	1.0
121	739	676	677	225	2.0	0.9
123	753	677	684	227	1.9	0.8
124	762	679	686	229	2.2	1.0
125	778	681	679	230	1.8	0.9
125	790	682	676	231	2.0	0.7
129	757	683	683	234	2.1	0.8
132	756	683	672	239	1.8	0.9
134	758	682	654	242	1.8	0.8
119	687	674	692	237	1.7	0.7
127	586	667	644	240	2.0	1.0
132	562	670	642	247	1.9	0.8
134	562	677	678	250	1.9	0.9
142	549	686	705	258	1.8	0.8
136	564	693	723	249	2.0	0.8
134	548	698	728	246	2.0	0.9
139	536	702	738	251	1.7	1.0
142	528	705	741	254	1.8	0.8
147	515	707	760	260	1.6	0.8
134	544	707	789	244	1.6	0.8

Table 6.3 Corncobs gasification

Temperature (°C)					ΔP (outlet II) (inch of water)	
18-inch	12-inch	5-inch	grate	exit	average	stdev
203	645	525	549	244	3.4	1.9
174	677	538	588	244	3.8	2.0
148	689	571	620	240	3.5	2.0
150	667	582	638	259	3.1	2.0
132	691	594	646	252	3.6	1.9
121	699	605	649	250	3.0	2.3
112	706	618	648	247	3.3	2.1
107	705	626	648	248	3.0	2.0
106	703	631	645	251	3.3	1.9
106	702	634	644	253	3.2	1.9
104	699	636	643	254	3.1	2.2
119	664	638	645	271	3.0	1.8
126	633	642	640	283	3.0	2.0
116	635	639	631	279	3.2	2.0
113	645	637	626	271	2.7	1.7
112	651	634	626	268	2.8	1.8
112	643	635	624	274	3.2	1.6
105	656	638	622	264	3.5	1.9
103	659	636	618	265	3.3	1.9
106	658	634	616	263	3.0	1.7
105	658	632	613	261	3.1	1.6
104	658	630	611	262	2.9	1.6
104	658	628	608	261	3.3	1.8
105	658	625	606	261	2.9	1.5
104	657	624	605	259	2.8	1.6
119	628	618	606	277	3.2	2.0
141	622	582	602	304	2.9	1.8
138	625	579	597	300	3.0	1.6
135	621	578	599	298	2.8	1.8
132	620	577	603	296	2.6	1.6
134	613	577	602	296	2.4	1.4
130	619	576	600	291	2.8	1.3
136	603	576	596	297	2.9	1.3
139	592	576	592	303	2.8	1.5
141	587	575	589	305	2.8	1.4
137	597	572	588	299	2.9	1.5

Table 6.4 Woodchips gasification

Temperature (°C)					ΔP (outlet II) (inch of water)	
18-inch	12-inch	5-inch	grate	exit	average	stdev
230	482	603	602	247	3.6	2.2
200	680	622	620	252	4.0	2.1
183	755	641	636	258	4.1	2.2
197	740	641	646	293	4.0	2.4
172	757	656	648	282	3.9	1.8
143	804	665	648	267	3.3	2.0
127	786	674	650	267	3.8	2.2
135	736	680	652	276	3.6	2.4
137	738	683	656	282	4.5	2.2
133	745	685	652	285	3.9	2.4
138	734	686	648	289	3.8	2.4
141	709	687	649	294	3.2	2.0
132	720	687	648	287	4.0	2.1
137	707	686	648	294	3.5	2.0
146	685	686	647	304	3.9	2.2
129	711	685	645	286	3.6	2.5
122	715	683	643	278	3.8	2.2
139	689	682	641	289	3.4	2.2
154	689	680	639	291	3.5	2.3
176	694	678	638	296	3.6	2.0
231	687	677	639	313	3.8	1.8
275	695	675	638	318	3.4	2.2
286	680	673	636	323	4.2	2.3
274	649	668	638	330	4.2	2.5
258	631	655	627	335	3.5	2.2
233	654	642	624	322	3.5	2.2
221	661	639	621	313	3.5	2.1
235	656	632	617	316	3.4	2.2
285	660	627	615	322	3.0	2.3
350	657	623	614	333	4.1	2.5
460	643	619	618	351	3.4	2.7
481	634	616	614	350	3.7	2.2

Table 6.5 Pressure drop comparison (unit: inch of water)

	inlet		18-inch		12-inch		grate		exit		outlet I		outlet II	
	average	stdev	average	stdev	average	stdev	average	stdev	average	stdev	average	stdev	average	stdev
no feed														
90V	-0.42	0.13	-0.36	0.14	-0.36	0.14	-0.36	0.13	-0.37	0.13	3.13	0.89	3.08	0.73
100V	-0.55	0.18	-0.53	0.17	-0.51	0.16	-0.51	0.19	-0.53	0.14	4.67	0.90	4.62	0.80
110V	-0.56	0.22	-0.49	0.25	-0.46	0.22	-0.48	0.21	-0.53	0.19	4.86	1.20	4.83	1.19
120V	-0.58	0.27	-0.53	0.26	-0.48	0.28	-0.53	0.26	-0.54	0.27	4.56	1.60	4.77	1.55
woodchips														
90V	0.03	0.08	0.00	0.09	0.01	0.10	-0.05	0.08	-0.04	0.09	1.12	0.47	1.27	0.44
100V	-0.09	0.12	-0.08	0.11	-0.12	0.12	-0.26	0.11	-0.30	0.15	2.43	0.54	2.38	0.58
110V	-0.18	0.12	-0.22	0.13	-0.27	0.12	-0.46	0.12	-0.54	0.15	3.94	0.82	3.76	0.80
120V	-0.30	0.13	-0.34	0.16	-0.38	0.17	-0.65	0.16	-0.76	0.21	4.75	1.07	4.79	1.19
corncobs														
90V	-0.03	0.09	-0.05	0.09	-0.16	0.11	-0.73	0.18	-0.83	0.19	0.90	0.46	0.87	0.44
100V	-0.22	0.10	-0.31	0.11	-0.43	0.14	-1.28	0.18	-1.34	0.11	1.91	0.54	1.78	0.50
110V	-0.44	0.14	-0.57	0.15	-0.74	0.18	-1.40	0.06	-1.40	0.07	2.87	0.66	2.82	0.71
120V	-0.55	0.22	-0.65	0.23	-0.79	0.27	-1.37	0.09	-1.37	0.10	3.30	1.11	3.07	0.97
DDGS														
90V	0.08	0.08	-0.27	0.12	-0.55	0.21	-1.40	0.08	-1.38	0.12	0.31	0.56	0.29	0.60
100V	0.07	0.08	-0.60	0.12	-1.14	0.20	-1.43	0.06	-1.42	0.06	0.43	0.66	0.49	0.55
110V	0.03	0.09	-0.97	0.12	-1.42	0.07	-1.42	0.06	-1.42	0.06	0.71	0.80	0.79	0.62
120V	0.03	0.10	-0.99	0.19	-1.43	0.06	-1.41	0.06	-1.43	0.06	0.93	0.93	0.75	0.97

Appendix D - Data Table for Experiment Documentation

Table 6.6 Test and analysis log for gasification experiment

Sampling of Tar in Syngas
Gasifier type:
Test #: Location/Date:
Feedstocks:
Particulate filter temperature (°C):
Weight of flask (g): Weight of sampling bottles (g):
Solvent for tar:
Solvent from T&P sampling:
Solvent from Soxhlet extraction:
Sampling start: Sampling end:
Total sampling duration (hr):
Gas flow rate (L/min):
Total amount of gas sampled (L):
Total tar mass (mg):
Drying temperature (°C): Drying duration (hr):
Remarks:

Appendix E - DDGS Properties Analysis

Table 6.7 DDGS properties (data provided by Land O'Lakes Purina Feed)

Midwest Sample #	Date Sampled	Date Reported	QC Sample #	Moisture	Protein	Fat	Pro+Fat	L Value	Total Starch
9340606	1/09/08 Wed	1/15/2008	08-0001	11.9	25.0	9.81	34.8	50.8	4.61
9344760	1/28/08 Mon	2/1/2008	08-0004	11.73	27.9	9.7	37.6	52.0	2.69
9345473	1/30/08 Wed	2/5/2008	08-0005	11.51	26.9	8.12	35.0	54.7	4.05
9355598	3/12/08 Wed	3/18/2008	08-0016	12.73	27.5	9.65	37.2	45.0	7.7
9357289	3/19/08 Wed	3/25/2008	08-0017	11.31	28.6	9.9	38.5	48.3	4.84
9358665	3/25/08 Tues	4/1/2008	08-0018	11.94	25.7	10.3	36.0	49.6	5.61
9361023	4/3/2008 Thurs	4/10/2008	08-0021	11.77	27.8	9.69	37.5	50.6	3.63
9362671	4/10/2008 Thurs	4/16/2008	08-0022	12.23	25.9	9.75	35.7	51.0	4.48
9364416	4/16/08 Wed	4/22/2008	08-0025	11.73	25.7	9.78	35.5	51.0	5.43
9366661	4/24/08 Thurs	4/30/2008	08-0026	11.57	26.5	9.69	36.2	49.5	4.35
9366688	4/24/08 Thurs	4/30/2008	Rick's Sample	10.51	28.5	9.38	37.9		
Averages				11.72	26.91	9.62	36.52	50.25	4.74
					Profat	36.52			

Appendix F - Biomass Properties (Gaur and Reed, 1998)

Name	Proximate analysis				Ultimate analysis				
	Fixed carbon (%)	Volatiles (%)	Ash (%)	HHV (kJ/g)	C (%)	H (%)	O (%)	N (%)	S (%)
Wood									
Beech	-	-	0.65	20.38	51.64	6.26	41.45	0	0
Black Locust	18.26	80.94	0.8	19.71	50.73	5.71	41.93	0.57	0.01
Douglas Fir	17.7	81.5	0.8	21.05	52.3	6.3	40.5	0.1	0
Hickory	-	-	0.73	20.17	47.67	6.49	43.11	0	0
Maple	-	-	1.35	19.96	50.64	6.02	41.74	0.25	0
Pinus pinaster	17.17	82.54	0.5	18.4	49.25	5.99	44.36	0.06	0.03
Poplar	-	-	0.65	20.75	51.64	6.26	41.45	0	0
Red Alder	12.5	87.1	0.4	19.3	49.55	6.06	43.78	0.13	0.07
Redwood	16.1	83.5	0.4	21.03	53.5	5.9	40.3	0.1	0
Western Hemlock	15.2	84.8	2.3	20.05	50.4	5.8	41.1	0.1	0.1
Yellow Pine	-	-	1.31	22.3	52.6	7	40.1	0	0
White Fir	16.58	83.17	0.25	19.95	49	5.89	44.75	0.05	0.01
White Oak	17.2	81.28	1.52	19.42	49.48	5.38	43.13	0.35	0.01
Madrone	12	87.8	0.2	19.51	48.94	6.03	44.75	0.05	0.02
Mango Wood	11.36	85.64	2.98	19.17	46.24	6.08	44.42	0.28	
Bark									
Douglas Fir bark	25.8	73	1.2	22.1	56.2	5.9	36.7	0	0
Loblolly Pine bark	33.9	54.7	0.4	21.78	56.3	5.6	37.7	0	0
Energy Crops									
Eucalyptus camaldulensis	17.82	81.43	0.76	19.42	49	5.87	43.97	0.3	0.01
Casuarina	19.58	78.58	1.83	18.77	48.5	6.04	43.32	0.31	0
Poplar	16.35	82.32	1.33	19.38	48.45	5.85	43.69	0.47	0.01
Sudan Grass	18.6	72.75	8.56	17.39	44.58	5.35	39.18	1.21	0.01
Processed Biomass									
Plywood	15.77	82.14	2.09	18.96	48.13	5.87	42.46	1.45	0
Agricultural									
Peach Pits	19.85	79.12	1.03	20.82	53	5.09	39.14	0.33	0.05
Walnut Shells	21.16	78.28	0.56	20.18	49.48	5.71	43.35	0.21	0.01
Almond Prunings	21.54	76.83	1.63	20.01	51.3	5.27	4.09	0.66	0.01
Black Walnut Prunings	18.56	80.69	0.78	19.83	49.8	5.82	43.23	0.22	0.01
Corncobs	18.54	80.1	1.36	18.77	46.58	5.87	45.46	0.47	0.01
Wheat Straw	19.8	71.3	8.9	17.51	43.2	5	39.4	0.61	0.11
Cotton Stalk	22.43	70.89	6.68	18.26	43.64	5.81	43.87	0	0
Corn Stover	19.25	75.17	5.58	17.65	43.65	5.56	43.31	0.61	0.01
Sugarcane Bagasse	14.95	73.78	11.27	17.33	44.8	5.33	39.55	0.38	0.01
Rice Hulls	15.8	63.6	20.6	14.89	38.3	4.36	35.45	0.83	0
Pine needles	26.12	72.38	1.5	20.12	48.21	6.57	43.72	-	0
Cotton gin trash	15.1	67.3	17.6	16.42	39.59	5.26	36.38	2.09	0

Appendix G - Relative Heating Value of Wood as a Function of Moisture Content

Table 6.8 The relative heating value of wood as a function of moisture content

Moisture (%)[a]	0	10	25	50	75	100
Heating value (%)[b]	100	90	78	63	52	44

[a]Moisture content is the weight of moisture as a percentage of wood oven-dry weight for a fixed weight of green wood
[b]Heating value is the amount of usable heat produced by wood at a given moisture content compared with that produced by oven dry wood.

Appendix H - Calibration of SRI8610 Gas Chromatograph (GC)

Molecule	Peak Area Data		Calibration Factor	Corrected Area	mole%
	Retention Time	Peak Area		Peak Area*Calibration Factor	Corrected Area/Total Corrected Area
H_2	1.8		150		
O_2	2.5		1.04		
N_2	2.9		1		
CO	7.7-10.6		0.823		
CO_2	6.8		0.611		
CH_4	5.8-6		1.276		
				Total Corrected Area=sum(corrected area)	

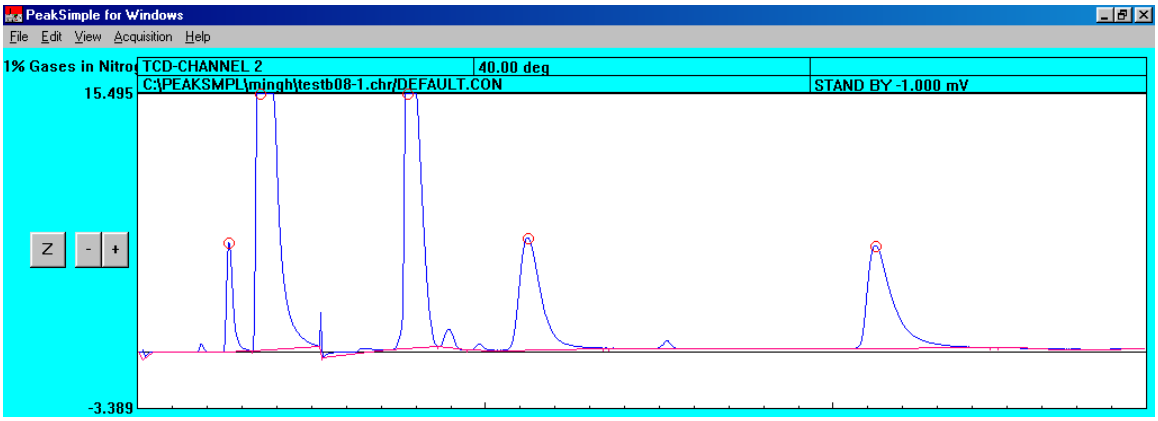

Appendix I - Calculation of flow rate, syngas density, and energy efficiency

Table 6.9 Calculation of flow rate

Calculation of flow rate							
Known							
d (m)	0.0254	D(m)	0.0508	P_1 (Pa)			
ε	1	R_D	300000	P_2 (Pa)			
β	0.5	$R_D (=V_1 * D/v_1)$		ΔP (Pa)	32.4	insert ΔP	
ρ_1 (kg/m^3)	0.8679	V_1 (m/s)	2.1771	$\tau (=P_2/P_1)$			
v_1 (m^2/s)	0.0000133			κ			
ρ (kg/m^3)	0.8679			$\varepsilon(Y)$			
π	3.14						
C	0.9758			ΔP (Pa)	q_v (cfm)		
q_m (kg/s)	0.0038			32.4	9.3		
q_v (m^3/s)	0.0044			69.7	13.7		
q_v (cfm)	9.3450			122	18.1		
				159.4	20.7		
Note:	*1 in = 0.0254 m*						
	C is the discharge coefficient;						
	ε is the expansibility factor;						
	Δp is the differential pressure;						
	ρ_1 is the density of the fluid at the upstream pressure tap;						
	ρ is the fluid density at the temperature and pressure for which the volume is stated;						
	β is the diameter ratio;						
	R_D is the Reynolds number referred to D.						
	1m^3/s = 2118.9cfm						
	1m^3/hr = 0.5886cfm						
	κ is the isentropic exponent (its value depends on the nature of the gas)						

Table 6.10 Calculation of syngas density

Calculation of syngas density								
Physical properties of gases								
Density of gases at standard temperature and pressure (0 ^{o} C, 1atm):								
ρ_{air} (kg/m^3)	1.29							
ρ_{H2} (kg/m^3)	0.0899							
ρ_{N2} (kg/m^3)	1.251							
ρ_{O2} (kg/m^3)	1.429							
ρ_{CO} (kg/m^3)	1.25							
ρ_{CO2} (kg/m^3)	2.16							
ρ_{CH4} (kg/m^3)	0.783							
*Density of gases at gasification temperature (49 ^{o} C) is calculated based on ideal gas law (ρ=P/R*T):*								
The density of gases at 49 ^{o} C, 1atm:								
ρ'_{air} (kg/m^3)	1.094							
ρ'_{H2} (kg/m^3)	0.076							
ρ'_{N2} (kg/m^3)	1.061							
ρ'_{O2} (kg/m^3)	1.212							
ρ'_{CO} (kg/m^3)	1.060							
ρ'_{CO2} (kg/m^3)	1.831							
ρ'_{CH4} (kg/m^3)	0.664							
Based on the syngas composition of woodchips gasification:								
H_2	20.04%							
O_2	3.15%							
N_2	61.64%							
CO_2	0.04%							
CO	15.01%							
CH_4	0.12%							
ρ_{syngas} (kg/m^3)	0.8679							
Note:	R = 8.314472 m^{3}Pa*K^{-1}*mol^{-1}							
	0^{o}C = 273.15K							

Table 6.11 Calculation of energy efficiency

Calculation of energy efficiency						
W_{bio} (kg)	6.87			Syngas composition		
MC	7.55%			Molecule	Wood Chips	
C%	44.26			H_2	20.04%	
$HHV_{woodchips}$ (MJ/kg)	17.54			O_2	3.15%	
E_{bio} (MJ)	111.43			N_2	61.64%	
t (min)	36			CO_2	0.04%	
q_v (cfm)	5.8			CO	15.01%	
HHV_{syngas} (MJ/m^3)	4.50			CH_4	0.12%	
E_{syn} (MJ)	26.60					
η (%)	23.9					
Note:	$1ft^3 = 0.0283m^3$					

Table 6.12 Gasification energy efficiency for woodchips

run	wood mass (lbs)	moisture content (%)	time (min)	η (%)
#1	6.87	7.55	36	23.9
#2	6.50	7.55	44	30.8
#3	4.76	8.05	31	29.8
#4	6.37	8.05	59	42.4
#5	6.49	8.05	60	42.3
#6	5.05	8.05	45	40.8
#7	6.49	8.05	64	45.2
#8	6.16	8.05	44	32.7

Appendix J - Thermodynamic data used by different companies (unit: MJ/Nm^3) (IEA, 2001)

Component	H2	CO	CH4	C2H6	C2H4	C2H2	Company
HHV	12.745	12.633	39.819	70.293	63.414		TU Wien
	12.769	12.622	39.781	69.693	63	58.059	NREL
	12.753	12.626	39.721	69.595	62.952		ECN
	12.766	12.641	39.847	70.402	63.998	58.975	DMT
	12.761	12.634	39.747	69.636	62.989	58.039	Carbona
	12.76	12.617	39.663	69.511	63.042	57.934	Univ. Sherbrook
	12.758	12.631	39.739				Vattenfall
	12.761	12.634	39.75	69.642	62.994	58.022	Nykomb
LHV	10.783	12.633	35.883	64.345	59.457		TU Wien
	10.788	12.622	35.814	63.748	59.036	56.078	NREL
	10.789	12.626	35.796	63.704	59.024		ECN
	10.8	12.6	35.8	63.71		56.03	Verenum
	10.757	12.641	35.787	64.333	59.938	56.924	DMT
	10.748	12.634	35.725	63.605	59.011	56.028	Carbona
	10.793		35.81				Vattenfall
	10.8	12.634	35.823	63.756	59.07	56.06	Nykomb
	10.797	12.635	35.821	63.749	59.068		TPS
	10.789	12.630	35.812	63.744	59.033	56.088	Bioelettrica
Component	**C3H8**	**C3H6**	**i-C4H8**	**i-C4H10**	**n-C4H10**	**C6H6**	**Company**
HHV	101.242	93.576	125.088	133.119	134.061		TU Wien
	99.091	91.879				142.893	NREL
						147.299	ECN
	101.794	94.343	121.843	131.972	133.981	146.329	DMT
	99.108	91.894		128.502		147.385	Carbona
	98.244					147.143	Univ. Sherbrook
	99.116	91.902	120.696	128.207	128.513	147.398	Nykomb
LHV	93.215	87.575	116.934	122.91	123.81		TU Wien
	91.163	85.934				141.41	NREL
						141.408	ECN
	93.548	88.191	113.806	121.592	123.517	140.301	DMT
	91.066	85.862		118.449		141.352	Carbona
	91.268	86.016	112.848	118.703	118.703	141.512	Nykomb
	91.164	85.925	113.371	117.668	118.569	159.502	Bioelettrica
Component	**NH3**	**H2S**					**Company**
HHV	13.072	25.105					ECN
		25.07					Kvaerner
	17.245	25.7					DMT
	17.094	25.123					Carbona
		25.096					Nykomb
LHV	10.128	23.142					ECN
		23.12					Kvaerner
	14.189	23.69					DMT
	14.079	23.134					Carbona
	14.132	23.152					TPS
	14.136	23.113					Bioelettrica